International Advanced Studies Institute
IASI

Science & Technology Series

# Detection and Analysis of Subsurface Objects and Phenomena

October 19-23, 1998

Naval Postgraduate School, Monterey, California, USA

## Chairmen

Barry Dillon, Head of Research
Naval Coastal Station
&
Xavier Maruyama, Professor
Naval Postgraduate School

Visit IASI's website at http://www.advstudies.org

# International Advanced Studies Institute

**(Science & Technology Series)**

## The First International Symposium on

# Detection and Analysis of Subsurface Objects and Phenomena

**Chairmen**

**Barry Dillon, Head**
**Science, Technology, Analysis and Special Operations**
**Department - Naval Coastal Systems Station**

**Xavier Maruyama, Professor**
**Naval Postgraduate School**

## PROGRAM

**All Sessions are Held in Room 101A-Spanagel Hall**

### Sunday, October 18

5:00 – 7:00 Registration – **Lobby of Ingersoll Hall**

### Monday October 19, 1998

7:30 – 8:30 Continental Breakfast – **Lobby of Ingersoll Hall**
Registration – **Lobby of Ingersoll Hall**

9:00 Opening Remarks

**Remote Detection and Physical Characterization of Subsurface Objects**

**Session Chairman : Jack Dvorkin, Geophysics Department, Stanford University**

9:05-9:35 Introduction
Jack Dvorkin, Geophysics Department, Stanford University

9:35-10:00 Crosswell Seismic Imaging
Jerry M. Harris, Geophysics Department, Stanford University

10:00-10:30 Coffee/Tea Break – **Lobby of Ingersoll Hall**

10:30-10:55 Feasibility of Reservoir Monitoring by 3-D Surface Seismic
Biondo Biondi, Geophysics Department, Stanford University

10:55-11:20 Quantifying the Amount of Gas Hydrates in Marine Sediments
Christine Ecker, Chevron; and
Jack Dvorkin and Amos Nur, Geophysics Department, Stanford University

11:20-11:45 Wave Propagation in Fine-Grained Marine Sediments: The Grain Material as an Effective Inelastic Medium
Klaus C. Leurer, Geophysics Department, Stanford University

11:45-12:10 Wave Propagation in Unconsolidated Sands: Dependence on Grain Size, Grain Shape, and Confining Pressure
Manika Prasad, Geophysics Department, Stanford University

12:10-2:00 Lunch – La Novia Room at Hermann Hall

2:00-2:45 Underground Imaging of Electrically Conducting Plumes
James G. Berryman, Lawrence Livermore National Lab

2:45-3:10 Ultra-Shallow Seismic Reflection in Unconsolidated Sediments: Theory and Applications
Ran Bachrach and Amos Nur
Geophysics Department, Stanford University

3:10-3:35 Petroleum Reservoir Rock Texture and Hydrocarbon Detection
Jack Dvorkin and Per Avseth
Geophysics Department, Stanford University

3:35 Coffee/Tea Break – **Lobby of Ingersoll Hall**

## Tuesday October 20, 1998

7:30 – 8:30 Continental Breakfast – **Lobby of Ingersoll Hall**
Registration – **Lobby of Ingersoll Hall**

**Threat Detection and Related Issues**

**Session Chairman : Xavier Maruyama, Naval Postgraduate School**

9:00-9:30 UNSCOM Inspection Regime in Iraqi Ballistic Missiles
Clay Bowen, Ph.D., Monterey Institue of International Studies

9:30-10:15 Microscopes for Subvisible Frequencies
Daniel van der Weide, University of Delaware

10:15-11:00 Coffee/Tea Break – **Lobby of Ingersoll Hall**

11:00-12:00 **Different aspects of Blast effects on buildings**
**Mohammed M. Ettouney, PE, Ph.D.**
**Principal, Weidlinger Associates, Inc.,**

12:00-2:00 Lunch – La Novia Room at Hermann Hall

2:00-2:45 Approaches to One-Side Radiographic Imaging for Detection of Illicit Materials
Esam M. A. Hussein and Edward J. Waller, Laboratory for Detection of Threat Materials, University of New Brunswick, Canada

2:45-3:30 Loss of Trace Amounts of Plastic Explosives from Airplane Parts Exposed to Seawater (The TWA-800 Investigation)
Frank T. Fox, Ph.D., FAA Security Equipment IPT

3:30-4:00 Coffee/Tea Break – **Lobby of Ingersoll Hall**

4:00-4:45 Deposition of Explosives on Porous Materials in the Development of Standards for Walk Through portals
Thomas Chamberlain, Aviation security R&D, FAA Technical Center

## Wednesday October 21, 1998

7:30 – 8:30 Continental Breakfast – **Lobby of Ingersoll Hall**
Registration – **Lobby of Ingersoll Hall**

**Underwater Phenomena and Sensing**

**Session Chair : Dr. Delbert C. Summey, Naval Coastal Station**

9:00-9:30 From Ocean Acoustics to Acoustical Oceanography, Inverting for Ocean Parameters
Herman Medwin, Professor Emeritus – Naval Postgraduate School

9:30-10:10 Using SOSUS to Track Whale Migration
Ching-Sang Chiu, Professor of Oceanography – Naval Postgraduate School

10:10-10:40 Coffee/Tea Break – **Lobby of Ingersoll Hall**

10:40-11:25 **Application of Advanced Sensors at the Swissair Flight-111 Survey Site**
**Barry Dillon, Head, Science, Technology, Analysis and Special Operations Department - Naval Coastal Systems Station**

11:25-11:55 Recent Advances in Subsurface Unexploded Ordinance (UXO) Detection Using Airborne Ground Penetrating SAR
Amir Finjany, James B. Collier and Ari Citak
Jet Propulsion Laboratory, California Institute of Technology

11:55-2:00 Lunch – La Novia Room at Hermann Hall

2:00-2:30 Chemical Sensing of Mines and Unexploded Ordnance in Marine Environments
William Chambers, Sandia national Laboratory

2:30-3:00 Chemical Sensing of Unexploded Ordnance with the Mobile Underwater Debris Survey System (MUDSS)
Murray Darrach, Jet Propulsion laboratory

3:00-3:30 Chemical Sensing for the Explosives
Anne Kusterbeck, naval Research Laboratory

3:30-4:00 The Mobile Underwater Debris Survey System (MUDSS)
Delbert Summey, Coastal Systems Station - Panama City, FL

4:00-4:30 Coffee/Tea Break – **Lobby of Ingersoll Hall**

4:30-5:20 **FIELDING TECHNOLOGY FAST**
**THE KAHO`OLAWE MODEL**
**James D. Putnam, Director, Contracts Operations Division, Pacific Division, Naval Facilities Engineering Command at Pearl Harbor**

## Thursday October 22, 1998

7:30 – 8:30 Continental Breakfast – **Lobby of Ingersoll Hall**
Registration – **Lobby of Ingersoll Hall**

**High-Speed Imaging Techniques and Applications**

**Session Co-Chairmen: Thomas McDonald, Jr. and George J. Yates**
**Los Alamos National Laboratory**

9:00-9:25 Underwater Mine Detection Utilizing Gated Intensifier Shutters Synchronized with Laser Reflectance Images From Submersed Targets
Nicholas S.P. King, Kevin L. Albright, Robert A. Gallegos, Vanner Holmes, Steven A.Jaramillo, Claudine R.Pena, Thomas E.McDonald Jr., George J. Yates, Los Alamos National Laboratory, Bojan T. Turko, Lawerence Berkeley National Laboratory and William Snuggs, Mike Stephenov, Naval Coastal Systems Center-Panama City

9:25-9:50 High Speed Cooled CCD Experiments
Claudine R. Pena, Kevin L. Albright, George J. Yates, Los Alamos National Laboratory

9:50-10:15 Miniature, Sub-nanosecond Lasers for High-Speed Imaging
Fred J Zutavern, Wesley D. Helgeson, Martin W. O'Malley, Alan Mar, and Guillermo M. Loubriel, Sandia National Laboratories and George J. Yates, Robert A. Gallegos, and Thomas E. McDonald, Los Alamos National Laboratory

10:15-10:45 Coffee/Tea Break – **Lobby of Ingersoll Hall**

10:45-11:10 Externally Rendered Objects (EROs)
Augusto Op den Bosch, Ph.D. Senior Research Engineer and Adrian Ferrier Research Engineer, Spectra Precision Software, Inc.

11:10-11:35 Range Gating Experiments through Scattering Media.
Jeremy Payton, Frank Cverna, Robert Gallegos, Tom McDonald, Dustin Numkena, Andy Obst, Claudine Pena-Abeyta, George Yates
Los Alamos National Laboratory

11:35-12:00 HyperSpectral and Image Fusion Using High Speed Back-illuminated CCD Sensors
George M. Williams, James R. Janesick, Serge Ioffe, Harry Marsh, Ryan Miller, and Scott Way, PixelVision Inc. and John Antoniades, John Fisher, Naval Research Labs

12:00-2:00 Lunch – La Novia Room at Hermann Hall
Luncheon talk by Dr. Frank Asaro – lawrence Berkeley National laboratory
"Determination of the Authenticity of the Plate of Brass"

2:00-2:25 RULLI; A Photon Counting Imager
Kevin L. Albright, Clayton Smith, and Cheng Ho

2:25-2:50 Using Optical Parametric Oscillators (OPO) for Wavelength Shifting IR Images to Visible Spectrum
Thomas E. McDonald Jr., Dustin M. Numkena, Jeremy Payton, George J. Yates, Los Alamos National Laboratory and Paul Zagarino, Sharpenit

2:50-3:15 Electron Bombarded CCD Imagers for Commercial and Military Systems
Eric Howard
Silicon Mountain Design

3:15-3:45 Coffee/Tea Break – **Lobby of Ingersoll Hall**

3:45-4:10 Camera System for High-Frame Rate Applications
George J. Yates, Thomas E. McDonald, Jr., and N. S. P. King, Los Alamos National Laboratory and Bojan T. Turko, Lawrence Berkeley National Laboratory

4:10-4:35 Digital Memory for a 16-port CCD Camera Readout at 40 MHz Pixel Rates
B.T. Turko,** N.S.P. King,* T. McDonald,* J. Millaud** and G.J. Yates*
(*Los Alamos National Laboratory; **Lawrence Berkeley National Laboratory )

4:35-5:00 A Method for Transmitting High Frame Rate Video Data to Remote Locations
Ernest L Brunholzl, Field Engineering Acqiris, Albuquerque, NM
Victor Hungerbueller, Engineering Manager, Acqiris SA, Geneva, Switzerland

## Friday October 23, 1998

7:30 – 8:30 Continental Breakfast – **Lobby of Ingersoll Hall**
Registration – **Lobby of Ingersoll Hall**

**Detection Technology for Non-Proliferation, Treaty Verification, Safeguards and Hazardous Waste Disposal**

**Session Chairman : Jim Morgan, Lawrence Livermore National Laboratory**

9:00 - 9:25 Nuclear radiation Detection Technology at Los Alamos National Laboratory
W. Robert Scarlett, M. W. Johnson and Avigdor Garvon, Los Alamos National Laboratory

9:25-9:50 Enriched Uranyl Fluoride Deposit Characterizations Using Active Neutron and $\gamma$ Interrogation Techniques with $^{252}Cf$
T. Uckan, M. S. Wyatt, J. T. Miahalczo and T. E. Valentine, Oak Ridge National Laboratory and T. F. Hannon, Bechtel Jacobs Company LLC

9:50-10:15 $^{252}Cf$ or Inherent Source Driven Correlations for Non-Intrusive Verification of Weapons Components in Containers
J. K. Mattingly, M. S. Wyatt, T. E. Valentine, J. T. Miahalczo and J. A. Mullens, Oak Ridge National Laboratory
and S. S. Hughes, Oak Ridge Y-12 Plant

10:15-10:45 Coffee/Tea Break – **Lobby of Ingersoll Hall**

10:45-11:10 Tactical Unattended Ground Sensors
Steven G. Peglow, Lawrence Livermore National Laboratory

11:10-11:35 Identification of Motion Events from Fusion of Micropower Impulse Radar and Other Sensor data
James K. Wolford, Jr, Donald J. Mullenhoff and David A. Kasimatis
Lawrence Livermore National Laboratory

11:35-12:00 Discussion

12:00 Lunch – La Novia Room at Hermann Hall

# Crosswell Seismic Imaging

**Jerry M. Harris, Geophysics Department, Stanford University**

Crosswell seismic imaging typically operates in a frequency band between 200 and 2000 Hz. The images produced from the crosswell geometry provide complementary coverage and resolution to surface seismic (50 Hz) and borehole logging (10,000 Hz) methods. The broadband signals used in crosswell imaging experience significant dispersion as well time delay during propagation; therefore, the attenuation and the velocity properties of rocks and fluids may be estimated from the data. In this talk, I will review acquisition procedures and summarize tomographic and reflection processing methodologies for crosswell surveys. In addition, I will describe three applications illustrating the need for high resolution imaging for aquifers and petroleum reservoirs:

(1) determining the geometry;
(2) characterization of flow properties, e.g., porosity and permeability;
(3) monitoring fluid movement and small changes in saturation.

# Feasibility of Reservoir Monitoring by 3-D Surface Seismic

**Biondo Biondi, Geophysics Department, Stanford University**

Oil and gas production causes changes in the physical properties of hydrocarbon reservoirs such as: fluid saturation, pore pressure, and temperature, that are, at least in principle, "visible" from reflection seismic surveys. The knowledge of the evolution of the reservoir can be used to greatly improve the efficiency of the recovery process. Therefore, monitoring reservoir changes with time-lapse seismic holds the promise to significantly improve reservoir characterization and reservoir management. Relating time-dependent changes in seismic to the underlying flow processes requires inputs from: (1) geological modeling/geostatistics; (2) flow simulation; (3) rock physics; and (4) seismic imaging. This paper
documents the results from a project that brings these disciplines together. In this study we have considered the forward modeling for a 3-D reservoir monitoring problem: creating a detailed geological model, performing flow simulation, relating the dynamic rock properties to seismic properties,
and, finally, imaging the reservoir at multiple times.

# Quantifying the Amount of Gas Hydrates in Marine Sediments

**Christine Ecker, Chevron; and**
**Jack Dvorkin and Amos Nur, Geophysics Department, Stanford University**

Marine seismic data and well log measurements at the Blake Ridge offshore South Carolina show that prominent seismic Bottom Simulating Reflectors (BSRs) are caused by sediment layers with gas hydrate overlying sediments with free gas. The goal of this investigation is to provide a theoretical tool for quantifying the amount of gas hydrate and gas near a BSR using marine seismic. In order to accomplish this goal, we develop a new theoretical rock-physics model that links the elastic wave velocities in high-porosity marine sediments to density; porosity; effective pressure; mineralogy; and water, gas, and gas hydrate saturation of the pore space. To apply this model to the data, we first obtain interval velocity using stacking velocity analysis. Then, we use the interval velocity together with the rock-physics model to calculate a porosity section under the assumption that the entire sediment is water-saturated. Such an inversion gives porosity anomalies where gas hydrate and free gas are present (as compared to typical profiles expected and obtained in sediment without gas hydrate or gas). Porosity is underestimated in the hydrate region and is overestimated in the free-gas region. We calculate the porosity residuals by subtracting a typical (without gas hydrate and gas) porosity profile from that with anomalies. Next we use the rock-physics model to eliminate these anomalies by introducing hydrate or gas saturation. As a result, we obtain a 2D saturation map. The maximum gas hydrate saturation thus obtained is between 15% and 20% of the pore space (depending on the version o the model used). These saturation values are consistent with those measured in the Blake Ridge wells (away from the seismic line). Free gas saturation varies between 1%-2%. The saturation estimates are extremely sensitive to the input velocity values. Therefore, accurate velocity analysis is crucial for correct reservoir characterization.

# Wave Propagation in Fine-Grained Marine Sediments: The Grain Material as an Effective Inelastic Medium

**Klaus C. Leurer, Geophysics Department, Stanford University**

In the present paper, an attempt is made to account for discrepancies found in comparing measured values for velocity and attenuation in clay-rich marine sediments and the corresponding theoretical values as resulting from Biot theory. It is assumed that the nature of expandable clay minerals in unconsolidated fine-grained marine sediments leads to deviations from the normally assumed ideal elasticity of the solid phase. In the proposed "effective grain model" (EGM), the elastic grain material is therefor replaced by an effective medium made up of a homogeneous elastic mineral phase containing isotropically distributed cylindrical, "penny-shaped" inclusions of low aspect ratio. These inclusions represent the intra-crystalline water layers in the expandable clay minerals. The two-phase nature of the grain material thus specified results in a wave-energy consuming squirt-flow from the inclusions into the pore space. Introducing the EGM into the Biot-Stoll model (BSM) via the complex bulk modulus of the dissipative grain material leads to a better fit to literature data on the attenuation of compressional waves than does the BSM alone. Since expandable clay minerals occur in nearly all clay-bearing sediments, it is concluded that the attenuation mechanism of the EGM may represent a universal contribution to the overall intrinsic inelasticity of unconsolidated fine-grained marine sediments in the frequency range from a few kilohertz to about 1 MHz.

# Wave Propagation in Unconsolidated Sands: Dependence on Grain Size, Grain Shape, and Confining Pressure

**Manika Prasad, Geophysics Department, Stanford University**

In order to get information about sediment properties from indirect seismic measurements, some a priori information about the dependence of velocity and attenuation on sediment parameters such as grain size and shape is required. I present here experimental results of P- and S-wave velocity and attenuation on sands. The results on dry and water saturated sediments are investigated for their dependence on grain size, grain shape, porosity, density, static frame compressibility and effective
pressure.
The main results of this study are:
(a) Grain size dependence of velocity and attenuation--an increase in grain size leads to an increase in velocity and attenuation; and
(b) Grain shape dependence--and increase in angularity causes velocity and attenuation to decrease.
These results will be compared with other, similar, measurements on sands.

# Underground Imaging of Electrically Conducting Plumes

**James G. Berryman, Lawrence Livermore National Lab**

The use of electrical resistance tomography for applications to underground contaminant remediation has now been established as a viable means of imaging conducting fluid plumes in the earth. A competing method using electromagnetic induction rather than d.c. imaging techniques also shows promise of being able to image both conductors and conduction deficits (presence of hydrocarbons) to map their locations underground, and potentially with both greater speed and higher resolution than d.c.. methods. Field tests in the shallow subsurface show that environmental clutter (for example, metallic pipes at the surface) has significantly more effect on some components of magnetic field than it does on others, which suggests that the less sensitive components may be the best ones to use for imaging the conductivities of most interest.

# Ultra-Shallow Seismic Reflection in Unconsolidated Sediments: Theory and Applications

**Ran Bachrach and Amos Nur, Geophysics Department, Stanford University**

Typical high-resolution shallow seismic methods target depths below 500m. However, obtaining high-resolution seismic reflection images at depths shallower than 5-10m is often assumed not to be possible. There is a great need for better physical understanding of the seismic response of the very shallow subsurface for evaluating the feasibility of acquisition and for optimal survey design in different conditions.
In this paper we address the problem of ultra-shallow seismic acquisition in unconsolidated sediments. We show that the velocity profile in the upper few meters of unconsolidated sediments is pressure dependent, and that the very near-surface P and S wave velocities (in undersaturated sediments) are always very low. Then we show that, given this velocity profile, ground roll will be attenuated greatly by scattering in the presence of very mild surface roughness. This attenuation of the high frequencies of the ground roll causes a separation of the reflection energy from the ground roll energy in the frequency domain. This separation enables us to image seismic reflections in at very shallow depths. We present field examples from three different locations where we have been able to obtain very shallow reflections (1-3m) in unconsolidated sediments. These findings show that in any unconsolidated material, ultra-shallow reflection imaging is possible given sufficient frequency bandwidth.

# Petroleum Reservoir Rock Texture and Hydrocarbon Detection

**Jack Dvorkin and Per Avseth, Geophysics Department, Stanford University**

At high porosity, velocity in reservoir rocks strongly depends on the position of the intergranular material. Velocity is high if the original grains are cemented at their contacts. It is low if the pore-filling material is placed away from the contacts. In the latter case we have truly unconsolidated sediments. In the former case we have high-porosity cemented rocks. Separating these two rock types is important for hydrocarbon identification. Due to the difference in the rock frame stiffness between the unconsolidated and high-porosity cemented rocks, seismic signatures of the former filled with water can be very close to those of the latter filled with hydrocarbons. This may complicate direct hydrocarbon detection. We separate the two rock types by diagnosing sand using rock physics theory. We conduct such diagnostic on well log data from two wells that penetrate the Heimdal formation (North Sea). We show that the Heimdal formation reservoir is composed of both unconsolidated and cemented high-porosity sands. The initial quartz cementation present in the latter is clearly seen in the cathode-luminescent SEM images. These images, combined with point XRD analysis, confirm our diagnostic that the high-velocity high-porosity sands in Heimdal contain quartz grains surrounded by quartz-cement rims. We find that the two different types of sand which are capped by similar low-impedance shales produce drastically different AVO signatures. The oil-filled high-porosity cemented sand shows a relatively strong zero-offset reflectivity which becomes less positive with increasing offset, while the oil-filled uncemented sand shows a negative zero-offset reflectivity with increasingly negative far-offset response. These results show that (1) rock diagnostic can be conducted not only on the log scale but also on the seismic scale; and (2) taking into account the nature of the rock improves our ability to identify pore fluid from seismic.

# Microscopes for sub-visible frequencies: scanning the near field in the microwave through infrared with micromachined probes

**Daniel van der Weide**
**Associate Professor and Director of the Center for Nanomachined Surfaces**
**University of Delaware**

How could we image an electron? Just take a picture of it. We would find, however, that the Rayleigh criterion limits how small an object we can resolve: it must be about half a wavelength in size. So shrink the wavelength. Now we've raised the photon energy so high that we will displace the electron, changing the object as we image it, a consequence of Heisenberg's uncertainty principle.
While we have learned through "squeezing" light that we can trade knowledge of position and momentum within the confines set by Heisenberg, could Rayleigh also be so accommodating? If we are willing to trade the parallel nature of conventional far field optics for serial image acquisition in the near field, the answer is yes. In this talk I will describe how we design, microfabricate and use near-field antennas and other sensors that also work as scanning force microscopes. These probes have cross-disciplinary applications: they can make images of an integrated circuit's topography and local electric or magnetic fields, but they can also be used to examine sub-surface defects in materials such as silicon and quartz, excite "artificial molecules" made with semiconductor quantum dots, probe moisture content in paper fibers, and perhaps map out the structure and dynamics of ion channels in neuronal membrane. Other probes with diodes at their tips can be used for imaging local temperature and topography or directly detecting local microwave and optical fields. These micromachined multifunctional probes are enabling us to do microscopy and spectroscopy at dimensions as much as $10^{-6}$ smaller than the wavelengths we use, shedding quite literally a new light onto the microscopic world.
Daniel W. van der Weide received the BSEE from the University of Iowa in 1987 and the MS (1990) and PhD (1993) in Electrical Engineering from Stanford. In Autumn 1995 he joined the Department of Electrical Engineering at the University of Delaware as an Assistant Professor, and is now Associate Professor as well as the director of the Center for Nanomachined Surfaces. During the two years prior to that, he was applying broadband electronic THz generation and detection techniques to coherent contactless spectroscopy of low-dimensional electron systems at the Max-Planck-Institut für Festkörperforschung (Solid-state Research) in Stuttgart.

Dr. van der Weide has held summer positions with Hewlett-Packard Co. and the Lawrence-Livermore National Laboratory, and has held full-time positions as an Engineer with Motorola, Inc. and as a Member of the Technical Staff at Watkins-Johnson Co.

He is the recipient of the ONR Young Investigator award, a Ford University Research Award, and the NSF CAREER award and the 1997 NSF Presidential Early Career Award for Scientists and Engineers (PECASE).

# Different aspects of Blast effects on buildings

**Mohammed M. Ettouney, PE, Ph.D.**
**Principal, Weidlinger Associates, Inc.,**
**New York, NY 10014**

The design and construction of buildings to provide life safety in the face of explosions is receiving renewed attention from engineers, building officials and legislators. From structural engineering viewpoint, there are several aspects to this subject. This presentation is subdivided into four parts. First we will consider some similarities / differences between seismic and blast loads and designs. Next we will discuss fragmentation effects, which is an aspect of blast loading that is not well understood. Third, an overview of current requirements of building design codes to mitigate progressive collapse in buildings is presented. Finally, we will consider the design features of a typical eight-story reinforced concrete building from blast protection perspective. We will address the design of floor slabs, columns, facades, atrium areas, and windows as well as the prevention of progressive collapse in the blast environment. We will present design modifications that may limit the occupant's exposure to extreme blast pressures and provide details that improve structural response characteristics

Dr. Ettouney has over 30 years of experience in Structural Engineering. He has been involved in both research and practical applications in this field. He has worked in academia, private industry and major consulting firms. His main interests are in Earthquake Engineering, Blast Engineering, submerged Structures, Structural Health Monitoring and Vibration and Acoustic Mitigation. He has authored and published more than 100 professional papers in these fields. Dr. Ettouney participated in writing seismic design codes for New York City and for the State of New York. He participates in numerous professional committees and activities. Dr. Ettouney holds a Ph.D. from Massachusetts Institute of Technology and an MBA from Long Island University.

# Loss of Trace Amounts of Plastic Explosives from Airplane Parts Exposed to Seawater

**Frank T. Fox, Ph.D.**
**Federal Aviation Administration, Security Equipment IPT**

Learning objective: Can trace amounts of unburned explosive be found on aircraft parts following an explosion over the sea and prolonged immersion of the parts in seawater?

Following the crash of TWA flight 800, it was decided to determine the effects of seawater on aircraft aluminum and cloth that had been contaminated with trace amount of plastic explosives. Wing aluminum parts from a commercial aircraft were obtained from a FAA salvage yard; seat cover and cargo liner glass fiber cloth was obtained from the FAA burn test laboratory. Four-inch squares were contaminated with accurately known trace amounts of plastic explosives using a water suspension process developed in this laboratory.

This procedure involves the gentle suspension of the compressed plastic-coated micro crystals of RDX and PETN, which make up plastic explosives, C4, DETA sheet and Semtex. The techniques of high-pressure liquid chromatography and particle sizing by light scatter were used to quantify the suspension containing explosive particles. The appropriate concentration is obtained by simple dilution followed by accurate pipetting of the quantified suspension. After evaporation of the water there remains a residue of the explosive particles with their original plastic coating as existed in the manufactured bulk material. Retention of the original plastic coating is important to retain the "sticky" character of the original explosive. Commercial explosives detection instruments require that a sample be taken from a test object surface by wiping with a swab. In that case the adhesive character of the test material must match the analyte sought. These deposits were intended to simulate preblast explosive. Contamination was also accomplished by exposing aluminum squares close to exploding C4, Semtex, and DETA sheet. This procedure was intended to capture unburned, postblast, explosive and decomposition products. The aluminum squares were wired to cyclone fence so as not to be lost during the explosion.

The aluminum aircraft parts were drilled in each corner and wired to the inside of plastic baskets. Two baskets were wired together at their "lip". This made for a sturdy system that protected the airplane parts and still allowed for a free flow of water around them. The baskets were placed in a nylon mesh divers bag and it had an anchor attached. The test objects were exposed to seawater by immersion in Brigantine Bay to a depth of six to eight feet. Samples were withdrawn and analyzed periodically. A commercial trace explosive analyzer was used for the analyses. Comparison was made to the effects of fresh water on similar samples to determine the effect of biological degradation of the explosives.

The experimental data led to the conclusion that there is little likelihood that blast deposited unburned plastic explosive remains for very long on cloth or aluminum aircraft parts after immersion in seawater. This is further complicated by the fact that there appears to be little post blast deposit of unburned explosive. The plastic explosives are rapidly leached or otherwise removed from immersed aircraft parts despite the low solubility. Microbial degradation or, more likely, the very end products of the multiple digestive processes that occur in the series of players in the food chain, seem to play a role in the removal of the plastic explosives. The last digestion products would be something that nothing in seawater wants to eat. Other workers in the field have suggested that this material may have micelle forming properties

# Deposition of Explosives on Porous Materials in the Development of Standards for Walk Through Portals

**R. Thomas Chamberlain, JD, Ph.D.**
**FAA William J. Hughes Technical Center,**

The Federal Aviation Administration (FAA) has been involved in evaluating Trace Explosives Detection Systems (TDS) for our airports. For this major undertaking the FAA's William J. Hughes Technical Center laboratory has been involved in the development of test standards and protocols that test performance of the various TDS systems on the commercial market. An extension of this is the development and testing of portals for screening of people.

Earlier work involved the production of explosives test standards that would closely approximate fingerprint derived plastic explosives contamination on electronic carry on items which have relatively non-porous surfaces. Now the FAA is involved in the use of walkthrough portals that could be used at airports or the entrances of buildings to detect trace amounts of explosives on individuals. This requires the development of standards on porous materials such as cloth. As part of the FAA's portal project, Idaho National Energy Laboratories has been involved in a series of tests to identify the location and quantities of explosives residues that are present on the person involved in the preparation of improvised explosive devices (IED). Several bombs have been constructed from explosives and the body and area around the building experiment were literally mapped in a semiquantitative manner. These measurements were critical in the next stage of the research in producing an appropriate standard for portal testing.

Several studies are presented in this presentation that describe our effort in the development of reproducible standards that are related to actual contamination that a bomb maker or handler displays on his or her person. Specific chromatographic procedures have been developed to accurately quantify explosives in the deposition process. We have attempted to follow the deposition of explosives on fabric and their removal by detection portals through the use of different microscopic techniques such as scanning electron microscopy.

Key terms: Portal, Trace Explosives, Standards

# Approaches to One-Side Radiographic Imaging for Detection of Illicit Materials

**Esam M.A. Hussein and Edward J. Waller**
**Laboratory for Detection of Threat Materials**
**Department of Mechanical Engineering**
**University of New Brunswick**

There are occasions, in the course of determining if an explosive threat exists, where access to both sides of an article to be interrogated is not possible, as in the detection of landmines or the inspection of baggage left unattended and abutted against a wall. In such cases, a one-side approach to imaging must be undertaken. This paper reviews existing approaches to radiological imaging and assesses their potential application to the
detection of explosives and narcotics.

# Using SOSUS to Track Whale Migration

**Ching-Sang Chiu, Professor of Oceanography**
**Naval Postgraduate School, Monterey, CA.**

To investigate the feasibility of automating the detection and censusing of blue whale vocalizations over a large coastal region using the Naval Postgraduate School (NPS) Ocean Acoustic Observatory (OAO), a four-day experiment was conducted along Central California in the summer of 1997. During the experiment, array data was archived continuously at the NPS OAO, a former US SOSUS array. In addition to shore-based acoustic monitoring, an aircraft was assigned to locate blue whales in the Monterey Bay National Marine Sanctuary, and a research vessel, manned with observers and instrumented with a towed hydrophone array, was used to confirm locations of the blue whales and classify the vocalized near-field signals. The shipboard measurements were required to provide a means to separate the source signal characteristics from their multipath signatures for the design of long-range auto-detection and censusing. The towed array data was deverberated, source level and characteristics were estimated, and call-to-call variability was studied. Determination of robust signal parameters is important to the design of auto-detection filters as well as optimal matched-signal (field) algorithms for long-range localization and tracking using the NPS OAO array. The progress toward proving the feasibility of these concepts is discussed.

**[Research supported by ONR]**

# Recent Advances in Subsurface Unexploded Ordnance (UXO) Detection using Airborne Ground Penetrating SAR

**Amir Fijany, James B. Collier, and Ari Citak**

*Jet Propulsion Laboratory, California Institute of Technology.*

## Abstract

In 1995, JPL, SRI, and U.S. Army Engineering and Support Center, Huntsville (USAESCH) teamed up to conduct an airborne SAR survey for detection of the Unexploded Ordnance (UXO) at the former Camp Croft Army Training Facility in Spartanburg, SC. SRI's UWB, ground penetrating, SAR was used for airborne survey of this site. Not only was the Camp Croft site of vast acreage but also the extent of UXO contamination was undocumented and unknown. In addition, this site presents significant complexity in foliage clutter and terrain relief. Although, airborne, ground penetrating, SAR is being increasingly used as an effective remote sensing technology for various applications it had not previously been successfully established as a viable tool for subsurface UXO detection. In addition, Camp Croft represented two unique challenges for subsurface UXO detection:

1. Highly negative signal-to-clutter environment, due to the dense foliage, and
2. Low-resolution measurement, due to the small size of the class of UXOs of interest with respect to the SAR wavelength resulting in a subpixel target.

The JPL team developed effective and advanced post-processing algorithms for detection of subpixel target in a highly negative signal-to-clutter environment, using the polarized UWB SAR data collected by SRI. These algorithms were first successfully validated against ground truth (found UXOs by walk through of the site) provided by USAESCH. They were then applied to a survey of a small area (100 acres) of Camp Croft. Subsequent inspection of this area by USAESCH clearly validated the effectiveness of JPL algorithms for both detection of subsurface UXOs and identification of clear areas. JPL's successful results of this challenging and real-life case study for the first time clearly established the ground penetrating airborne SAR as a viable remote sensing tool for a rapid and cost-effective survey of large sites. Upon this successful validation, Former Buckley Field, CO, which is a 60,000 acres site close to city of Denver, was considered for a first large-scale application of the JPL technology. In order to achieve an adequate processing rate, thus making such a large-scale application possible, JPL has been developing an automated testbed. Also, a set of new algorithms have been developed to specifically increase the processing rate. In order to validate these algorithms, a data set acquired by SRI airborne SAR of a minefield in Yuma Proving Ground has been used. The application of the algorithms on this data set, has shown successful detection of surface and subsurface anti-tank mines. In this talk, we present our results of Camp Croft and Yuma Proving Ground experience, and discuss the foundation of JPL algorithms. We also discuss new techniques in terms of both data acquisition and processing which will be used for survey of Former Buckley Field.

*Key Words*: Airborne, Ground Penetrating SAR, Image Processing Algorithms, Subpixel Target Detection, UXO.

Brief Biography of Principal Author:

Dr. Amir Fijany is a Senior Member of Technical Staff with the Ultra Computing Group, Information and Computing Technologies Research Section, at the Jet Propulsion Laboratory, California Institute of Technology. He received the BS and MS degrees in electrical engineering from University of Tehran in 1980, and the D.E.A. and Ph.D. degrees in electrical and computer engineering from University of Paris XI (Orsay), France, in 1981 and 1988, respectively. In July 1987, he joined JPL and since May 1996 he is also a Visiting Associate at the California Institute of Technology. His research activities include signal and image processing, SAR data processing, parallel algorithms, advanced computer architectures, and application of parallel computing to scientific and Grand Challenge problems. He holds five U.S. patents on the design of parallel architectures for signal processing and robotics applications. He has received numerous NASA Technical Innovation Awards. He is the recipient of two NASA Major Monetary Awards for the development of scientific contributions with significant value to the advancement of the aerospace technology program of NASA. He has authored/co-authored over 60 articles in archival journals and conference proceedings as well as one book and three book chapters. Dr. Fijany is a Senior Member of IEEE.

# Chemical Sensing of Mines and Unexploded Ordnance

William B. Chambers, Philip J. Rodacy
James M. Phelan, Stephen D. Reber

Sandia National Laboratories

Sandia National Laboratories has conducted research in chemical sensing and analysis of explosives for many years. Recently, that experience has been directed towards detecting mines and unexploded ordnance (UXO) by sensing the low-level explosive signatures associated with these objects. The objective of this work is to develop a miniature, portable chemical sensing system which can be used to classify buried or submerged objects to determine whether there are explosive molecules associated with them. We will describe a prototype system which consists of a sampler, concentrator, and detector. Two separate sampling systems have been designed, one for water collection and one for soil/vapor sampling. The water sampler utilizes a flow-through chemical adsorbent phase to extract and concentrate the explosive molecules. The soil sampler employs a light-weight probe for extracting and concentrating explosive vapor from the soil. Explosive molecules are thermally desorbed from the concentrator and trapped in a focusing stage for rapid desorption into an Ion Mobility Spectrometer. The system is capable of sub-part-per-billion detection of TNT and related explosive munition compounds. We will present the results of field and laboratory tests which demonstrate the feasibility of using such a system to classify buried or submerged objects.

**William B. Chambers**
Senior Member Technical Staff
Analytical Chemistry Department
Sandia National Laboratories
Albuquerque, NM 87185-0343

phone: 505/844-3849
fax: 505/844-7910
e-mail: wbchamb@sandia.gov

## Education

B.Sc. Biology/Chemistry, University of New Mexico, 1973.

## Professional Experience

Senior Member Technical Staff, Analytical Chemistry Dept., Sandia National Laboratories, 1996-present
Member Technical Staff, Analytical Chemistry Dept., Sandia National Laboratories, 1985-1996;
Lab Manager/Chemist, Academy Corporation, Albuq., NM, 1981-1985;
Lab Manager/Chemist, EDA Instruments, Albuq., NM, 1980-1981;
Lab Scientist, New Mexico Environment Dept., Scientific Laboratory Div., Albuq., NM, 1974-1980.

## Representative Sandia Technical Assignments

Advanced Materials Analysis for Sandia Research and Development Laboratories;
Trace Explosives Analysis applied to Landmine and Unexploded Ordnance Detection;
Environmental and Materials Analysis for USN, USS IOWA Explosion Investigation;
Consultant to IAEA on Nuclear Fuel Transport Cask Contamination;
Systems Analysis of Analytical Methodology for Verification of U.N. Chemical Weapons Treaty.

## Publications

Chambers, W. B., Rodacy, P. J., Woodfin, R. L., Jones, E. E., Gomez, B. J., "Chemical Sensing System for Classification of Mine Like Objects", Proceedings SPIE Aerosense '98 Conference: Detection and Remediation Technologies for Mines and Minelike Targets III, Orlando, Fl., 1998.
Chambers, W.B., Maestas, L., et.al., "Weapon Interaction Study: An Analysis of Weapon Materials Compatibility", SAND97-2947. Sandia National Laboratories, Albuq., NM.
Chambers, W.B., Graff, E.W. 1995. SNL/NM Weapon Hardware Characterization: Process Development Report. SAND94-2872. Sandia National Laboratories, Albuquerque., NM.
Chambers, W.B., Granstaff, V.E. 1993. Application of Surface Complexation Modeling to the Understanding of Transportation Cask Weeping. SAND93-1467. Sandia National Laboratories, Albuquerque, NM.
Nelson, G.C., Tallant, D.R., Chambers, W.B., Borders, J.A. 1993. Materials Analysis Related to the USS IOWA Incident. SAND93-0103. Sandia National Laboratories, Albuquerque, NM.
Chambers, W.B., Keenan, M.R., Tissot, R.G. 1992. Statistical Sampling and Chemical Analysis of Complex Weapon Components. SAND92-2219. Proceedings of the DOE Dismantlement Technology Forum, Livermore, CA.
McGuire, R., Stanbro, W. Chambers, W.B., Kempf, R. 1992. Chemical Weapons Treaty Verification Technology Research and Development: Equipment Field Trial Report. CRDEC-CR-180. U.S. Army Chemical Research, Development, and Engineering Center. Aberdeen Proving Ground, MD.

## Professional Societies

American Chemical Society (ACS)
Society of Applied Spectroscopy (SAS)

# CHEMICAL SENSING OF UNEXPLODED ORDNANCE WITH THE MOBILE UNDERWATER SURVEY SYSTEM (MUDSS)

**M. R. Darrach, A. Chutjian**
Jet Propulsion Laboratory, California Institute of Technology
4800 Oak Grove Drive
Pasadena, CA 91109 USA

**Abstract**

The ability to sense explosives residues in the marine environment is a critical tool for identification and classification of underwater unexploded ordnance (UXO). Trace explosives signatures of TNT and DNT have been extracted from multiple sediment samples adjacent to unexploded undersea ordnance at Halifax Harbor, Canada. The ordnance was hurled into the harbor during a massive explosion fifty years earlier, in 1945 after World War II had ended. Laboratory sediment extractions were made using the solid-phase microextraction (*SPME*) method in seawater, and detection using the Reversal Electron Attachment Detection (*READ*) technique and, in the case of DNT, a commercial gas-chromatography/mass spectrometer (*GC/MS*). Results show that, after more than 50 years in the environment, ordnance which appeared to be physically intact gave good explosives signatures at the parts-per-billion level, whereas ordnance which had been cracked open during the explosion gave no signatures at the 10 parts-per-trillion sensitivity level. These measurements appear to provide the first reported data of explosives signatures from undersea UXOs.

**I. Introduction**

The detection of undersea UXOs is a matter of vital concern to several United States agencies, including the Department of Defense (US Navy, Army Corps of Engineers), and the Environmental Protection Agency. This issue has been highlighted as a result of the Base Realignment and Closure (BRAC) Act in which formerly used defense sites (FUDS) will be returned to the civilian sector. Central to the problem of undersea UXOs is their detection, by both physical means (*e.g.*, forward- and side-scanning sonars, magnetic-field gradiometers, electro-optical sensors) and chemical means (*e.g.*, seawater and/or sediment sampling and detection). A suite of these physical and chemical sensors has been incorporated into the so-called Mobile Undersea Debris Survey System (MUDSS) (1). The present study is aimed at testing the hypothesis that sediment sampling near a UXO, followed by chemical extraction and detection, can be a viable method of

verifying an active target. To our knowledge, this is the first chemical evaluation under actual environmental conditions of sediment adjacent to old, live UXOs (2). The site chosen for the sediment sampling was offshore of Rent Point in Halifax Harbor, Canada. A fire in 1945 caused detonation of an ammunition storage complex, which scattered large quantities of UXOs. After the explosions subsided underwater UXOs lay undisturbed for 50 years. All of the ordnance at Halifax could be expected to be live, with few if any inert rounds

Samples collected were brought back to the laboratory, and any explosives materials extracted using solid-phase microextraction (*SPME*). The extracted species were detected using the Reversal Electron Attachment Detection (*READ*) technique and, for verification in some cases, a commercial gas-chromatography/mass spectrometer (*GC/MS*). The *READ* system uses the fact that explosives have an extremely large cross section for attachment of zero-energy electrons, *via* the so-called *s*-wave attachment phenomenon. The *SPME/READ* technique is highly selective towards those molecules which adsorb to the *SPME* fiber, *and* have large electron attachment cross sections at ultralow electron energies. Its use as opposed to, for example, use of more accessible *GC/MS* or *HPLC/MS* methods, offers the possibility of good selectivity, free of interferences from other chemical species present in sea water

## II. EXPERIMENTAL

### Sediment Acquisition Procedure

A site off Rent Point in the Bedford Basin, adjacent to the ammunition-storage bunkers used by the Canadian Armed Forces was chosen for collection of the samples. Members of the Harbor Inspection Dive Team of the Canadian Armed Forces located, photographed, and acquired sediment samples at distances of between 6-12" from the UXO. The sediment-water slurry sample for each target was then returned to the surface to be labeled and frozen. The holding times of nitroaromatic and nitramine explosives in water have been studied extensively (3), and it is found that trace explosives can be up to 90 days provided the samples are stored in silanized containers and frozen immediately after collection.

### Explosives-Sediment Extraction Procedure

Considerable work has been carried out at several laboratories on characterizing the dissolution and extraction of explosives in seawater and ground soil (4). Based on these results, the extraction procedure was sonication of the sediment sample after the addition of methanol. After sonication the soil and liquid layers

were allowed to separate and the liquid layer pipetted into a separate glass beaker which was then vacuum desiccated. After desiccation was complete, water was added to each sample and the solution sonicated again. The extraction of explosives from the aqueous solution was effected by solid-phase microextraction (*SPME*) (5). The poly(dimethylsiloxane) divinylbenzene (PS-DVB) fiber used in the *SPME* has been found to have the highest relative efficiency of the commercially-available fibers for TNT extraction

Also, present within the collected sediment were numerous fragments of the propellent "cordite", typically composed of a mixture of nitrocellulose, nitroglycerin and lubricants. Because of the high selectivity of the *READ* detection system to TNT, RDX, PETN, no false positive results were found due to the cordite in the sediment.

**The READ System Used With SPME**

Details of the operation of the *READ* have been given elsewhere and its operation with explosives discussed (6-8). Briefly, the *READ* system uses the fact that the explosives molecules have an extremely large cross section for attaching zero-energy electrons. This cross section varies as (electron velocity)$^{-1}$. Hence the attachment rate (or ionization efficiency) is favored for slow electrons. Referring to the block diagram in Fig. 1, the *READ* system provides a large density of electrons with zero- and near-zero velocities by stopping and reversing, using a shaped electrostatic mirror, the current from an electron gun column. The analyte is introduced to this stopping region, and upon attachment each explosives type forms a characteristic negative-ion fragmentation pattern. Using a quadrupole mass spectrometer, the *READ* monitors one or more fragment peaks to detect the species, and with calibration to provide concentration levels. The explosives molecules are thermally desorbed from the *SPME* fiber by injection into an oven connected to the *READ* where the explosive vapors pass through the gas line into an adjustable jet separator and then into the *READ*.

**III. RESULTS AND DISCUSSION**

Shown in Fig. 2 is the time evolution of the fiber desorption where the mass peak $m/e$ = 167 $u$ of TNT is monitored. Typically, an *SPME* extraction of a sediment sample was sequentially analyzed with *SPME* extractions of a spiked sample of known concentration, then a seawater blank. The *SPME* results for the sediments collected near the Halifax UXOs are summarized in Table 1. The negative-ion signal detected by the

*SPME/READ* system as a function of calibrated samples of TNT in water is shown in Fig 3. A new READ device is currently undergoing testing which will improve the sensitivities by a factor of at least 100.

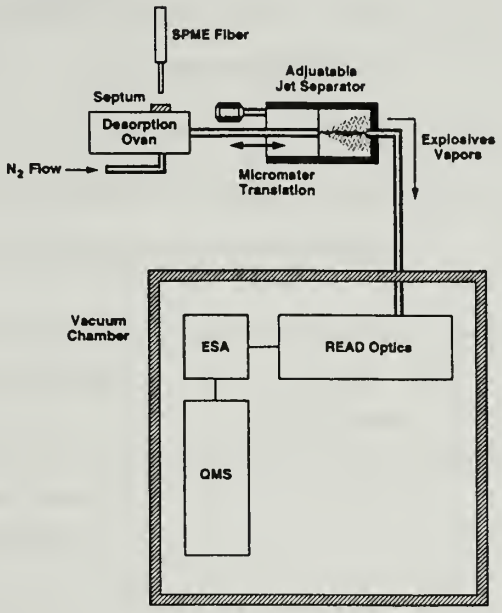


**Figure 1.** Schematic diagram of the *SPME/READ* system used in this study. Electron reversal and attachment, and ion extraction take place within the *READ* optics. The electrostatic analyzer (*ESA*) ensures the sign of charge by deflecting the negative ions after attachment in the *READ* optics to the quadrupole mass spectrometer (*QMS*).

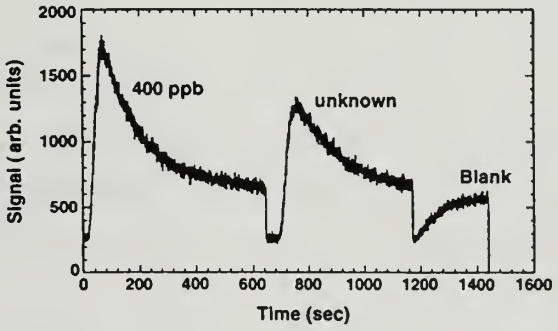


**Figure 2.** Display of the *SPME/READ* TNT negative-ion fragment signal at $m/e$ =167 $u$. Time is shown after injection of extractions from a 400 ppb standard TNT solution, a sediment-extraction sample of unknown concentration, and a blank.

As an independent test of the *SPME/READ* analysis, the solvent-extracted material from three different sediment samples were split and analyzed by *GC/MS* for the presence of trace TNT or DNT. The *GC/MS* results obtained from analysis of the sediments are also summarized in Table 1.

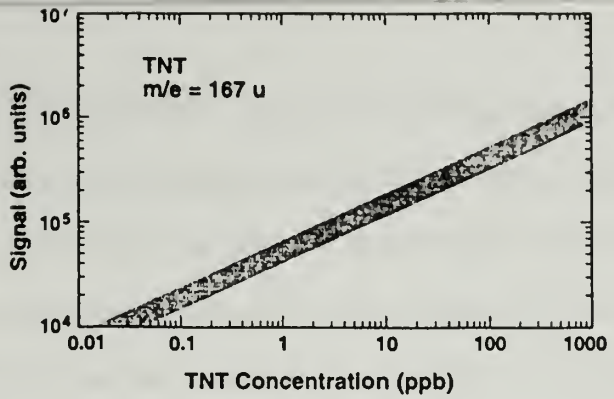


**Figure 3.** Sensitivity curve of the *SPME/READ* system to TNT concentration in. The shaded region represents the sensitivity, and its error, in determining the TNT concentration corresponding to the indicated signals.

| Target Number | Target Description | Sample Identification | Results |
|---|---|---|---|
| 1 | 5" shell, poor condition broken open | A, B, C, D | no explosives detected |
| 2 | 5" shell, very poor condition broken open | E, F, G, H | no explosives detected |
| 3 | 5" shell, good condition intact | I, J | no explosives detected (confirmed by *GC/MS*) |
| | | W, X | TNT detected at low ppb concentrations |
| 4 | 9" shell, semi-buried appeared intact | K, L | DNT detected at high pptr concentrations |
| | | M, N | no explosives detected |
| 5 | 5" shells, very poor condition broken open | O, P, Q, R | no explosives detected (confirmed by *GC/MS*) |
| 6 | 5" shell, semi-buried intact | T | DNT detected at low ppb concentrations (confirmed by *GC/MS*) |
| | | S, U, V | no explosives detected (confirmed by *GC/MS*) |

**Table 1. Summary of the SPME/READ Explosives Tests on Samples Collected at Halifax, Nova Scotia, Canada.**

In general, the results herein indicate that sediment collected near UXOs that visually appeared to be broken open showed *no* evidence for TNT. Samples near targets that appeared intact showed trace explosives

up to parts-per-billion concentration levels. For the intact rounds, positive results were found at only two of the four cardinal points, indicating a directionality to the source. *Intact* munitions appear to be releasing their contents as a slow leak, very likely through pinholes in the eroded casing, or through the screw threads linking the fuse assembly to the main charge. A prevalent, directed bottom current could assist this directionality. One may also presume from the detection results that, in the fifty years since the Halifax explosion, *broken* munitions have had their contents dissolved, reacted, biodegraded or even photodegraded. One may also conclude that trace explosives can very likely be detected at even *further distances* from a UXO, certainly with diminished concentration levels but well within present *SPME/READ* detection limits.

It is clear that in any UXO disposal strategy one would gain further information about a UXO site from chemical examination of the sea-bottom sediments. Hence the chemical information offers another diagnostic dimension which is quite orthogonal to that from optical, magnetometer, and sonar instruments which are presently being deployed for UXO detection and classification. Chemistry will be an important tool in any explosives-ordnance disposal strategy.

**Acknowledgements**

This work was performed at the Jet Propulsion Laboratory, California Institute of Technology, and was supported by the Office of Naval Research, and the Department of Defense/Strategic Environmental Research and Development Program through agreement with the National Aeronautics and Space Administration.

**References**

1. The MUDSS is a JPL-USN Coastal Systems Station collaboration sponsored under the Department of Defense/Strategic Environmental Research and Development Program (SERDP).
2. Fauth, M. I. *Determination of the Fate of Fragmented or Unexploded Munitions and Munitions Ingredients in the Environment*, DTIC AD-B120489(L) C.1 (1988).
3. Grant, C. L.; Jenkins, T. F.; Meyers, K. F.; McCormick, E. F. *Env. Toxic. Chem.* **1995,** *14*, 1865.
4. Bruggemann, E. E. *HPLC Analysis of SEX, HMX, TAX, RDX and TNT in Wastewater*; Army Medical Bioengineering R&D Lab, Report USAMBRDL-TR-8206; Fort Detrick, MD,1983.
5. Jenkins, T. F.; Miyares, P. H.; Meyers, K. F.; McCormick, E. F. *Anal. Chim. Acta* **1994**, *289*, 69.
6. Bernius, M. T.; Chutjian, A. *Anal. Chem.* **1990**, *62*, 1345.
7. Boumsellek, S.; Chutjian, A. *Anal. Chem.* **1992**, *64*, 2096.
8. Boumsellek, S.; Alajajian, S. H.; Chutjian, A. *J. Am. Soc. Mass Spectrom.* **1992**, *3*, 243.

# FIELDING TECHNOLOGY FAST
# THE KAHO`OLAWE MODEL

**By James D. Putnam**

**Abstract.** The Navy's $280 million ordnance clearance project of the island of Kaho`olawe has a strong focus on quickly incorporating new or improved technology into field operations. On a policy level recent reports by the Defense Science Board and the DOD Unexploded Ordnance Clearance and Remediation Contracting Integrated Process Team are critical of current practices within the DOD and benchmark the Kaho`olawe effort as the way to accelerate technology incorporation into a project. The Navy contract provides a non-traditional and innovative means for industry and research activities to demonstrate directly in the field new technologies. New ideas that provide production or quality improvements may be directly fielded.

The Department of Defense estimates that as much as 55 million acres on 2,100 formerly used defense sites (FUDS) and 130 installations identified for closure are potentially contaminated with unexploded ordnance.[1] If only 5% of the suspected acreage actually requires remediation with cleanup costs running up to $20,000 per acre (up to $45,000 in emergency situations), the total bill for the taxpayers is potentially astronomical. Estimates on the magnitude of the problem in the United States exceed $15 billion. I don't know what the acreage estimates of UXO contamination are on a global basis. When one considers that the United States has not been an active war zone this century (except on a very limited basis in Hawaii and Alaska) and UXO contamination is primarily from training, testing, and development ranges, the worldwide area contaminated must be staggering. Consider the amount of the European, Asian, and African landmasses that have been the sites of major armed conflict with attendant UXO left behind. The impact of the land mine is probably best depicted by estimates from the International Red Cross that 2000 people every month are injured or killed by landmines alone.[2] In the late 1980's I was the Navy construction contracting officer in Guam, and we frequently found World War II American and Japanese UXO during excavations. Much of this ordnance was still capable of high order detonation even after fifty years.

My small part of this national and international problem is a 29,000 acre island called Kaho`olawe. This Hawaiian island was used for fifty years as an active live-fire target range utilized by armed forces of the United States and many of our allies. Every type of conventional munitions in the DOD inventory was expended on Kaho`olawe from small arms to large bombs deliveried from land, sea, and air platforms.[3] The entire island is on the National Register of Historic Places and is considered a *wahi pana* or sacred place by Native Hawaiians.[4]

The island was first used by the military during World War II when the Territory of Hawaii was placed under martial law. In 1943 the first ordnance was exploded on the island as U.S. forces rehearsed the invasion of the Gilbert Islands. In 1953 President

Eisenhower took the island and gave control to the Navy by executive order with a proviso that it would be returned to the state in a "reasonably safe" condition for human habitation.[5] During the Korean War era, the range saw an increased use for air delivered general purpose bombs. In February 1965 five hundred tons of trinitrotoluene (TNT) were detonated on Kaho`olawe's southern shore to simulate a nuclear explosion for testing blast effects on guided missile equipment. The resulting crater, known as Sailor's Hat, has formed an aquatic ecosystem which has become a habitat for two endangered species of brine shrimp. The Vietnam period saw the entire island use as a range with mock airfields laid out for aerial bombardment and gunnery as well as targets for Naval and land fired artillery. The Army and Marines used the island for small unit tactics and weapons firing. In 1990 President George Bush issued a memorandum to discontinue use of Kaho`olawe as a weapons range.

In 1993 congress passed legislation which authorized transfer of the title to the island and the waters surrounding it for two miles back to the State of Hawaii.[6] This law provided for the "clearance or removal of unexploded ordnance" and environmental restoration of the island as required to assure "meaningful safe use of the island for appropriate cultural, historical, archaeological, and educational purposes as determined by the State of Hawaii." Finally, the law established a trust fund in the Treasury of the United States in an amount of $400 million that could be incrementally funded by congress. Of this amount 11% of any monies appropriated go to the State of Hawaii for island restoration.

After a $20 million model UXO project performed with an existing Pacific Division environmental remediation contract in 1995-1996 and four years of discussions and negotiations between the State of Hawaii and the Navy, a contract was awarded in July 1997. This contract to Parsons-UXB Joint Venture is for $280 million and includes in the scope ordnance detection, disposal, environmental remediation, construction, engineering, historic properties, and natural resource support.[7] This contract integrates the site investigation and ordnance disposal work where previous contracts generally separate the site study and the remediation. In other words, one contractor is responsible to the Navy for the full scope and range of site planning, ordnance detection, disposal, remediation, and closure. All contract site work must be completed by November 2003.

The contract has a number of innovative features that encourage early and expeditious implementation of new or improvements to existing technology. First, the contract is designed with a performance-oriented statement of work. The contract tells the contract what standard of cleanup is desired, it is, then, the contractor's responsibility to apply the appropriate technology to meet the standards. For this contract the Department of Defense Explosive Safety Board sets the standards. Desired detection levels are set at a minimum level of 85% probability of detection with a 90% confidence level consistent with terrain and overgrowth characteristics. Future land use as determined by the State of Hawaii and minimum size and depth of probably ordnance types set the clearance criteria standards.[8]

A second aspect of the contract that is innovative in ordnance clearance work is an award fee feature. This feature measures contractor performance against stated criteria that the Navy uses to determine the amount of award fee, or profit, the contractor receives. A key award fee criterion is introduction of new technology that will have a beneficial impact on cost, production, or quality of the work. The Navy opens the door to the contractor to be proactive, and will provide rewards, for bringing new or improved technology to the job. The basis for evaluation of any new technology is whether it will reduce cost (or increase production at the same cost), meet contract standards, meet production requirements (estimated at 5000 acres a year), be field deployable, and reliable. Any innovations will be field demonstrated and validated on Kaho`olawe or in conditions approximating Kaho`olawe. The Navy maintains an ordnance quality assurance range on the island, and the contractor has a demonstration range on Maui that may be used.

In the first year of the contract before ordnance clearance operations commenced on Kaho`olawe, one vendor demonstrated an upgrade to the currently contemplated detection platform, the Geonics EM-61. The vendor claimed the upgrade would increase the probability of detection and the confidence level. Testing by the contractor under field conditions showed that the upgrade would not meet contract standards. The point is that the door is open and if the upgrade had performed as claimed, it could be immediately incorporated into the contract.

Similarly, the Navy and the contractor are jointly pursing two initiatives with Sandia National Labs, one involving enhancements to the detection platform and attendant advanced signal processing, the other involving chemical detection. If either or both of these technologies are demonstrated as feasible and meet the guidelines mentioned above, they can be immediately incorporated into production or given to industry to provide a field useable unit (under a cooperative agreement or similar arrangement).

As project director for this effort my challenge is attempt to remove as much of the UXO on the island as possible. The budget is fixed and current estimates indicate that we should be able to perform surface clearance on 100% of the island and subsurface detection on perhaps 50%. This result would mean that significant portions of the island may have to be restricted as to future use and the state will be required to impose institution controls limiting access and use. Needless to say, politically this in an untenable situation with the Navy being criticized by State of Hawaii legislators, executive agencies and Native Hawaiian groups. We are looking to technology improvements to leverage project resources and allow us to increase production by reducing cost per acre.

From a field management perspective we see the largest problem as the false alarm rate (FAR) requiring field UXO disposal teams to excavate an unreasonable "empty holes." This problem is exacerbated on Kaho`olawe by the soil composition and geology. Kaho`olawe Island is a single volcanic dome composed of tholeiitic basalt base rock (containing up to 20% magnetite) covered by very diverse soil types. The quantity of magnetite in the basalt limits the functionality of conventional flux-gate and cesium

vapor magnetometers.[9] In addition, certain rocks were observed to produce a magnetic response that mimicked that of iron objects. The model project mentioned above field tested all families of currently fielded ordnance detection technologies with only time-domain EM meeting the probability of detection and confidence requirements of the contract. Terrain conductivity meters, flux-gate magnetometry, cesium-vapor magnetometry, and ground penetrating radar detection systems were all rated poor.[10]

The Defense Science Board recommends that the Department of Defense set as an objective the demonstration of a reduction in the false alarms by about a factor of ten within the next 3-5 years. The Board recommends an increase during this period the annual research and development budget to $20 million as being required to meet this goal.[11] Innovations to new, emerging, or existing technology are absolutely required if the goal of 100% UXO cleanup of Kaho`olawe is to be achieved. The contract facilitates faster incorporation of technology advancements and the contractor and the Navy are motivated to expedite any innovations which can be demonstrated to meet our guidelines. We look to the scientific community to help us solve our problem and have the largest funded UXO project in the United Sates to work with.

---

James D. Putnam works as the director, Pacific Contract Operations Division, Pacific Division, Naval Facilities Engineering Command, Pearl Harbor, Hawaii. He is the Pacific Division's project director for the Kaho`olawe ordnance cleanup directing technical and contracting staffs. He has a B.A. from DePauw University and a J.D. from the University of Iowa College of Law.

---

[1] **Report of the Unexploded Clearance and Remediation Contracting Integrated Process Team**, Office of the Deputy Undersecretary of Defense (Environmental Security).
[2] As reported in the **Report of the Defense Science Board Task Force on Unexploded Ordnance (UXO) Clearance, Active Range UXO Clearance, and Explosive Ordnance Disposal (EOD) Programs,** April 1998. Issued by the Office of the Under Secretary of Defense for Acquisition and Technology. [Hereinafter cited as DSB Report].
[3] **Cleanup Plan, UXO Clearance Project Kaho`olawe Island Reserve, Hawaii**, prepared for Contract N62742-95-D-1369 by Parsons-UXB Joint Venture, July 1998. [Hereinafter cited as Cleanup Plan]
[4] ibid.
[5] **Executive Order 10436** signed February 20,1953.
[6] **Title X of the Fiscal Year 1994 Department of Defense Appropriation Act** (PL 103-139, 107 Stat. 1418. 1479-1484).
[7] **Contract N62742-95-D-1369** awarded by the Pacific Division, Naval Facilities Engineering Command, Pear Harbor on July 29,1997.
[8] **Department of Defense (DOD) 6055.9-STD: DOD Ammunition and Explosives Safety Standards**, Chapter 12-Real Property Contaminated with Ammunition and Explosives, 19 June 1996.
[9] Cleanup Plan
[10] ibid.
[11] DSB Report

# Underwater Mine Detection Utilizing Gated Intensifier Shutters Synchronized with Laser Reflectance Images From Submersed Targets

Nicholas S.P. King, Kevin L. Albright, Robert A. Gallegos, Vanner Holmes,
Steven A.Jaramillo, Claudine R.Pena, Thomas E.McDonald Jr., George J. Yates

Los Alamos National Laboratory
Los Alamos, New Mexico

Bojan T. Turko
Lawerence Berkeley National Laboratory
Berkeley, California

William Snuggs, Mike Stephenov
Naval Coastal Systems Center
Panama City, Florida

Los Alamos National Laboratory (LANL) designed and developed a high repetition rate intensified shuttered CCD camera (ISCCD) for use in the United States Marine Corps Airborne Mine Detection and Surveillance (AMDAS) system initiated under the sponsorship of the Naval Coastal Systems Center. The camera system, designated LANL GY-6, was one of several key components of the AMDAS system which was designed to identify minefields in beach areas designated as potential landing zones for assault troops. The AMDAS concept is to raster the beach area with a pulsed 532nm laser beam and record time-phased reflectance images from stretegic locations/distances with a shuttered camera system operated as a real-time range-gated sensor to liminate/minimize noisy (atmospheric clutter, reflections, etc.) scene components in the laser flight path. The laser and camera are carried by a low-flying (approximately 1000 ft) high-speed (approximately 500 knots/hr) aircraft transmitting image data to remote recording media where the data are analysed with image recognition algorithims to determine absence or
presence of minefields in the rastered beach area. The GY-6 was designed for synchronous reset for synchronizing with the laser and subsequent continuous readout at 4000 frames per second (f/s) for sub-array of 125x125 pixels (or 1000 f/s for full array of 244x380 pixels), with ISCCD shutter capable of 5-10 ns exposures. The GY-6 design, electro-optic characterization data, and performance in laboratory/field experiments will
be presented.

# High Speed Cooled CCD Experiments

Claudine R. Pena, Kevin L. Albright, George J. Yates
Los Alamos National Laboratory

Experiments were conducted using cooled and intensified CCD cameras. Two different cameras were identically tested using different variables. Camera gain and dynamic range were measured by varying micro-channel plate voltages and controlling flux using neutral density (ND) filters to yield ADU values. A Xenon strobe (5us FWHM blue light 430nm) and a doubled Nd.yag laser (10ns FWHM green light 532nm) were both used as pulsed illumination sources for the cameras. Images were captured on PC desktop computer system using commercial software. Camera gain and integration time values were adjusted using camera software. Mean values of camera volts versus input flux were also obtained by performing line scans through regions of interest. Experiments and results will be discussed.

# Miniature, Sub-nanosecond Lasers for High-Speed Imaging

Fred J Zutavern, Wesley D. Helgeson, Martin W. O'Malley,
Alan Mar, and Guillermo M. Loubriel
Sandia National Laboratories, Albuquerque, New Mexico

George J. Yates, Robert A. Gallegos, and Thomas E. McDonald
Los Alamos National Laboratory, Los Alamos, New Mexico

High gain photoconductive switch (PCSS) technology is being employed to develop compact, high power, short-pulse lasers for high speed imaging applications. PCSS technology is being used in two distinct ways: (1) to inject short current pulses directly into semiconductor lasers (short pulse pumping), and (2) to drive electro-optical components which control the pulse width and timing of lasers that are pumped with long current pulses (greater than 100 ns). Arrays of wide-strip, single heterojunction lasers are readily gain-switched when pumped with a short, high-voltage pulse from a high gain PCSS. Under conditions that optimize peak power, the individual lasers in the array deliver approximately 100 nJ in 75 ps wide pulses. For example, we have produced 44 microjoules with an array of 500 lasers and 2 microjoules with an array of 20 lasers. The PCSS-driven laser diode array is a very compact and reliable system which may be appropriate for many types of applications. The entire system is powered by a standard 9V battery and can be held in the palm of a hand. On the other hand, even higher energies can be obtained by mode-locking or Q-switching long pulse pumped lasers. High speed Pockels cell drivers are used for Q-switches, pulse selectors, and regenerative amplifiers in more conventional types of short pulse lasers. PCSS have demonstrated 350 ps rise time and 50 ps rms jitter and voltage stand-off above 100 kV. PCSS driven Pockels cells have the additional convenience of optical triggering which is critical for low jitter applications in noisy electrical environments. The test results of a reduced jitter 8 kV Pockels cell driver for laser triggering will be presented. Other properties of high gain GaAs PCSS such as lifetime, repetition rate (1-10 kHz), and optical triggering requirements (5-200 nanojoules) will also be described. PCSS longevity continues to improve with GaAs contact research and development. At present we have tested switches which have lasted 5(107 pulses at 10 A and 2(106 pulses at 80 A. The p-contact, which has limited switch lifetime in the past, was dramatically improved with a new process for GaAs. We are presently developing a similar process for the n-contact which should lead to further increases in device lifetime.

Fred J Zutavern
Dept. 9323, MS 1153
PO Box 5800 (Shipping: 1515 Eubank SE)
Sandia National Laboratories
Albuquerque, NM 87185-1153 (Shipping: 87123)
505-845-9128, fax 845-3651
Email: fjzutav@sandia.gov
SNL location: Kirtland AFB, Area IV, Bldg 962, room 2423, lab 2224

# Externally Rendered Objects (EROs)

Augusto Op den Bosch, Ph.D.
Senior Research Engineer
And
Adrian Ferrier
Research Engineer
Spectra Precision Software, Inc.

**E**xternally **R**endered **O**bjects (EROs) were originally conceived to allow a **V**irtual **E**nvironment **A**pplication (VEA) to display vehicles that have external dependencies. An example of such a vehicle is an ROV (remotely operated vehicle, e.g. a submarine). Without the ERO technology, a VEA would have to be reprogrammed for each new type of object or vehicle that needed to be displayed and controlled. Our solution is to place the smarts needed to control and display this type of object outside the VEA and to provide a common access methodology.

An ERO is an independent self-contained and dynamic vehicle that can exist as a guest in a VEA. The location and behavior of an ERO is outside the control of the VEA in which it exists. In addition, an ERO is in charge of defining its own 3-D representation and appearance. The ERO may or may not have its own user interface. The minimum requirement for an ERO is to have a view independent 3-D rendering scheme.

EROs have unique properties that make them very powerful and versatile. An ERO can be dynamically inserted into a live VEA. This takes place without the environment having any prior knowledge of the ERO. Both VEA and ERO can exist without the other. An ERO can be created before the VEA is launched and can continue to operate after the VEA is terminated. The behavior of an ERO can be controlled by an additional application that may or may not have anything to do with the VEA where the ERO is being displayed. The same ERO can be inserted into multiple VEAs. A VEA can load multiple EROS. In addition, multiple applications can control the same ERO or a single application can control multiple EROS.

All these properties make the ERO technology an ideal choice for tracking and visualizing real vehicles in a virtual sub sea environment. For each real object, a corresponding ERO will be in charge of collecting and displaying all the relevant information of itself in a host environment. This host environment can be setup to load the corresponding bathimetry or topology surface data along with additional static objects that can enhance the scene.

This paper will describe the principles associated with the design and implementation of EROs. Examples of ERO applications, with an emphasis on underwater vehicle tracking, will also be presented.

# Range Gating Experiments through a Scattering Media.

Jeremy Payton, Frank Cverna, Robert Gallegos, Tom McDonald, Dustin Numkena,

Andy Obst, Claudine Pena-Abeyta, George Yates

Los Alamos National Laboratory

This paper discusses range-gated imaging experiments performed recently at Redstone Arsenal in Huntsville Alabama. Range gating is an imaging technique that uses a laser and camera to image objects through scattering media such as dense smoke or fog. Range gating uses the fact that the speed of light travels at $3*10^8$m/s. Using this principle we can calculate the time it will take the laser light to travel a known distance, then provide a trigger so that an optical shutter utilizing a gated Micro Channel Plate Image Intensifier (MCPII) opens when the reflected light returns from the target. The gate width on the MCPII was set to equal the laser pulse width (~8ns) for the highest signal to noise ratio. The gate allows the light reflected from the target and a small portion of the light reflected from the smoke in the vicinity of the target to be imaged. We obtained good results in light and medium smoke but the laser we were using did not have sufficient intensity to penetrate the thickest smoke. We did not diverge the laser beam to cover the entire target in order to maintain a high flux that would achieve better penetration through the smoke. We were able to image an Armored Personnel Carrier (APC) through light and medium smoke but we were not able to image the APC through heavy smoke. The experiment and results will be presented.

# RULLI; A Photon Counting Imager

Kevin L. Albright, Clayton Smith, and Cheng Ho

RULLI is an acronym for Remote Ultra-Low Light Imager. The system responds to individual photons using a modification to conventional image intensifier technology and very fast TIM (time interval meter) electronics. Each photon received at the detector is resolved in three dimensions (X,Y, and time). The accumulation of photons over time allows the system to image with very low light levels such as starlight illumination. Using a low power pulsed laser and very fine time discrimination, three dimensional imaging can be accomplished with vertical resolution of a few cm.

# Using Optical Parametric Oscillators (OPO) for Wavelength Shifting IR Images to Visible Spectrum

Dustin M. Numkena, Thomas E. McDonald Jr., Jeremy Payton, George J. Yates

Los Alamos National Laboratory

Paul Zagarino

Sharpenit

We have concluded preliminary investigations into coherent imaging using Optical Parametric Oscillators (OPO) for wavelength conversion of near IR images to visible spectrum. A nonlinear crystal, second harmonic generator (SHG), was used for degenerate optical parametric up-conversion. A Potassium Titanyl Phosphate (KTP) doubling crystal was used to convert incident 1540nm flux to 772nm. Experiments included investigation of spatial resolution and responsivity of the OPO. Spatial resolution of 3-1/2 lp/mm was attained with reasonable CTF in both horizontal and vertical axis. Measured responsivity for this OPO configuration compared well with that attained from image intensifier-based systems. Equipment used for this experiment included an ORION SB2-2R pulsed solid state laser used as a light source and a CCD camera/frame grabber to capture and record all data. The experiment and results will be discussed.

# Electron Bombarded CCD Imagers for Commercial and Military Systems

Eric Howard
Silicon Mountain Design

Due to recent process advances, Electron Bombarded CCD (EBCCD) imagers are now viable low-light imaging solutions in both commercial and military markets. While there are many similarities between the two markets, each still has certain aspects that must be addressed in the system design of an EBCCD camera. Some of the results of our imager characterization are presented along with a discussion of the tradeoffs between designing low light imaging systems for the commercial and military markets.

Eric Howard
Silicon Mountain Design
5055 Corporate Plaza Dr. Suite 100
Colorado Springs, CO 80919
(719) 599-7700
(719) 599-7775 fax
ehoward@smd.com

# Camera System for High-Frame Rate Applications

George J. Yates, Thomas E. McDonald, Jr., and N. S. P. King
Los Alamos National Laboratory, Los Alamos, NM, USA

Bojan T. Turko
Lawrence Berkeley National Laboratory

A CCD camera system having a high-frame rate and fast shutter capability is being developed by the Los Alamos National Laboratory for the imaging of dynamic phenomena. The CCD pixel array size is 512x512 and has 16 parallel output ports. With a 75 MHz per port pixel clock rate the camera frame rate can reach up to 3500 frames per second. A microchennel plate image intensifier provides gain for low light applications and also provides camera gating. The intensifier can achieve sub-nanosecond gating by incorporating a strip line electrical geometry that provides impedance matching to reduce pulse reflections and dispersion. A computer controlled frame grabber records data from the digital output and stores the data in a local memory for transfer into a non-volatile storage medium such as removable disk drives. The imaging system and potential applications will be discussed.

# Digital Memory for a 16-port CCD Camera Readout at 40 MHz Pixel Rates

B.T. Turko,** N.S.P. King,* T. McDonald,* J. Millaud** and G.J. Yates*
(*Los Alamos National Laboratory; **Lawrence Berkeley National Laboratory)

A 16-port very high frame rate CCD camera, developed at the Los Alamos National Laboratory, requires a custom designed digital memory. We describe a modular memory capable of supporting a variety of multi-port CCD sensors. The LANL camera, using EG&G/Reticon, Inc. HS0512J sensor, makes 512x512 pixel video frames split into 16 segments. Each segment is served by an individual video channel. The segment format is 256 video lines of 64 pixels each, digitized in 10-bit words. Combined, the data make 160-bit wide words, sent to the memory for storage at the rates of up to 40 MSPS. The distance between the camera and the memory should exceed 50 feet.

In order to achieve a flexible, expandable system, the memory is split into two modules serving eight video ports each. Each module has four slots for RAM boards. A single RAM board capacity is eight frames. With all slots occupied, the memory can store up to 32 frames. A programming logic controls the memory modules, either one alone or the two combined together, depending on how many video ports are configured. The memory operates either in a write mode or in a read mode.

Data write mode.

The camera normally operates continually, sending data, the vertical and horizontal synchronization pulses and the pixel clock signal to the memory. An ARM signal from computer is sent before the commencing the recording in order to enable the write mode. Upon the FIDU command from the camera operation logic, the memory will start storing video frames until full.

Data readout mode.

Prior to data readout the computer has to download the address of the frame and/or its segment to be read out. The data is read out serially in 10-bit words, each one representing the signal magnitude of an individual pixel. The rate is dependent on the read clock rate sent by the computer. Each clock pulse stores the addressed pixel's data into the P.C. memory. Its trailing edge advances the pixel address. The number of clock pulses defines the number of consecutive video frames and/or sections read out.

Before using the memory in either mode, parameters pertinent to the video format of the CCD camera must be entered. These include the number of lines per frame, number of pixels per line and the number of frames to be recorded. During the period between the lines the recording stops in order to save memory space. However, due to the data latency in A/D converters of the CCD camera, the write cycle must be extended beyond the video line by several pixel clock pulses. The ADC latency is thus also one of parameters to be entered.

In preliminary tests the data was transferred from camera to the memory over 70 feet long twisted pair cables at up to 50 MHz pixel clock frequency. Relatively low cost and flexibility in adapting this memory to a number of different high-speed digital CCD cameras makes it a useful tool in many applications.

# A Method for Transmitting High Frame Rate Video Data to Remote Locations

Ernest L Brunholzl, Field Engineering Acqiris, Albuquerque, NM
Victor Hungerbueller, Engineering Manager, Acqiris SA, Geneva, Switzerland

High resolution, high frame rate video applications typically have an overabundance of data to forward on to other locations. This problem manifests itself throughout the system, starting with the high speed A/D converter that is necessary for capturing the camera data and on through the processing end transmission systems.
Acqiris is taking a different approach, recognizing that large memory capture alone is not enough. By incorporating a fast real time processor immediately following the A/D converter, many functions can be accomplished in real time, prior to data storage, processing and transmission. This method can significantly improve data quality and greatly reduce the amount of data for subsequent transmission.

# Underwater Mine Detection Utilizing Gated Intensifier Shutters Synchronized with Laser Reflectance Images from Submersed Targets

**Nicholas S.P. King, Kevin L. Albright, Robert A. Gallegos, Vanner Holmes, Steven A.Jaramillo, Claudine R.Pena, Thomas E.McDonald Jr., George J. Yates**

Los Alamos National Laboratory
Los Alamos, New Mexico

**Bojan T. Turko**
Lawerence Berkeley National Laboratory
Berkeley, California

**William Snuggs, Mike Stephenov**
Naval Coastal Systems Center
Panama City, Florida

## ABSTRACT

Los Alamos National Laboratory (LANL) designed and developed a high repetition rate intensified shuttered CCD camera (ISCCD) for use in the United States Marine Corps Airborne Mine Detection and Surveillance (AMDAS) system, which was initiated under the sponsorship of the Naval Coastal Systems Center. The camera system, designated LANL GY-5/6, was one of several key components of the AMDAS system, which was designed to identify minefields in beach areas designated as potential landing zones for assault troops. The AMDAS concept is to raster the beach area with a pulsed 532nm laser beam and record time-phased reflectance images from strategic locations/distances with a shuttered camera system operated as a real-time range-gated sensor to eliminate/minimize noisy (atmospheric clutter, reflections, etc.) scene components in the laser flight path. The laser and camera are carried by a low-flying (approximately 1000 ft) high-speed (approximately 500 knots/hr) aircraft transmitting image data to remote recording media where the data are analyzed with image recognition algorithms to determine absence or presence of minefields in the rastered beach area. The GY-5/6 was designed for asynchronous reset for synchronizing with the laser and subsequent continuous readout at 4000 frames per second (f/s) for sub-array of 128 x 128 pixels (or 1000 f/s for full array of 244x380 pixels), with ISCCD shutter capable of 5-10 ns exposures. The GY-5/6 design, electro-optic characterization data, and performance in laboratory/field experiments are presented.

## BACKGROUND

The purpose of AMDAS and follow on programs such as Mine Detection Laser Technology (MDLT) and Magic Lantern Adaptation (MLA) is to use pulsed lasers and fast optical shutters in a range-gated LADAR configuration to search for and detect and identify hidden minefields in beach areas where Marine Corp troops are expected to be deployed. The successful identification of minefield locations can prevent troop casualties by either destroying the mines prior to troop landing or by selecting alternative mine-free locations confirmed by the LADAR.

The system concept for AMDAS is shown in figure 1. An airborne laser rasters the region of beach intended for Marine Corp troop landing. The illuminated beach region is imaged by reflected laser light relayed onto an intensified/shuttered CCD camera that is also airborne. The intensifier is gated to record images from strategic depths corresponding to suspect mine field deployment. The images are telemetered to a shipboard base station where they are processed to determine the presence of minefields. Because of the size of mines and extent of the minefield, the large area coverage, and optical scene clutter in the laser beam's flight path, the image data rate is too high for real-time manual operator detection and classification. Therefore, computers are required for data storage and image processing of the images.

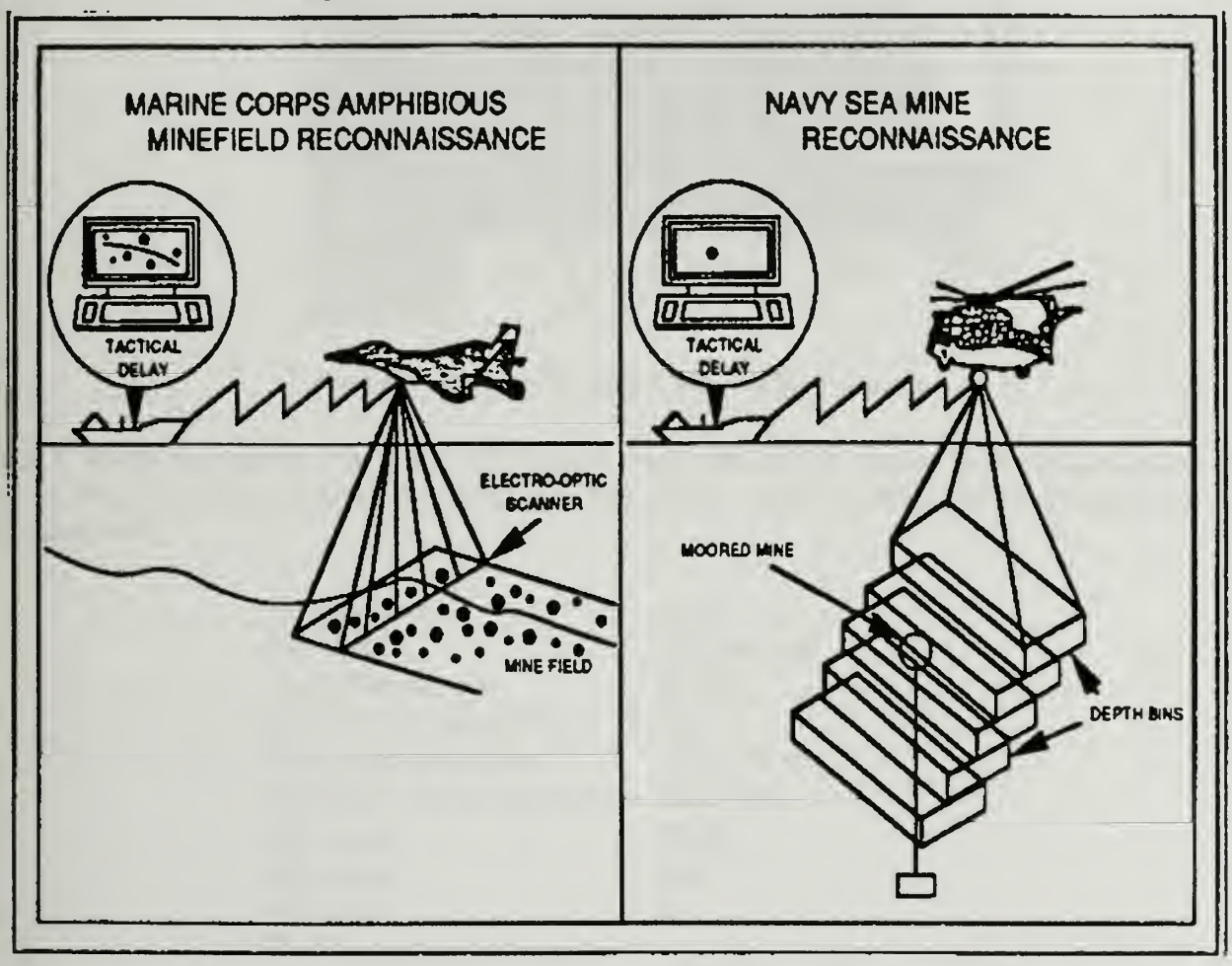


Figure 1. Navy/Marine Corps operational system concept of the AMDAS program.

## BASIC CAMERA DESIGN

The GY-5/6 camera is a single port CCD camera designed for high-speed readout (reference 1). The CCD is a Fairchild model 222 Inter-Line Transfer (ITL) CCD, with 244 x 380 pixels. The CCD is fiber optically coupled to an ITT model F4111 Generation II microchannel plate (MCP) image intensifier (MCPII) for shuttering (reference 2). The MCPII is modified according to Los Alamos National Laboratory design specifications, which include (1) electrically conductive but optically transmissive nickel undercoating of the S-20 photocathode to permit gating/shuttering in the few nanosecond

regime, and (2) high strip current MCP and short persistence P-48 phosphor to allow high repetition rate operation for compatibility with the fastest CCD readout rate of 4KHz. The GY-5/6 camera package is shown in figure 2, and measured responsivity data are given in Table 1.

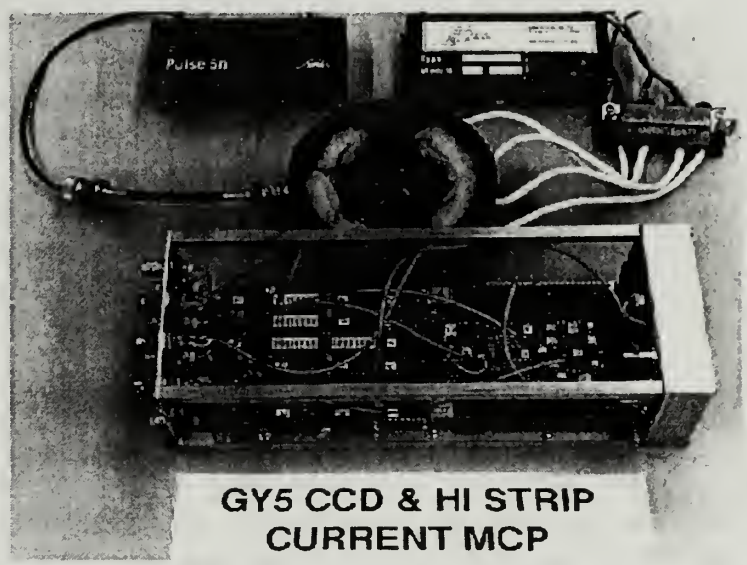


Figure 2. Photograph of GY 5/6 AMDAS camera.

Table 1. Measured responsivity of GY-5/6 camera. The MCPII/CCD coupled response per unit area as well as the single pixel response to "delta" function light source from 10ns FWHM 532nm laser pulse are tabulated.

| | |
|---|---|
| Area illuminated: | 16 $mm^2$ |
| Pixel area: | 1080 $micron^2$ |
| Pixels illuminated: | 14,815 |
| Photosite area/pixel area: | 20% |
| Peak power/photosite: | 1.36 E-15 W |
| Equivalent energy/photosite: | 1.36 E-17J |
| CCD signal: | 25mV |
| CCD noise: | 5mV |
| CCD S/N: | 5:1 |
| GY-5/6 sensitivity threshold: | |
| | 2.72 E-10 W/photosite (power/pulse) |
| | 2.72 E-18 J/photosite |
| | 1.25 E-12 J/cm sqd |

## THE AMDAS CONFIGURATION

The principal AMDAS requirements are found in Table 2. The camera system required the use of four (4) 1KHz GY-5/6 cameras to accomplish the 4KHz rate, by time phasing of MCPII shutter openings and CCD readouts in a "Gatling Gun" arrangement. The system block diagram is in figure 3, and it's associated timing diagram in figure 4.

Table 2. Principal requirements for the AMDAS camera.

| | |
|---|---|
| Image pixelization | 256 x 256 pixels |
| Frame rate | 3000 to 4000 f/s |
| Optical shutter time | 5ns to 5 microsec |
| System pixel rates | 200 to 290 Mpixels/s |
| Dynamic range | 10-bits Interscene |
| | 8-bits Intrascene |
| Noise-equivalent radiance | 20 photons/pixel |
| Inter-frame image lag | 5% |
| Data output | analog: 1.5V/50 ohms |
| | digital: 8-bits parallel |

## PRELIMINARY FIELD EXPERIMENTS

The first series of field tests were performed in a controlled seawater environment "tank" constructed at EG&G Santa Barbara Ca. Targets were submersed at different depths and water turbidity factors varied. A probe laser provided pulses of 532nm light in the few nanosecond FWHM range and the GY-6 MCPII shutters were synchronized to open properly time-phased and only long enough to record reflectance images from specific target location depths in the tank. In this manner, the GY-5/6 sensitivity and resolution were calibrated in environments similar to those expected in "pier" tests in actual/real ocean-based experiments where mine field decoys and related targets were to be imaged. Both series of tests were conducted using only one GY-5/6 camera. The setup for the "tank" tests and some data are shown in figure 5. Some of data is shown in figure 6.

## REFERENCES


1. G.J. Yates, N.S.P. King, "High-frame-rate intensified fast optically shuttered TV cameras with selected imaging applications", (invited paper) SPIE, Vol. 2273-26, Ultrahigh- and High-Speed Photography, Videography, and Photonics Conference, San Diego, CA, July 24-29, 1994.

2. N.S.P. King et al, "Nanosecond Gating Properties of Proximity-Focused Microchannel-Plate Image Intensities", Los Alamos Conference on Optics, SPIE Vol. 288, pp. 426-433, April 7-10, 1981, Santa Fe, New Mexico.

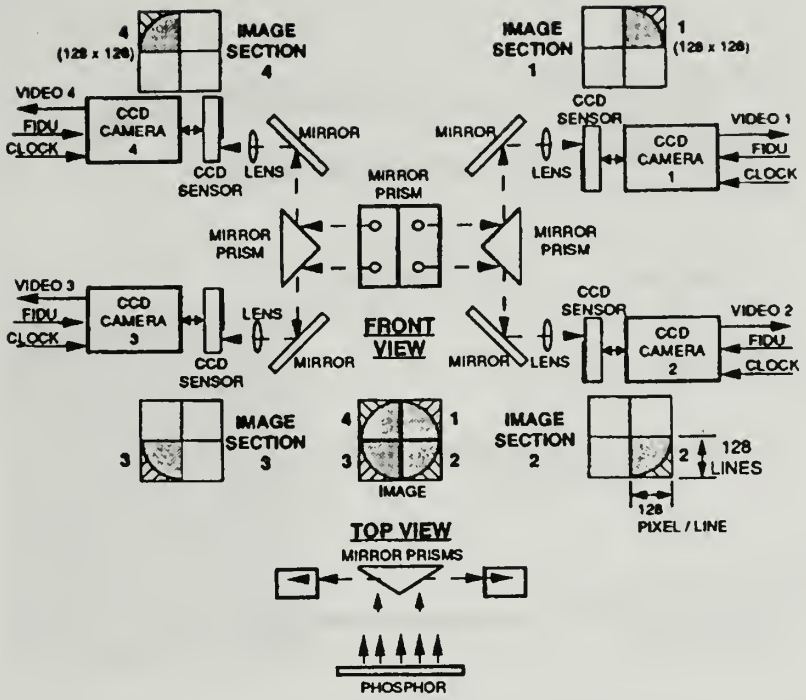


Figure 3. AMDAS system block diagram.

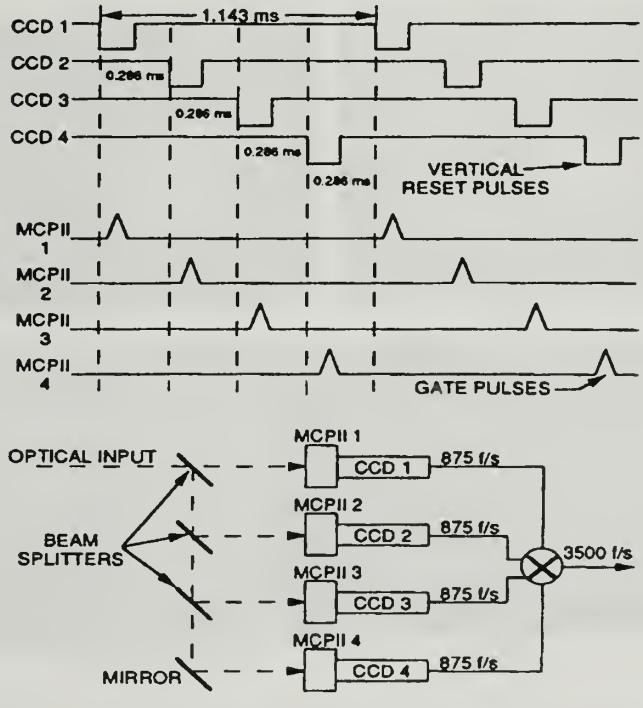


Figure 4. Block and timing diagram for gatling gun system.

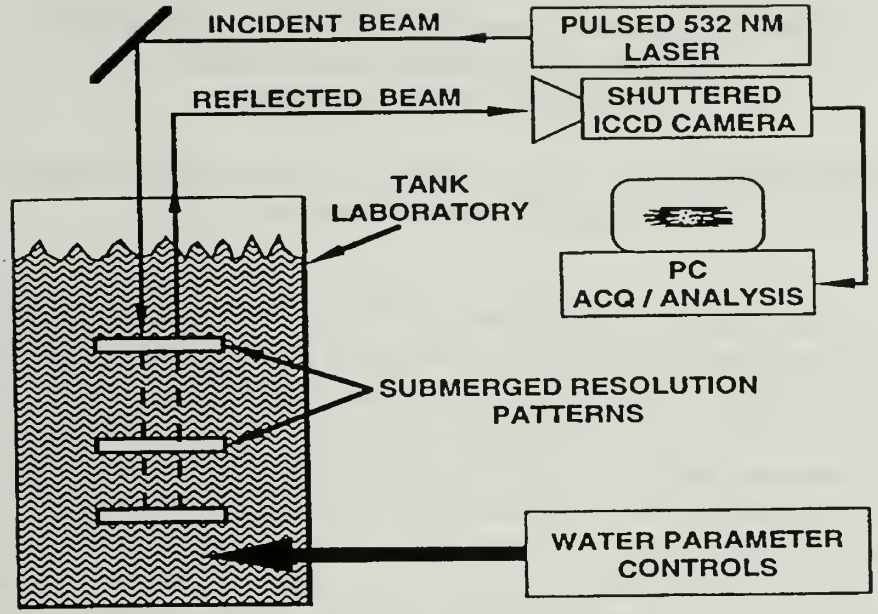


Figure 5. Simplified experiment diagram for depth profile imaging for Mine Detection Studies.

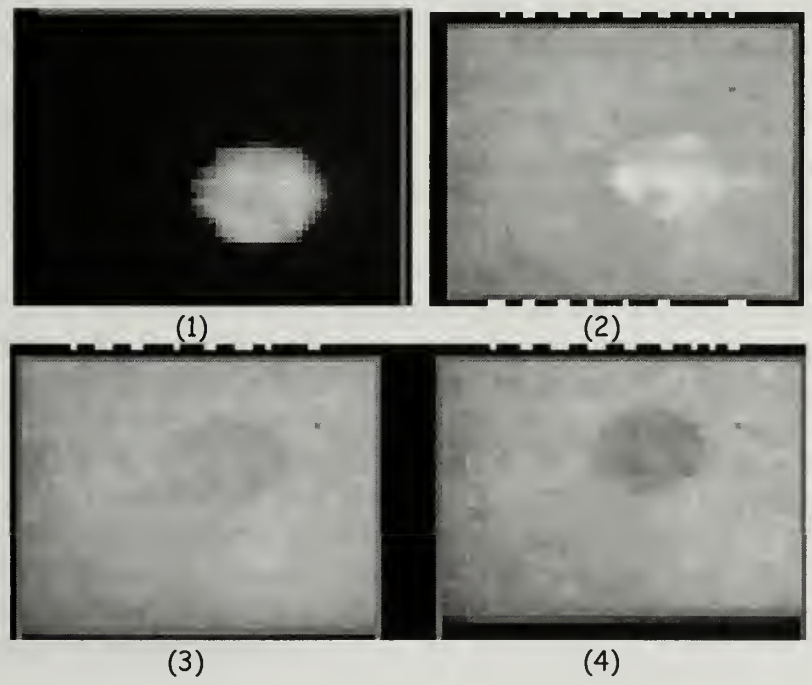


Figure 6. Images obtained using LANL GY-6 gated image intensifier shutters to image reflected laser images from submerged pattern (black glossy disk) in the EG&G/SBO Tank are in (b) for the disk imaged in air (1) and at depths 1.4 meters (2), 5.6 meters (3), 7.0 meters (4) in the Tank under constant water turbidity (not quantified here).

# Miniature, Sub-nanosecond Lasers for High-Speed Imaging

**Fred J Zutavern, Wesley D. Helgeson, Martin W. O'Malley,
Alan Mar, and Guillermo M. Loubriel
Sandia National Laboratories**

**George J. Yates, Robert A. Gallegos, and Thomas E. McDonald
Los Alamos National Laboratory**

High gain photoconductive switch (PCSS) technology is being employed to develop compact, high power, short-pulse lasers for high speed imaging applications. PCSS technology is being used in two distinct ways: (1) to inject short current pulses directly into semiconductor lasers (short pulse pumping), and (2) to drive electro-optical components which control the pulse width and timing of lasers that are pumped with long current pulses (greater than 100 ns). Arrays of wide-strip, single heterojunction lasers are readily gain-switched when pumped with a short, high-voltage pulse from a high gain PCSS. Under conditions that optimize peak power, the individual lasers in the array deliver approximately 100 nJ in 75 ps wide pulses. For example, we have produced 44 microjoules with an array of 500 lasers and 2 microjoules with an array of 20 lasers. The PCSS-driven laser diode array is a very compact and reliable system, which may be appropriate for many types of applications. The entire system is powered by a standard 9V battery and can be held in the palm of a hand. On the other hand, even higher energies can be obtained by mode-locking or Q-switching long pulse pumped lasers. High speed Pockels cell drivers are used for Q-switches, pulse selectors, and regenerative amplifiers in more conventional types of short pulse lasers. PCSS have demonstrated 350 ps rise time and 50 ps rms jitter and voltage stand-off above 100 kV. PCSS driven Pockels cells have the additional convenience of optical triggering which is critical for low jitter applications in noisy electrical environments. The test results of a reduced jitter 8 kV Pockels cell driver for laser triggering will be presented. Other properties of high gain GaAs PCSS such as lifetime, repetition rate (1-10 kHz), and optical triggering requirements (5-200 nanojoules) will also be described. PCSS longevity continues to improve with GaAs contact research and development. At present we have tested switches which have lasted 5(107 pulses at 10 A and 2(106 pulses at 80 A. The p-contact, which has limited switch lifetime in the past, was dramatically improved with a new process for GaAs. We are presently developing a similar process for the n-contact which should lead to further increases in device lifetime.

# EXTERNALLY RENDERED OBJECTS (EROS)

By:

Augusto Op den Bosch
Senior Research Engineer
Spectra Precision Software, Inc.

Adrian Ferrier
Research Engineer
Spectra Precision Software, Inc.

## ABSTRACT

**E**xternally **R**endered **O**bjects (EROs) were originally conceived to allow a **V**irtual **E**nvironment **A**pplication (VEA) to display vehicles that have external dependencies. An example of such a vehicle is an ROV (remotely operated vehicle, e.g., a submarine). Without the ERO technology, a VEA would have to be reprogrammed for each new type of object or vehicle that needed to be displayed and controlled. Our solution is to place the smarts needed to control and display this type of object outside the VEA and to provide a common access methodology.

An ERO is an independent, self-contained, and dynamic vehicle that can exist as a guest in a VEA. The location and behavior of an ERO is outside the control of the VEA in which it exists. In addition, an ERO is in charge of defining its own 3-D representation and appearance. The ERO may or may not have its own user interface. The minimum requirement for an ERO is to have a view independent 3-D rendering scheme.

EROs have unique properties that make them very powerful and versatile. An ERO can be dynamically inserted into a live VEA. This takes place without the environment having any prior knowledge of the ERO. Both VEA and ERO can exist without the other. An ERO can be created before the VEA is launched and can continue to operate after the VEA is terminated. The behavior of an ERO can be controlled by an additional application that may or may not have anything to do with the VEA where the ERO is being displayed. The same ERO can be inserted into multiple VEAs. A VEA can load multiple EROs. In addition, multiple applications can control the same ERO or a single application can control multiple EROs.

All these properties make the ERO technology an ideal choice for tracking and visualizing real vehicles in a virtual sub-sea environment. For each real object, a corresponding ERO will be in charge of collecting and displaying all the relevant information of itself in a host environment. This host environment can be setup to load the corresponding bathymetry or topology surface data along with additional static objects that can enhance the scene.

This paper will describe the principles associated with the design and implementation of EROs. Examples of ERO applications, with an emphasis on underwater vehicle tracking, will also be presented.

*Note: Spectra Precision Software Inc. has a patent pending on the ERO technology.*

# INTRODUCTION

The development of the ERO technology was motivated by the need to have dynamic elements in a VEA. These elements are dynamic in two senses. First of all, both the geometric and the behavioral components of the element are defined outside the VEA. Secondly, these elements have lifetimes independent of the VEA. Dynamic ERO elements can be plugged into the VEA during runtime as needed.

There have been attempts in recent years to provide users with "customizable" VEAs [1,2,3]. These high level Libraries, Toolkits, or Applications sit on top of graphic libraries such as OpenGL [4] in order to facilitate the creation of VEAs. Typically, the task of defining the objects that perform in an environment can be divided into two categories: Appearance and Behavioral Definition. Typically, object appearance is defined outside the VEA through the use of a variety of geometric formats such as VRML, DXF and 3D Studio in their corresponding editors. The definition of behavior, however, is more complex as it has no commonly accepted format.

A simple approach to capturing object behavior is to directly code the behavior in the VEA [2,5,6]. The problem with this approach is its rigidity. Any change will involve updating the source code of the VEA. An alternate method involves the use of complex communication protocols [7] to allow an external application (i.e., simulation engine) to transmit an object's state information to a VEA for visualization. This approach is also problematic because general object behavior tends to be too complex for a description protocol to fully capture it. In addition, VEA and object parser development are complicated by the many required rules of a rich protocol. In other words, implementing simple objects is hindered by the large required protocol set and the implementation of complex objects is hindered by limitations in statically defined behaviors.

Additional scenarios exist where the geometry of virtual objects is driven by behavior. When geometry is altered due to behavior, the approaches outlined above fail to perform. Objects with dynamic geometry (e.g., waving flags, altered ground surfaces, and running water) are typically handled as special cases that end up breaking the code or raising special exceptions in a protocol.

We propose that the description of the behavior and the geometry of a virtual object should be contained and then accessed in a generic way by the VEA. The entire definition of the object is external to the VEA and remains completely flexible and modular. The following section explains how to design these types of objects, as well as a VEA capable of hosting dynamic, self-defining, external objects.

# TECHNOLOGY

## *VEA Overview*

The basic rendering cycle of most VEAs can be represented by a simple diagram (Figure 1). First, user input is captured. Second, some amount of processing or parsing is required to update the state of the objects in the system. Then, the viewing transformations are introduced. Lastly the scene is rendered.

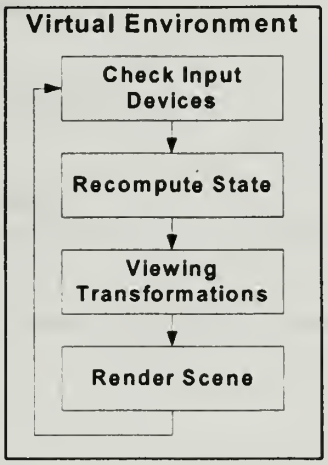


**Figure 1: The Basic VEA Rendering Loop**

The actual rendering process takes place through a series of function calls. These functions can be implemented within the application itself, although this is not a requirement. Typically, rendering functions are in dynamically linked libraries (DLLs) such as OpenGL that can be accessed by the VEA at run time.

An ERO expands this basic VEA template by acting just like a DLL. An ERO provides some standardized interfaces that allow the VEA to access its rendering routines. Using this scheme, an ERO acts like a plug-in component. There are many examples of commercial systems that use similar concepts to modularize, customize, and expand functionality. Plug-ins used by web browsers are good examples of externally developed elements that can be accepted by a host system through a common published interface. Some plug-ins can even perform 3-D rendering, and some are virtual environments themselves (e.g., Cosmos VRML plug-in). However, what sets EROs apart from general plug-in technologies is the fact that none of these concepts can render 3-D objects inside a VEA while simultaneously interacting with other applications.

## *VEA/ERO System Architecture*

This section will present the architecture of a VEA capable of loading, initializing, and rendering EROs. The VEA/ERO interface details will be discussed in the next section.

Figure 2 shows the execution of a rendering cycle containing a very basic ERO. This architecture is only adequate for *Inert EROs* (e.g., buildings, backgrounds, trees, etc.). If the EROs internal state changes then the VEA will only display the change on the next rendering cycle. The changes in the ERO will not be apparent until the environment is forced to refresh. This is common in modern event driven systems where an idle loop is executed until the program receives user input.

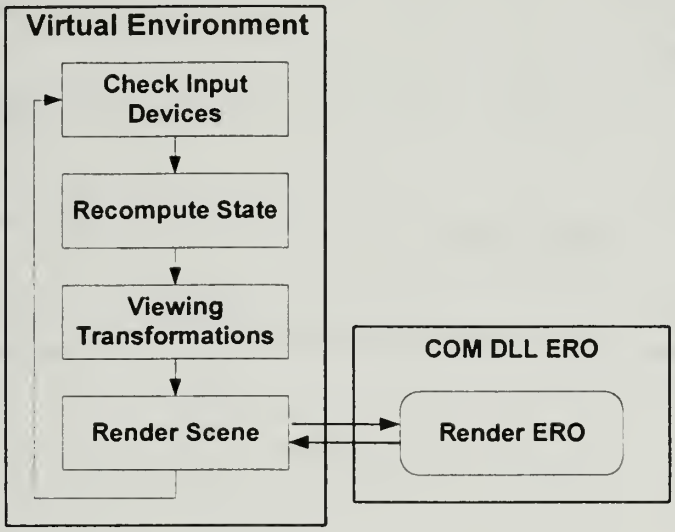


**Figure 2: An Inert ERO Member**

A less passive approach is illustrated in Figure 3, where an ERO can notify the VEA that its state has changed and trigger an environment refresh. The system will drop out of the idle loop and update the scene. EROs that are geometrically *self generating* can be supported by this architecture.

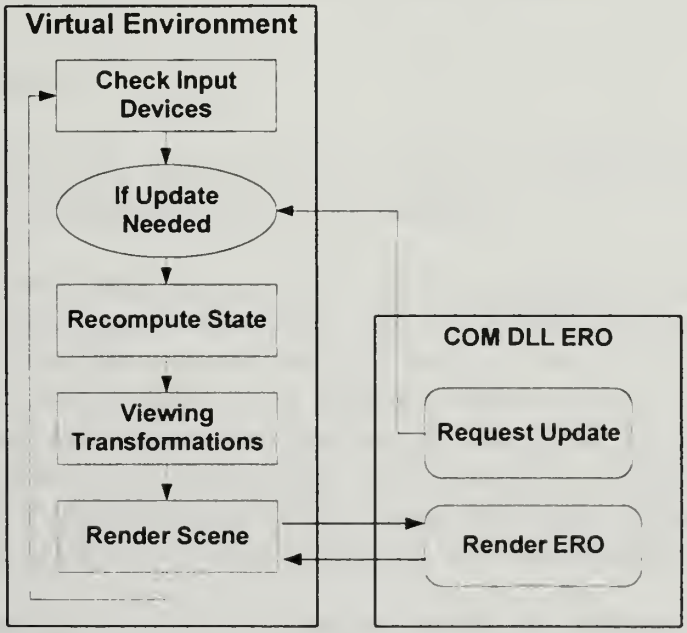


**Figure 3: An Active ERO Member**

This approach is sufficient for simple EROs and can be expanded to support *controlled* EROs as shown in Figure 4.

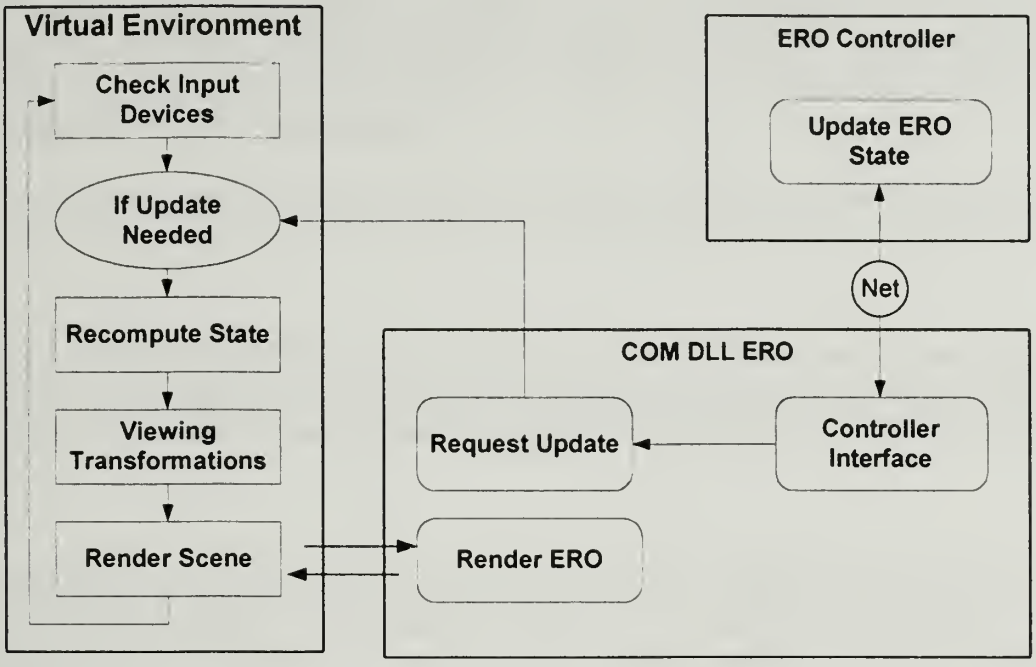


**Figure 4: An Externally Controlled ERO**

A VEA with the architecture shown above is capable of supporting all ERO types. *Inert* EROs may not take advantage of the additional interfaces supported by this type of environment. In order to support multiple EROs, a VEA can be equipped with an ERO "manager". This manager could provide the VEA with a higher level methodology to load, unload and render EROs.

## *ERO Interface Definition*

EROs are COM DLL objects [8]. COM objects are based on defined interfaces. EROs define at least two COM interfaces: IERORender and IEROController.

The IERORender interface is used directly by the VEA to manage the rendering of instantiated EROs. This interface may also be used by the VEA to initialize communications between the instance of the ERO in the environment and any external data source or controller. During initialization, EROs can take advantage of this interface and provide a setup dialogue to the user. The IERORender interface also provides a layer through which the VEA can specify and retrieve specific rendering parameters. For example, the VEA can ask the ERO how much space it will occupy for depth of view calculations. The VEA can also use the IERORender interface to tell the ERO what transformation to use to move from real space to rendering space.

The IEROController interface contains no standard functions and may be empty. This is a contradiction to the COM approach; however, it allows the encapsulation of external controls and behaviors. The external controller interface is customized to suit the type of ERO. The only

constraint is the interface name and the interface ID. Since this is a non-standardized 'private' interface, the VEA will never contact the ERO using this object interface.

The render interface provides a simple set of functions to allow the object to be a guest of the VEA. The behavior of an ERO is either generated within the ERO, or influenced through the communications interface. It is up to the ERO designer to implement an interface that can adequately support the ERO's requirements.

The interface functions currently defined in the IERORender interface will be discussed below.

*InitRender*

This interface is called by the VEA when the ERO is loaded. The ERO may do anything necessary to initialize itself. It is expected that a typical use of this function call is to display a dialogue box that allows the user to specify the rendering properties of the ERO and its expected maximum refresh rate.

*SetOffset*

This is an initialization function used by the VEA to set the translation required to convert from ERO space to rendering space. All interactions with the VEA should be transformed to rendering space using this offset. The VEA will calculate an appropriate offset and call this ERO function before rendering it.

*UpdateScheme*

During ERO initialization, the VEA uses this function to allow the ERO to register an update scheme. Three schemes are available: No updates, event driven updates, and periodic updates. Inert EROs do not request updates. Controlled EROs typically request event driven updates. Self-Generating EROs will typically make a request to the VEA for a periodic update. For event driven updates, the VEA provides the ERO with the parent window to which the ERO may send messages. The ERO requests updates by posting a repaint message to the VEA window. ERO driven refresh requests are important to controlled EROs since they may require immediate update for feedback. It is advisable to limit the number of concurrent EROs that request refreshes in this fashion. Too many refresh requests can hinder the performance of a VEA. The alternate method to secure a regular refresh is to register an update period with the VEA. The ERO uses this interface to request an update frequency in the VEA. The VEA determines the actual period from all the EROs that request periodic updates. Therefore, an ERO should use an internal clock to decide if an update is warranted.

*Draw*

The VEA calls this interface during each refresh. This interface contains a collection of drawing functions to plot the visual representation of the ERO. The VEA takes care of any viewing transformations that may be required. Since the drawing calls belong to the ERO, the ERO may alter its geometry to suit its behavior.

*UpdateSelf*

If an ERO has registered a periodic refresh request with the VEA, then the VEA will call this function at least the specified frequency. If multiple EROs have requested periodic updates, the actual period is the smallest requested period; therefore, the ERO should check a $\Delta t$ and update only on its own period. The ERO is not required to alter its state on every call of *UpdateSelf*. Inert, Controlled, or periodic EROs that do not require an update should always return zero.

*GetAttitude*

The VEA may get the bulk attitude of the ERO transformation matrix at any time. The ERO is expected to provide this information in matrix form and to keep it current. This matrix is expected to be in rendering space.

*SetAttitude*

A VEA may set the bulk attitude transformation matrix at any time. The VEA will provide this information in matrix form.

*GetClippingEnvelope*

The ERO must provide the parameters of a sphere that completely contains the object. This allows the VEA to calculate an appropriate viewing volume that contains all the objects in the scene.

*InitCommunciation*

This interface is called by the VEA when the ERO is loaded. The ERO may do anything necessary to initialize its communications between itself and a possible ERO controller. If the ERO has no controller or no need to initialize communications with a controller, then this will be an empty function. It is expected that a typical use of this function call is to display a dialogue box allowing the user to specify the communication settings. The external controller is expected to provide a similar function through the same IEROController interface. Alternately, this method may also be used to start input from a file, mouse, spaceball, or any other data source.

The following section will present examples of ERO implementations.

# EXAMPLES

Since their original conception, EROs have been used in many projects at Spectra Precision Software. This section will present some examples to illustrate the power and flexibility of EROs. All the EROs in this section are *Controlled EROs*. A controller application, different from the VEA, dictates the behavior of the ERO.

## *Remotely Operated Vehicle ERO*

The use of ROVs (Remotely Operated Vehicles) in the petroleum exploration industry is extensive. The task of operating such vehicles is difficult and risky due to the extreme conditions under which ROVs operate. ROV operators rely on video cameras mounted on the ROVs for navigation cues. Additional sensors transmit ROV position and attitude; however, this information is presented in two-dimensional plan and profile views. Operating ROVs is a challenge due to limited position and orientation feedback and low visibility. When the high cost of ROVs is considered, a system to improve navigation and feedback is invaluable. Spectra Precision's VEA "TerraVista" was capable of visualizing bathymetry data but lacked the capability to interact with ROVs. The idea to define dynamic objects outside the TerraVista code base proved to be an ideal solution.

Figure 5 shows the ROV ERO architecture used. In this application, the controller does not have a direct connection to the ERO because it runs on a separate computer. The controller communicates to a server that relays information across a network. The server that the ROV ERO connects to receives the information and updates the position of the ERO. This is in turn reflected in the VEA when it renders the ROV. This configuration provides the greatest flexibility because it allows the visualization to take place in multiple remote locations.

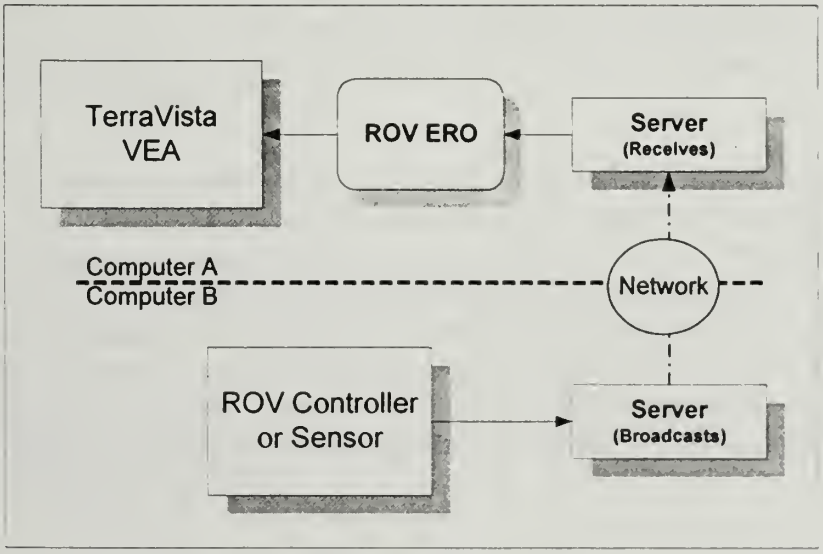


**Figure 5: ROV ERO Architecture**

Figure 6 is a screen snapshot of the ROV in TerraVista and a test controller. In order to take the snapshot, it was necessary to run the test controller and TerraVista on the same computer. The ROV test controller is a small operator-simulation program to test the ROV ERO components offline. In the real world scenario, the controller is replaced with a data gathering and management program that receives ROV location and orientation information from sensors and broadcasts it across the network. The ROV operator uses existing equipment to control the ROV.

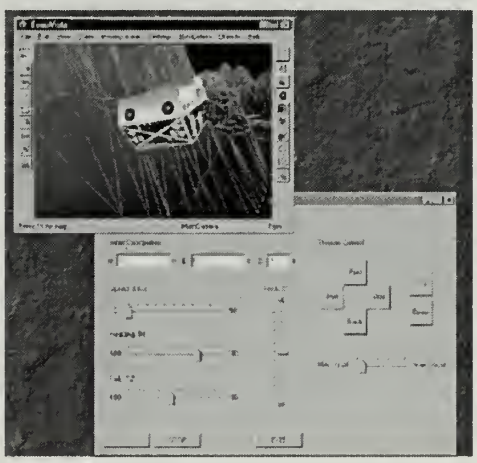

**Figure 6: Remotely Operated Vehicle ERO**

## *Sonar Swath Visualization ERO*

One of the most critical issues in the collection of underwater bathymetry data is the high cost of the operation combined with the lack of immediate feedback of data gathered. Without real-time data visualization, it is possible to miss entire segments. These errors may be found only after a costly operation has been completed.

The requirement to visualize the data while it is being collected motivated the development of a new scene element. The ERO architecture allowed the development of an ERO that could define its own geometry, without requiring changes to the VEA. The ERO was to store and render bathymetry information as it was gathered, and represent itself as the last few swaths of data. Since sonar data tends to be redundant, it is necessary to filter the collected points. Inline data filters can lower the amount of information required to accurately represent the surface. The "Decimator" is an application developed by Spectra Precision Software to filter raw data produced by scanning instruments. The Swath-Visualization ERO (Figure 7) receives the filtered data points from the Decimator and realizes itself in the VEA.

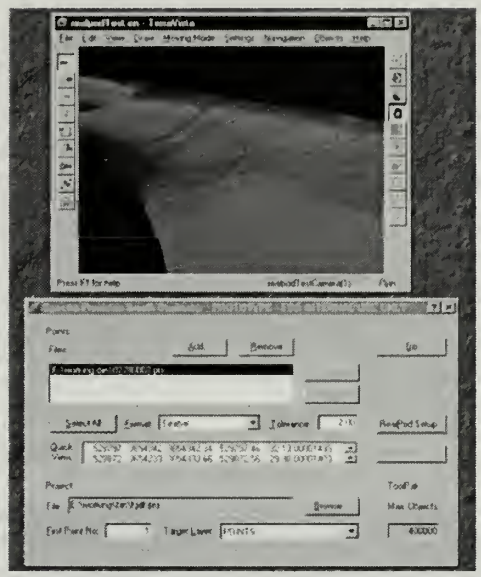

**Figure 7: The Swath-Visualization ERO and Decimator**

The ERO stores a user-specified number of swaths. This information is used by the rendering routines that are accessed by TerraVista to render a surface section. The Decimator can store all the filtered points and upon completion it can convert them into a TIN (Triangular Irregular Network). This TIN surface can be imported into TerraVista to become a reference to the swath lines represented by the ERO. Figure 8 shows the architectural diagram of this system.

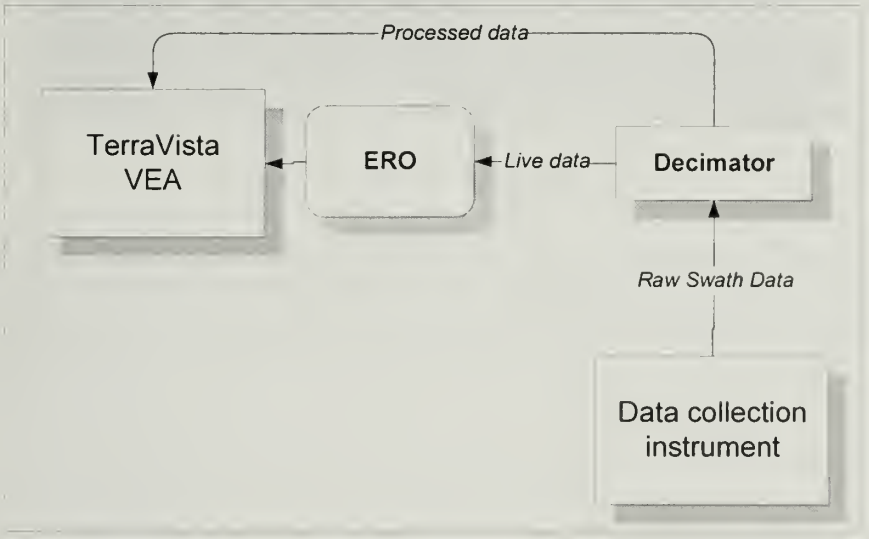


**Figure 8: Swath ERO Architecture**

## *Subsea Drilling Operations*

Sub-sea Drilling is an example of a complicated task that can benefit from visualization. The drill operators on the ocean surface are miles above the drill head. Decisions must be made based on the information provided by numerous instruments.

Since the position and speed of the drill head is known at all times, it is possible to design a controller program that transfers this data into an ERO. The drill ERO renders the rotating head of the drill and the bore accumulated from the drill head history. The speed of the drill head is used to color sections of the boring to provide progress indicators to the drill operator. Figure 9 shows a snapshot of the drill ERO with a test controller.

**Figure 9: Subsea Drilling ERO**

This ERO has an architecture identical to the ROV ERO (Figure 5). Therefore, engineers and executives thousands of miles from the drilling site can monitor a remote operation. Further, the entire drilling operation can be stored and played back to allow offline analysis and training of junior drill operators.

## CONCLUSION

The concept of EROs is a simple one, yet has unlimited power and flexibility. Given a working knowledge of OpenGL, or any standard graphics library, the design and implementation of EROs is a simple matter. The use of COM as a mechanism to access and render elements in a VEA provides the flexibility needed to break the constraints of object behavior definition. The VEA becomes an open rendering system that can host unique objects. Since the implementation of geometry and behavior is contained within the ERO, the ERO may exhibit any range of new functionality. The open communication interface offers no restrictions. Once objects are created they can be shared by any VEA that supports the same interface.

*Note: Spectra Precision Software Inc. has a patent pending on the ERO technology.*

## REFERENCES


[1] Web site: Sense8 (http://www.sense8.com) Interactive 3-D software development tool.

[2] Web site: SVE (http://www.cc.gatech.edu/gvu/virtual/SVE/docV2.0/sve.book_1.htm) User's Guide Version 2.0.

[3] Web site: Performer (http://www.sgi.com/Technology/Performer/index.html) SGI Performer Library.

[4] Woo, M., Neider, J., and Davis, T. (1997). *OpenGL Programming Guide*. Addison Wesley Developers Press, Reading, MA.

[5] Opdenbosch, A., and Rodriguez, W. (1993). Interactive Visualizer: Object and View Manipulation Algorithms. *Journal of Theoretical Graphics and Computing*, 6:48-57.

[6] Opdenbosch, A. (1994). *Design/Construction Processes Simulation in Real-time Object-Oriented Environments. Ph.D. thesis*, Department of Civil and Environmental Engineering, Georgia Institute of Technology, Atlanta, GA.

[7] Web site: Descriptions of DIS PDUs ( http://www.pitch.se//fmv/default.htm). Specifications of Protocol Data Units (PDUs) for Distributed Interactive Simulation (DIS) Protocol.

[8] Rogerson, D. (1997). *Inside COM*. Microsoft Press, Redmond, WA.

# *Range Gating Experiments through a Scattering Media*

Jeremy Payton, Frank Cverna, Robert Gallegos, Tom McDonald, Dustin Numkena,
Andy Obst, Claudine Pena-Abeyta, George Yates

Los Alamos National Laboratory

## ABSTRACT

This paper discusses range-gated imaging experiments performed recently at Redstone Arsenal in Huntsville Alabama. Range gating is an imaging technique that uses a pulsed laser and gated camera to image objects at specific ranges. The technique can be used for imaging through scattering media such as dense smoke or fog. Range gating uses the fact that light travels at $3*10^8$m/s. Knowing the speed of light we can calculate the time it will take the laser light to travel a known distance, then gate open a Micro Channel Plate Image Intensifier (MCPII) at the time the reflected light returns from the target. In the Redstone experiment the gate width on the MCPII was set to equal the laser pulse width (~8ns) for the highest signal to noise ratio. The gate allows the light reflected from the target and a small portion of the light reflected from the smoke in the vicinity of the target to be imaged. We obtained good results in light and medium smoke but the laser we were using did not have sufficient intensity to penetrate the thickest smoke. We did not diverge the laser beam to cover the entire target in order to maintain a high flux that would achieve better penetration through the smoke. We were able to image an Armored Personnel Carrier (APC) through light and medium smoke but we were not able to image the APC through heavy smoke. The experiment and results are presented.

Keywords: Range Gating, Micro Channel Plate Image Intensifier(MCPII), CCD Cameras.

## I. Introduction

Range Gating is a well known imaging technique that can be used to image through scattering media such as smoke, fog, and turbid waters(1)(2). Using range gating we are able to record only the light that is being reflected from the vicinity of the target(see Figure1). We use a pulsed laser, which has a higher intensity than the background light. The imager consists of a Micro Channel Plate Image Intensifier (MCPII) coupled to a Charge Coupled Device (CCD) camera. The MCPII is shuttered with a gate pulse of about 8ns in width.

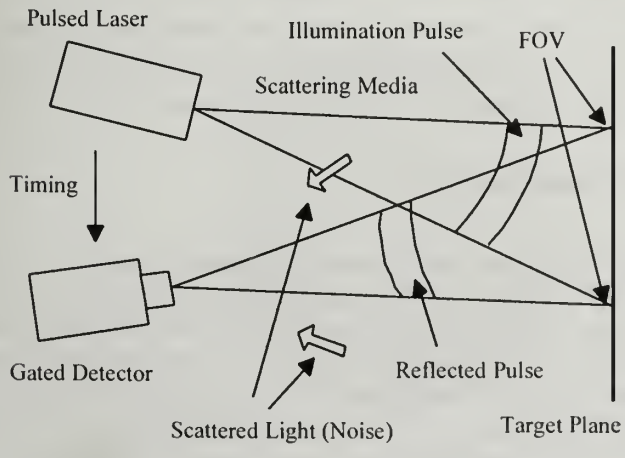


Figure 1: Illustration of range gated imaging. The laser source illuminates the target with a short pulse and provides a timing signal to the gated detector. The gated detector is set to accept light from the vicinity of the target plane and reject most of the light scattered by the intervening medium.

For These experiments our primary target was an Armored Personnel Carrier about 500m down range from a 100ft tower where our equipment was located. Figure 2 shows a block diagram of our equipment set up. Although three cameras are shown in the block

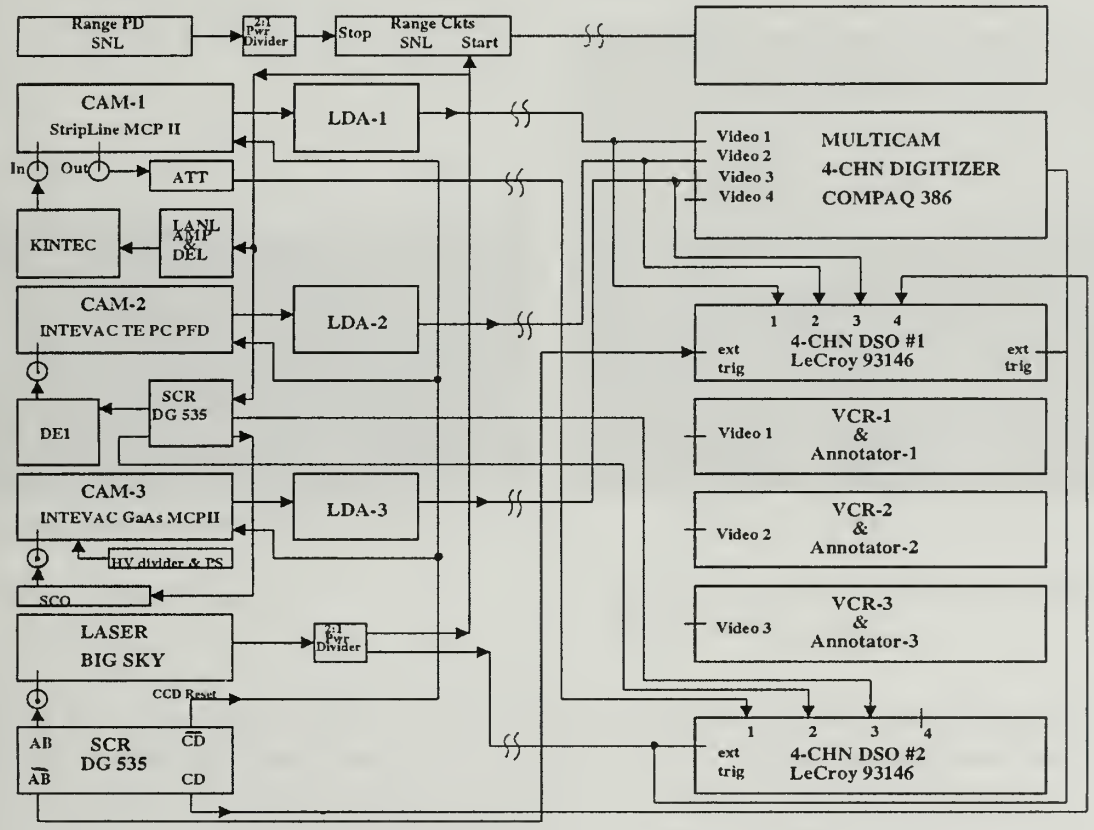


Figure 2: Block Diagram of System

diagram only one was actually used due to technical difficulties and safety requirements. A Big Sky Laser was used in the experiments. The laser operated at a wavelength of 532nm, had a pulse length of 8ns, and an energy of approximately 30mJ/pulse. Timing was provided by a Stanford DG 535 pulse generator. A frame grabber card installed in a Compaq computer was used to capture images from the camera and associated display and analyzing software was used to display and record the images. As a backup the image data were recorded on a VCR and on a LeCroy storage 9314L oscilloscope.

## II. Experimental Results

In the Redstone experiments smoke was used as the scattering media. We qualitatively classified the smoke into three levels of density, Light, Medium, and Heavy. The smoke was produced by burning fog oil and then using a jet engine starter to blow the smoke across the field. Light smoke has a density such that an observer can just see the APC by eye. Medium smoke is at a level such that the target can easily be lost to the observer. Heavy smoke is at a level that the target can definitely not be seen. The illustrations in Figure 3 show the test range at Redstone Arsenal with and without smoke. The range was about 5km long and about ½ to 1km wide. In Figure 3b you can see the

fog oil just beginning to drift across the field. The range is about 450m and the APC can be seen by an observer with appropriate optics.

Figures 4a and 4b show the APC as it looked from about 20m from an ordinary camera and from about 500m from one of our range gated cameras with a 300mm

Figure 3a: Range without Smoke

left from a digital camera.

Figure 3b: Range with Smoke

on the right notice the hotspot in the middle of the target.

telephoto lens. The field of view in the two images is approximately the same. One can clearly see in the range-gated image the shape of the APC. Portions of the wheels and tread can be observed. The bright spot in the middle of the APC is due to the non-uniform intensity of the laser beam. No attempt was made to obtain a more uniform laser beam profile in order to increase penetration of the smoke.

Figure 5 shows a series of range gated images taken through light, medium, and heavy smoke. Figure 5a shows the APC imaged through light smoke. One can see the APC but not as many details can be seen due to the fact that the gain of the MCPII was adjusted high in order to ensure detection of the return signal. Figure 5b shows the APC covered with medium smoke, which is at a level that almost completely obscures the target and an observer could easily miss or lose the APC in the smoke. Again, the gain on the MCPII was adjusted high and, the recorded image was saturated and had no detail. Had the gain

Figure 5a: APC through light smoke

Figure 5b: APC in Medium Smoke there is no detail due to high intensifier gain.

Figure 5c: APC covered in Heavy smoke and not visible to without data extraction.

been adjusted lower, more detail of the APC would have been observed. Figure 5c shows imaging through heavy smoke. Except for an indication of the high intensity spot of the laser, no reflected signal from the APC was recorded. A higher energy laser pulse would have been required to penetrate the smoke and provide a recordable return signal from the APC.

In Figure 6a the APC is covered in heavy smoke. Although no detail of the APC is evident in the picture, it may, nonetheless, be possible to extract data from such imaging using data analysis techniques. Figure 6b shows a data enhancement of the image in Figure 6a, which brings out a bright-spot return from the APC. We speculate that the bright return in the lower left corner of the image is a reflection from a small pool of water near the APC. The speckled pattern seen in the images is the typical granular light distribution associated with laser light.

Figure 6a: APC in Heavy smoke

Figure 6b: APC after Data Extraction

## III. Conclusion

We have demonstrated the use of range gating in imaging through smoke and scattering media. With range-gating techniques we where able to image a target in three different levels of smoke. Although the photon return was low through the heavy smoke, it is speculated that a laser that has a greater pulse energy would be able to correct this problem.

## IV. Bibliography

1. I. P. Csorba, *Image Tubes* (Howard W. Sams & Co., Inc., 1985), Section 9.3, "Active Gated Image Intensifier System," pp. 142-143.

2. George J. Yates, Robert A. Gallegos, Thomas E. McDonald, F. J. Zutavern, W. D. Helgeson, G. M Loubriel," Range-Gated Imaging for Near-Field Target Identification," SPIE 22nd International Congress on High-Speed Photography and Photonics, January 96

# A Photon Counting Imager

**Kevin L. Albright, R. Clayton Smith, Cheng Ho, S. Kerry Wilson, Jeffery Bradley, Alan Bird, Don E. Casperson, Miles Hindman, Rob Whitaker, James Theiler, Robert Scarlett, William C. Priedhorsky**

Los Alamos National Laboratory

P.O. Box 1663, MS D454, Los Alamos, NM 87545

**Abstract:**

The Remote Low Light Imaging (RULLI) system responds to individual photons using a modification to conventional image intensifier technology and fast timing electronics. Each photon received at the detector is resolved in three dimensions (X, Y, and time). The accumulation of photons over time allows the system to image with very low light levels, such as starlight illumination. Using a low power pulsed laser and very fine time discrimination, three dimensional imaging has been accomplished with a vertical resolution of five cm.

## Introduction

In standard high speed imaging, a focal plane array (FPA) will accumulate photo-electrons either directly from the scene illuminated by a strobed light source, or from a gated image intensifier. Thus the FPA acts as a photonic memory with the integrated scene information stored until the information is accessed. After accumulating the photons which originated from the scene and moment of interest, the pixels in the focal plane array are read out in a parallel-serial process. The serial transfer of a line of data through the output amplifier is often the rate-limiting step. Recent advances in focal plane arrays such as parallel or multi-port readouts and high bandwidth output amplifiers have increased the frame rate capabilities of high-speed cameras to many thousands of frames per second.

In contrast, this detector system processes each photon event as it occurs. The detector is made up of a standard micro-channel-plate (MCP) image-intensifier front end with high gain for photon counting and with a wire-wound crossed delay-line (CDL) anode. Thus it is referred to as an MCP/CDL detector. The detector signals are input into fast front-end electronics, called Pulse Absolute Timing (PAT) channels. The PAT channel converts the analog signal from the detector into the raw time information needed to determine the position and time of arrival of the photon with respect to the photo-cathode. Final data display is provided through custom processing software.

By sensing each photon for position and time of arrival, several important new approaches to imaging are possible. First is the ability to image with near noiseless performance. For low light conditions, this enables long integration times with contrast improvement, since only scene-generated photons are collected. For visible photons this is achieved without having to cool the detector. Second is the ability to debiur an image based solely on the scene contrast. Since the MCP/CDL is not integrating photons in the sense of a FPA, post processing of high contrast elements within the scene enable a reordering of the image over time. Third is the ability to image in three dimensions, when using a synchronously pulsed light source. This gives a very flexible imaging system that can provide much more information than standard focal plane systems. A report was published that rigorously treats various applications of this system [1].

## The detector

The detector is operated in a photon counting mode. The detector uses a low noise S-20 photocathode for photon detection, and a triple ( Z) stack of micro-channel-plates (MCPs) for electronic gain (up to $10^7$).

The front end components, the photocathode and MCPs, are from a resistive anode tube design that is a commercial product.

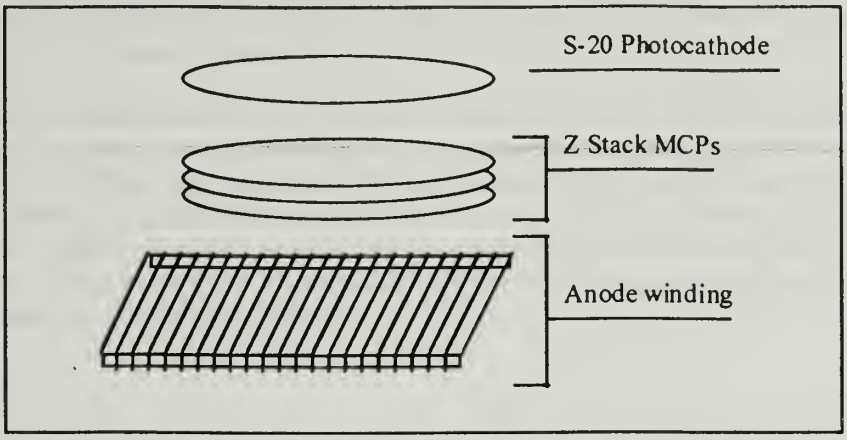


Drawing of basic elements of micro-channel-plate crossed-delay-line detector.

The remainder of the tube is the CDL wire anode [2,3]. It consists of two windings, each about 100 feet long, wound around a 3.5 in. square copper ground plane with insulating ceramic edges. One set of ceramic edges is larger in height from the ground plane than the other. Thus there is an inner wire winding in one direction (Y axis), and an slightly larger orthogonal winding for the other direction (X axis). In the drawing below, the Yaxis wires are cut away for clarity. Each winding is composed of a bifilar coil of Cu-Zr wires, that is two wires are spooled simultaneously with a fixed space between them. They are pulled with substantial tension so that as the wires pass over the ceramic insulator, they form a taught flat grid in parallel to the copper ground plane. Effort has been made to ensure the wires maintain their tension through the tube processing, which includes a 300 deg C bake-out cycle. The bifilar construction of each winding yields a balanced transmission line for the high frequency signals to propagate along, with a slight (18V) bias from one line to the next. The end of the wire is carefully clamped with a thin (0.002 in) nickel foil strip wrapped around it. Each nickel strip is then attached to a vacuum feedthrough pin in order to make electrical connection outside the tube.

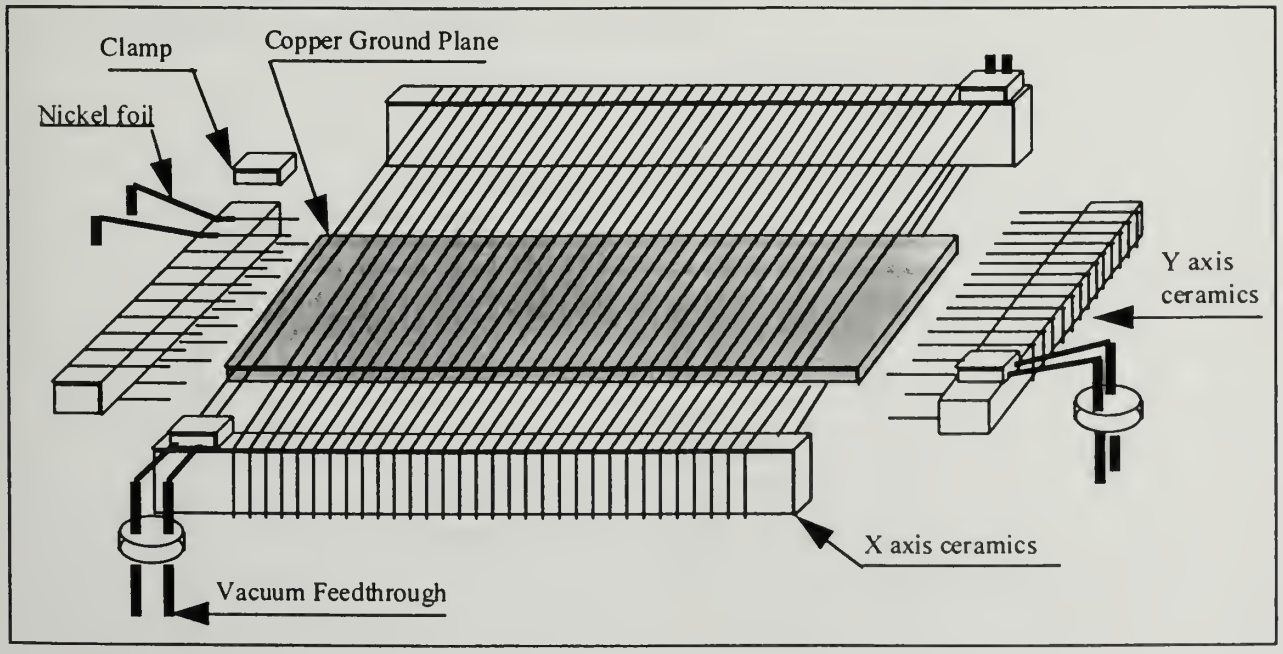


Drawing of wire-wound crossed delay line anode.

Thus, there is a three level structure through which the cloud of electrons move, giving rise to simultaneous signals on the outer winding, the inner winding, and lastly being absorbed into the copper ground plane. There are the same three levels seen from the back side, which are shielded from seeing electrons by the innermost layer, the solid copper ground plane.

The Z stack MCPs are biased so that the last plate is in saturation, giving a nearly constant electron gain for each photon that is detected. The amplified electrons are moderately accelerated (700V) from the last MCP to the wire-wound delay-line anode where they spread and strike an area at least a few wire diameters wide. From the interaction, a signal is impressed on each wire due to electrons that are captured, secondary electrons that are released or absorbed, and currents induced by the electrons passing through the small bifilar field (18V). This current signal propagates to each end of the winding where it is extracted through vacuum feedthroughs to external preamplifiers.

**The electronics**

The pulse absolute timing, or PAT, electronics are comprised of a wide bandwidth four channel preamplifier at the detector, and four VME modules. One double width VME module is used for each PAT channel and it has an associated single width memory module sitting next to it in the VME chassis. There are four PAT channels in the system. The electronics of each PAT channel are designed around a custom 1X3 in. hybrid electronics module called a time interval meter (TIM). The TIM includes a number of internal circuits; a constant fraction discriminator (CFD) front end, a dual interpolator stage, and a ten bit time to digital converter (TDC). The TIM of each channel is connected to one of the ends from the two windings of the detector anode, hence the need for four channels. About 80 ns after a trigger, that is a photon signal from the detector, the TIM generates a fine count number. The fine count is the difference between the time of a trigger and the clock phase of a very stable 100 MHz system clock, expressed with 20 ps of accuracy. The fine count is passed through a lookup table, which provides correction for linearity and other artifacts. External to the TIM, but triggered from it, is a course counter, which keeps track of time in 10 ns increments over the course of a collection period. The two count values, fine and course, are passed on to a fast FIFO for intermediate ordering. The fast FIFO is followed by a slow FIFO, which parallels the data, and synchronizes the data with a VSB interface. At the interface, a periodic time stamp is inserted which keeps the data in records of know time duration. The data from each channel, and time stamps, are stored in a fast RAM memory card (128 or 256 Mb) which sits on the VSB bus. When the acquisition is complete, the data is transferred to a hard disk array.

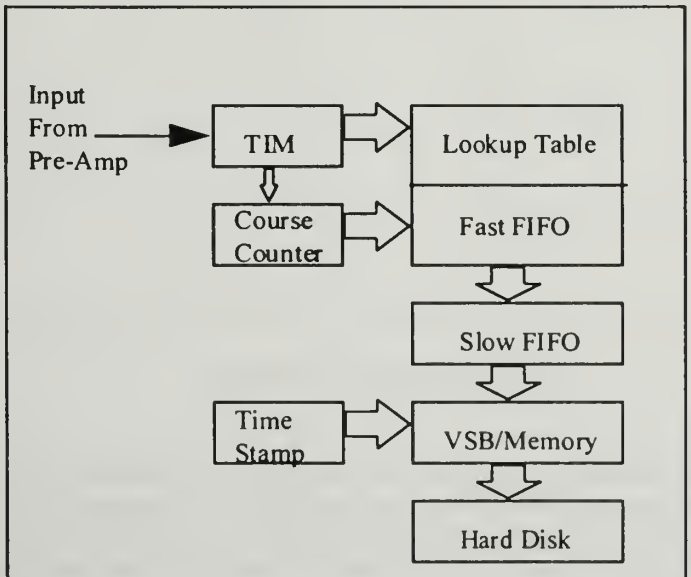


Block diagram of the Electronics System.

**TIM electronics**

Time is measured by recording the cycle number of the reference clock and the clock phase at which an event arrived. First the CFD latch and the dual interpolator latches form a pulse whose duration is proportional to the phase plus 1 clock width. This pulse duration is used to switch a constant current source to a capacitor and store an analog voltage that is proportional to the arrival phase. Also the pulse edge is used to select an unambiguous cycle of the clock. Those two values combine to compute the time.

The CFD used in the TIM is a modification of one originally designed by Bojan Turko and R. Clayton Smith. It was shown that this circuit was capable of detecting signals with amplitude variation of 40 dB, while maintaining a time walk of less than 100 ps [4]. The circuit is built using two high speed ECL comparators. The first comparator sets the threshold of the input signal, triggering on the leading edge of the detector pulse. The second comparator sees a slightly integrated version of the input signal, and compares it to a reference level called compensation, which is usually set close to ground. The first comparator passes a logic level to the data input of an ECL D flip flop, while the second comparator triggers the clock input of the same D flip flop. With this dual trigger approach, and the slight integration of the input signal, the CFD is able to maintain a stable firing time even if the pulse amplitude varies over a range of 100:1. The complementary outputs of the D flip flop are fed to the inputs of the dual interpolator stage.

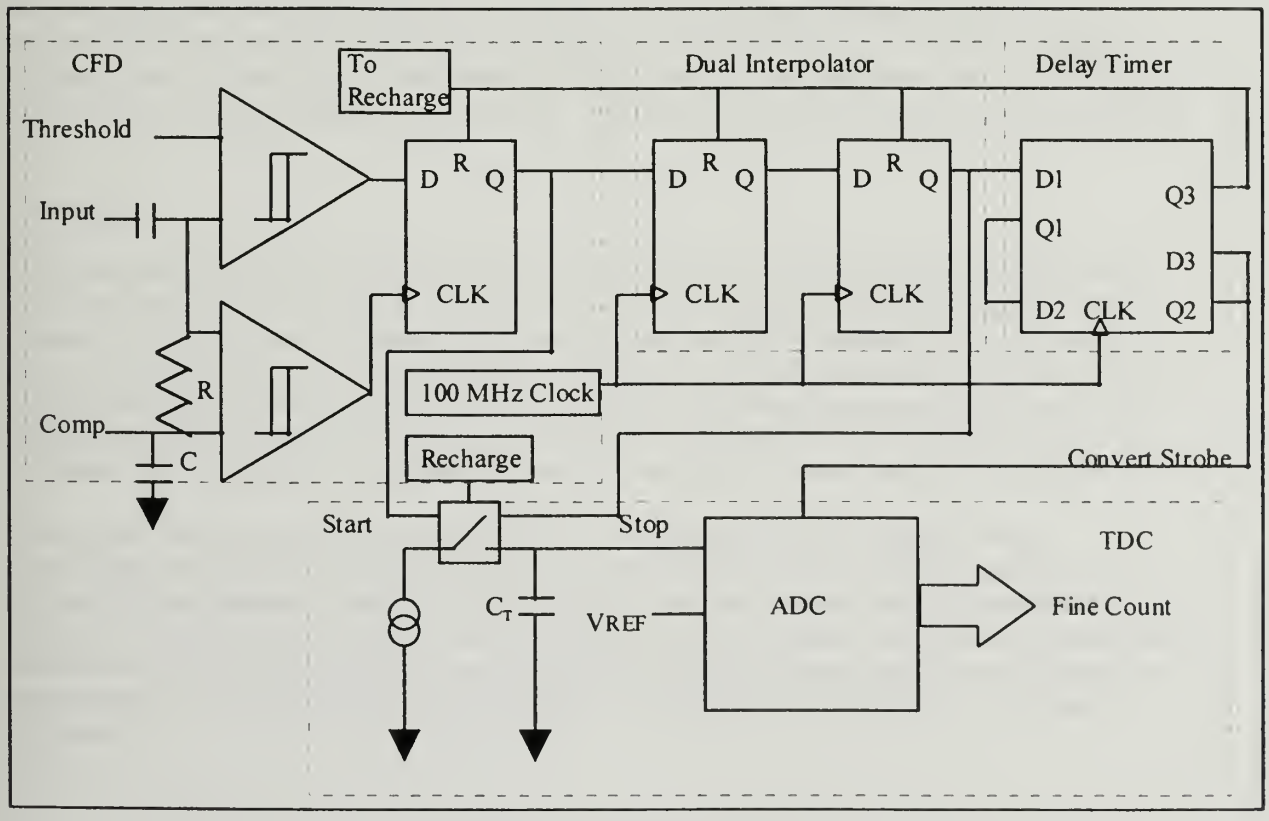


Schematic of TIM hybrid circuit.

The ADC is a 10 bit 40 MHz Flash ADC chip, and requires 20 ns of setup and hold time. After halting the discharge of the timing capacitor, $C_T$, the CFD trigger signal from the second stage of the dual interpolator is clocked through two periods of the 100 MHz system clock through two more stages of D flip flops. After the 20 ns delay, the ADC is triggered to convert the voltage remaining on the capacitor to a digital output. A final stage of D flip flop is used to delay the CFD trigger signal for 10 ns. The output of this

final delay is used to send a reset signal to all the gates, and to a recharge circuit which brings the voltage on the capacitor back to the initialized level.

Data Processing:

Post processing, or photon event reconstruction, is the step where the position of the photon relative to the photocathode is calculated, based on the raw timing data sets previously stored on disk. The photon event reconstruction software compares the relative time it takes a pulse to arrive at each end of the delay line with the sum equal to the total delay of the winding. Using this test for appropriate pairing, the data set is reduced by a small amount as some data pairs are rejected. The data is then matched, in order associate appropriate pairs from each axis, so that a two dimensional position is determined for the initial photon event. By summing these spatial events over time, the analysis yields a two dimensional data set equivalent to a "frame". For FPA based imaging, a frame is usually taken as both fixed in spatial and in temporal dimensions. The temporal dimension here can be adjusted for as long a time as is needed for developing sufficient photon statistics in constructing the image.

For three dimensional imaging, a pulsed light source is used that is time synchronous with the PAT system. The source employed in several recent experiments is a Hamamatsu PLP-01 solid state diode laser. This laser has a pulse width of 85 ps at 655 nm wavelength, and was operated synchronously by dividing down the 100 MHz system clock to 1.56 MHz. By ordering the data into pulse synchronous time bins, an additional level of association is calculated that results in a distance determination with resolution of 5 cm or better. Three dimensional structures from a 3X3X3 ft. box to a polystyrene target with the LANL logo in 2 in. letters have been imaged with this system. These experiments are described in detail elsewhere [5].

Conclusion:

The approach of imaging by photon counting is not new. But most systems suffer from deadtime issues which limit their useful counting rates to no more than a few thousand to a hundred thousand counts per second. This system currently operates at 10 times that rate, and has the potential of another factor of three or more increase in photon rate. The high speed electronics, which have made this performance possible, are built using hybrid electronics techniques. Even higher performance is expected out of newer ASIC IC designs that are being proposed. In fact, an very high precision, though lower speed ASIC IC has been developed which can achieve better than 10 ps accuracy with very low power and space requirements.

The system described was first proposed in 1993. A prototype was rapidly constructed which demonstrated the utility of the approach, especially as applied to UV imaging. An intermediate prototype was developed and operated from 1994 to 1996. By mid-1997, the PAT version of the system was developed. Also in 1997, a new tube vendor was producing robust detectors, which could be used in field experiments as well as the laboratory. Several field experiments have been conducted over the past year proving that the system has several unique capabilities which complement existing low light imaging techniques.

**Acknowledgements**

This work was performed under the auspices of the U.S. Department of Energy.

**Bibliography**

1. Priedhorsky, W.C., Smith, R.C., and Ho, C., "Laser Ranging and Mapping with a Photon-Counting Detector", *Applied Optics*, **35**, 441-452 (1996).
2. Williams, M.B., . Sobottka, S.E., Shepherd, J.A., "Delay line readout of MicroChannel Plates in a Prototype Position-Sensitive Photomultiplier Tube", *Nuclear Instruments and Methods in Physics Research*, **A320**, 105-112 (1991).
3. Baron, M.H., and Priedhorsky, W.C., "Crossed Delay Detector for Ground and Space Based Applications", *Proc. SPIE*, **2006**, 188-197 (1993).
4. Turko, B.T., Smith, R.C., "A precision timing discriminator for high density detector systems", *IEEE Trans. Nucl. Sci.* **39**, 1311-1315 (1992).
5. Ho, C., Albright, K.L., Bird, A.W., Bradley, J., Casperson, D.E., Hindman, M., Priedhorsky, W.C., Scarlett, W.R., Smith, R.C., Theiler, J., Wilson, S.K., "Demonstration of Literal Three-Dimensional Imaging", submitted to *Applied Optics*.

# Using Optical Parametric Oscillators (OPO) for Wavelength Shifting IR Images to Visible Spectrum

Thomas E. McDonald Jr., Dustin M. Numkena, Jeremy Payton
George J. Yates
Los Alamos National Laboratory

Paul Zagarino
Sharpenit

## ABSTRACT

We have carried out preliminary investigations into coherent imaging using Optical Parametric Oscillators (OPO) for wavelength conversion of near IR images to visible spectrum. A nonlinear crystal, second harmonic generator (SHG), was used for degenerate optical parametric up-conversion. A Potassium Titanyl Phosphate (KTP) doubling crystal was used to convert incident 1540nm flux to 772nm. Experiments included investigation of spatial resolution and responsivity of the OPO. Spatial resolution of 1.3 lp/mm was attained in both horizontal and vertical axis. Measured responsivity for this OPO configuration compared well with that attained from image intensifier-based systems. Equipment used for this experiment included an ORION SB2-2R pulsed solid state laser used as a light source and a CCD camera and frame grabber to capture and record all data. The experiment and results are discussed.

## BACKGROUND

Imaging in the near IR is a goal of some projects that are being carried out at the Los Alamos National Laboratory under the joint Department of Energy and Department of Defense technology development program. Such a capability is useful in a number of applications including LADAR and range gated imaging. We have specifically been investigating range gated imaging in the region of 1.5 microns wavelength, where the eye damage threshold is 3 to 4 orders of magnitude higher than that at the shorter wavelengths from about 1.2 microns into the visible (Ref. 1).

The fundamental difficulty in imaging at 1.5 microns is the lack of photocathode materials that can detect 1.5-micon photons. Whereas photocathode materials have been developed that can detect photons over the wavelength range of approximately 100 to 1200 nm (Ref.2), the energy in a 1.5 micron photon is too low to stimulate photoemission in currently available photocathode materials. Alternate detection approaches must be found if imaging is to be possible at the 1.5 micron wavelength. One possible approach that has been developed with a degree of success is referred to as transferred electron (TE) photocathode, which was conceived and patented by Bell in the 1970's (Ref. 3) and within the past few years further developed by Intevac Advanced Technology Division of Santa Clara, CA. (Ref. 4) Although details of the Intevac development are propriety, basically the transferred electron photocathode approach uses an externally applied electric field to increase the energy level of excited electrons sufficiently to escape into the vacuum region of the intensifier.

We have conducted several range gated imaging experiments using visible wavelength photocathodes (Ref. 5 ). Our earlier unpublished studies investigated the use of the Intevac TE photocathode intensifier in a planar diode configuration coupled to our own high speed stripline image intensifiers (Ref. 6). This combination would exploit the IR sensitivity of the TE photocathode and the fast shuttering capabilities of the stripline geometry intensifiers.

An alternate approach that is being considered by us at Los Alamos is the use of nonlinear optical crystals to double the frequency (or half the wavelength) of the 1.5 micron return signal to produce a signal in the region of 750-micron that can be detected by conventional photocathodes or CCD cameras. This approach of frequency doubling, or second harmonic generation, is commonly used to produce the second or third

harmonic wavelengths of a laser beam from a fundamental, such as the production of a 532 nm beam from a 1064 nm Nd:YAG laser. In this investigation we are considering whether a nonlinear crystal could also be used to up-convert 1.5-micron laser light returned from a target in a gated imaging system and be detected by a CCD camera or a conventional image intensifier. Issues to be considered include flux density into the nonlinear crystal, which affects conversion efficiency and output signal strength, light acceptance angle, which defines the system field of view, and spatial information invariance through the conversion process. Our first experiment was to determine if the spatial information (the image data) in the incoming signal remained undistorted through the nonlinear conversion process.

## EXPERIMENTAL SETUP

A laboratory laser, the ORION SB2-2R, manufactured by MPB technologies, Inc. of Dorval, Quebec, Canada, was used to observe imaging through a nonlinear optical crystal. In the ORION laser, the fundamental laser beam is produced by a Nd:YAG oscillator, which generates an 8ns, 30mJ pulse at 1064nm wavelength. Up to 6 different beams of differing frequencies and pulse widths are produced by routing the fundamental beam through various stimulated Brillouin and Raman cells and nonlinear optical crystals. The beam we used for our imaging experiments had a pulse width of 20ps at a wavelength of 1540nm. The beam is routed through a nonlinear optical crystal, a KTP (Potassium Titanyl Phosphate) second harmonic generator, to produce a 772nm wavelength beam.

A bar pattern of approximately 1.3 lp/mm was placed in front of the KTP second harmonic generator crystal and a CCD camera was placed behind the crystal in order to observe the spatial modulation of the beam produced by the bar pattern through the crystal. A schematic diagram of the ORION laser showing the placement of the optical target pattern in given Fig. 1.

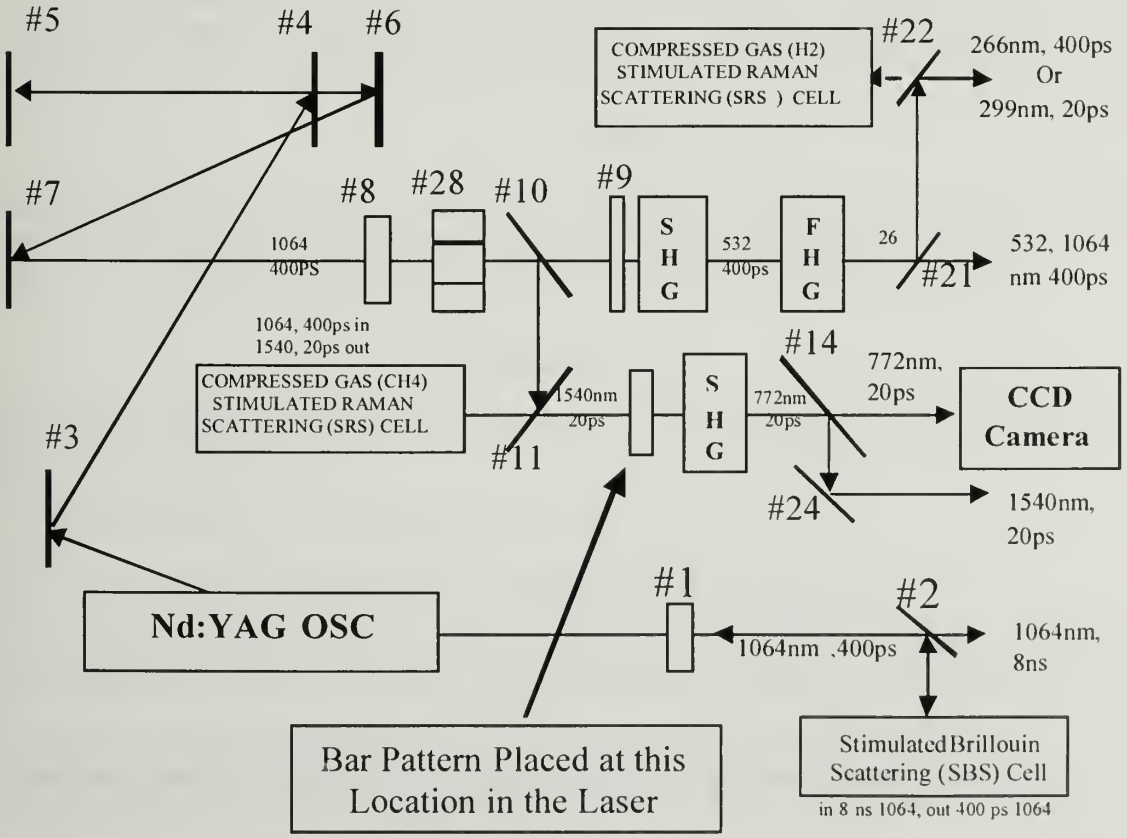


Fig. 1 Block Diagram of ORION laser showing location of 1.3 lp/mm bar pattern in the 1540nm beam line and location of CCD camera after the second harmonic generation nonlinear optical crystal.

## EXPERIMENTAL RESULTS

Images were taken of the frequency doubled laser beam with the Cohu CCD camera and recorded using a Big Sky frame grabber. The recorded images are shown in Fig. 2a and 2b. The bar pattern used in these images had approximately 1.3 line-pairs/mm. Fig. 2a is taken with the lines running in a direction horizontal to the camera and Fig. 2b is taken with the lines running vertical to the camera. Although we observed fringe patterns in the images, spatial modulation is definitely maintained.

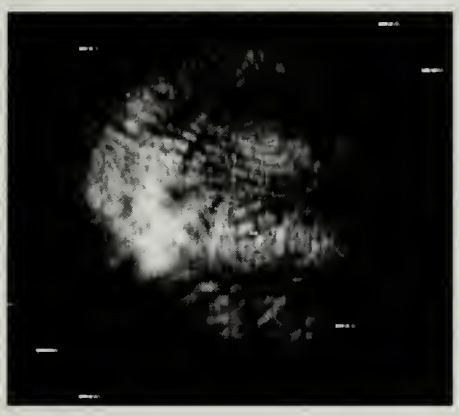

Fig. 2a

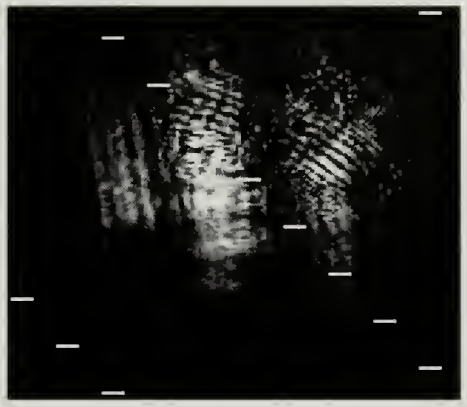

Fig. 2b

Fig. 2 Image recorded by camera of Laser beam after the second harmonic generator crystal (1.54mm--772nm). Spatial frequency of the line pattern is 1.3 lp/mm. Figure 2a is with the pattern in the horizontal orientation and Figure 2b is with the pattern in the vertical orientation.

## CONCLUSIONS

It appears that spatial modulation is maintained through the nonlinear crystal conversion process; however, a great deal of fringing and some distortion is present . Our next step in the assessment is to examine imaging at a low flux level and determine the lower practical bounds or the process.

## REFERENCES


1. David Sliney and Myron Wolbarsht, *Safety with Lasers and Other Optical Sources-A Comprehensive Handbook*, 1980 Plenum Press, NY

2. I. P. Csorba, *Image Tubes*, Howard W. Sams & Co., Inc.,

3. R. L. Bell, Long-wavelength Photoemission Cathode, Patent Number 3,958,143

4. K. A. Costello, G. Cavis, R. e. Weiss and V. W. Aebi, Transferred electron photocathode with greater that 5% quantum efficiency beyond 1 micron, SPIE Proceedings, Vol. 1449, P. 40-50, March 1991.

5 J. Payton et al, "Range Gating Experiments Through A Scattering Media", ISIA Conference on Detection And Analysis of Subsurface Objects and Phenomena, High-Speed Imaging Techniques and Applications Session, Naval Post Graduate School, Monterey, Ca., October 19-23, 1998.

6 . M.C. Thomas., G.J. Yates, and P.A. Zagarino, " Fast Optical Gating Using Planar-Lead MCPIIs and Linear Microstrip Impedance Transformers," SPIE Vol. 2273-26, Ultrahigh-and High-Speed Photography, Videography, and Photonics Conference, San Diego, Ca., July 24-29, 1994.

Camera System for High-Frame Rate Applications

George J. Yates, Thomas E. McDonald, Jr., and Nicholas S.P. King
Los Alamos National Laboratory, Los Alamos, New Mexico

Bojan T. Turko
Lawrence Berkeley National Laboratory, Berkeley, California

## ABSTRACT

A CCD camera system, designated GY-11, having a high-frame rate and fast shutter capability is being developed by the Los Alamos National Laboratory for the imaging of dynamic optical phenomena. The CCD pixel array size is 512x512 and has 16 parallel output ports. With a 75 MHz per port pixel rate, the camera frame rate can reach up to 3500 frames per second. A microchannel plate image intensifier provides gain for low light level applications and also provides camera gating. The intensifier can achieve sub-nanosecond gating by incorporating a stripline electrical geometry that provides impedance matching to reduce pulse reflections and dispersion. A computer controlled frame grabber records data from the digital output and stores the data in a local memory for transfer into a non-volatile storage medium such as removable disk drives. The entire camera system will be discussed.

## BACKGROUND

Los Alamos National Laboratory (LANL) engineers, technicians, and physicists have designed, developed, and fielded several high speed TV based camera systems for use in the nation's underground nuclear weapons test (UGT) program which was conducted at the Neveda Test Site (NTS) over the last three decades, commencing in 1968 and ending in 1993 with the moratorium banning further nuclear testing.

The salient requirements were for (1) fast optical shuttering in the 1-20ns range to capture rapidly evolving two dimensional images corresponding to temporal and spatial evolution of neutron chain reactions, i.e. geometries and intensities of neutron production from fission/fusion processes of nuclear devices, and (2) fast readout of the recorded images in the 1-10ms range to permit telemetry of the test data before onset of camera destruction by shock waves following detonation of the nuclear device under test.

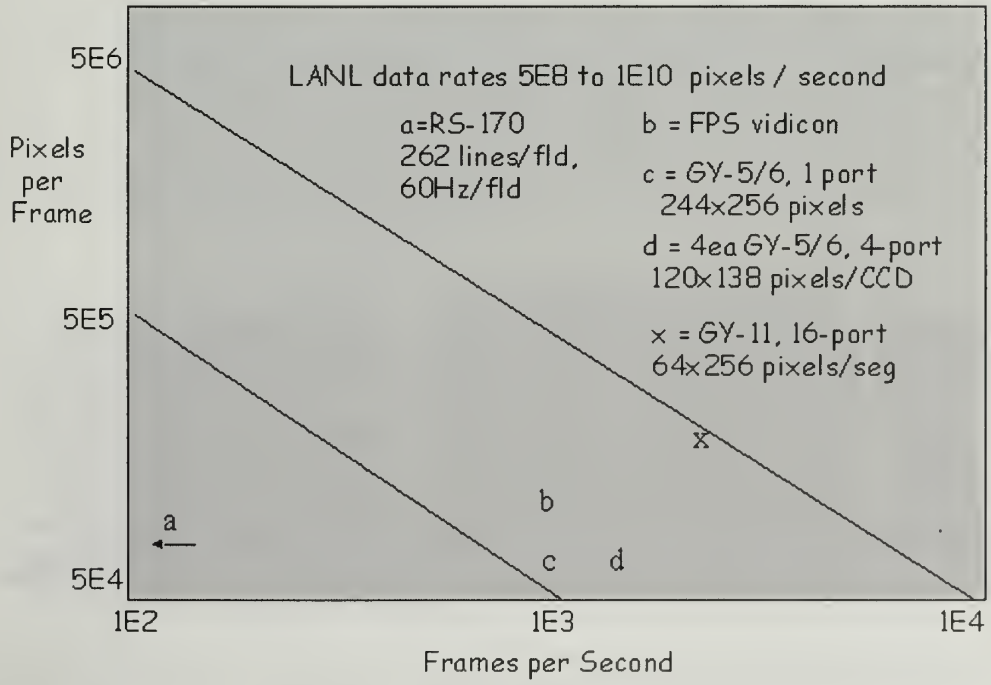


Figure 1. LANL camera design range.

Performance and characteristics of LANL UGT cameras are shown in figure 1, and reported in numerous papers including internal (reference 1) and open literature publications (references 2,3,4). Since the recent ban on nuclear weapons testing, the Laboratory's mission has extended to that of principle responsibility for Science Based Stockpile Stewardship (SBSS) of the nation's nuclear arsenal. This involves time-resolved imaging of transient phenomena including shockwave propagation in variously shocked strategic materials and components using dynamic x-ray and proton radiography techniques pioneered/developed at Los Alamos. The high speed imaging capabilities of the UGT cameras have been adapted for use in the SBSS experiments, thereby expediting field testing (reference 5). These cameras have also been used in non-nuclear military imaging applications to demonstrate "proof-of-principle" benefits of range-gated LADAR in improving signal-to-noise ratio of images in scattering media for a number of applications, including (1) strategic target detection for the US Air Force at Wright Laboratory, Eglin Air Force base; (2) mine field detection in sea water for the US Navy and Marine Corps at NCSS facilities, Panama City, (reference 6); (3) imaging of military vehicles through smoke and fog for the US Army, Redstone Arsenal (reference 7).

## CAMERA DESIGN FEATURES

The GY-11 camera has evolved from earlier GY-Series of high speed intensified and shuttered solid state cameras. The design incorporates many of the best features of the earlier cameras, including real-time 100MHz analog processing circuitry for detection of peak charge from individual CCD pixels. This is an essential requirement for pre-processing of "raw" CCD analog signals prior to digitization of slew rate limited video signals from the CCD that can arise at high pixel rates; 100MHz ECL/TTL logic circuitry for CCD clock signal generation followed by level-shifting amplifiers for driving the CCD clock line(s) capacitances based upon "charge pump" circuitry to minimize the power dissipation at high clock rates; stripline design microchannel plate (MCP) image intensifiers (MCPII) for transmission line "like" geometry, impedance matched to the MCPII characteristic impedance of 4-6 ohms when gated in the 100-500ps range; microstrip design tapered lines for impedance transformation between 50-ohm gate pulse generators and the approximately 5-ohm MCPII load; real-time control, measurement, and recording of MCPII gate-width and gain variables, with 10-bit resolution, and updated each vertical sync interval of the camera for data logging along with the video image for individual frames. These systems and components have been previously described in detail elsewhere (references 8,9,10,11) and only salient characteristics will be summarized in this paper for completeness.

The GY-11 package (see figures 2,3 ) is a new robust mechanical design featuring a multilayer printed circuit "mother" board (PCB) that (1) provides a high speed stripline design analog transmission buss for relaying the 16 video outputs from the Reticon HS0512J multiport CCD to on-board ADCs and MUX circuitry and to output connectors for external recording; (2) high speed digital buss for transmission of clock signals to the CCD "header" PCB which houses the CCD and MCPII components of the camera; (3) accommodates plug-in PCBs for the digital clock logic and MCPII circuits, as well as 10-bit 50MHz ADCs and 16-channel analog MUX and positioning/rastering circuitry for near real-time sequential viewing of the 16 segments of the Reticon HS0512J multiport CCD.

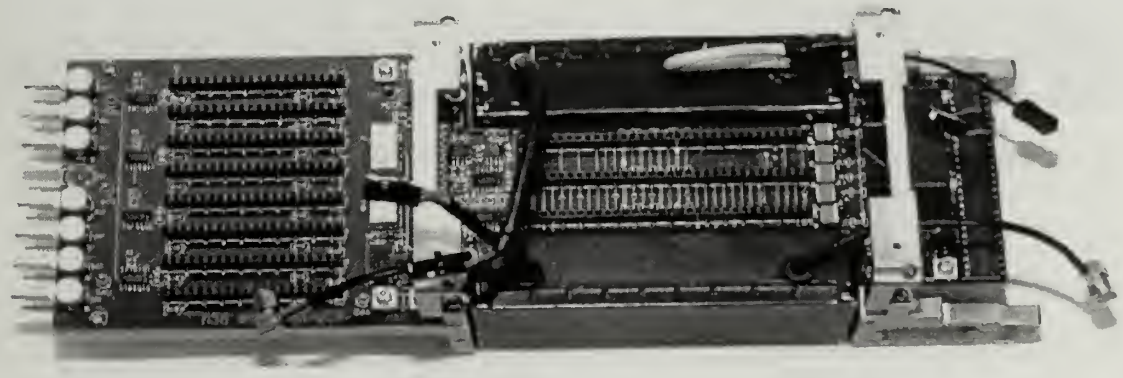

Figure 2 Photograph of GY-11 mainframe, without MCPII/CCD module connected (connector at right, normal to motherboard). PCB connectors for eight of the ADC s are shown to the left and CCD clock logic PCBs at right center. Analog video output connectors are at far left.

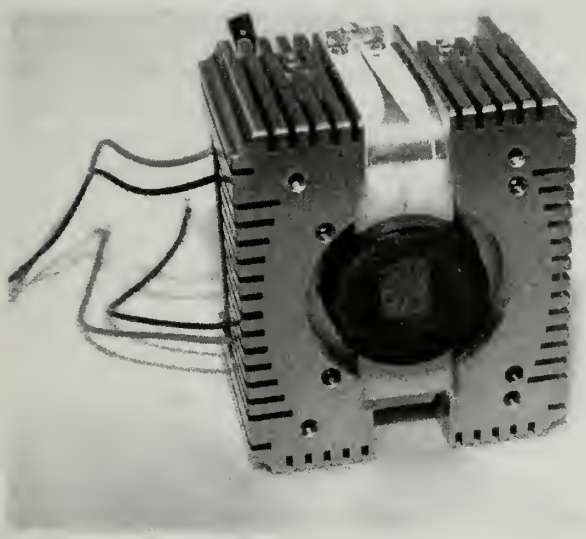

Figure 3. Photograph of GY-11 MCPII/CCD housing. The stripline MCPII with 12x18mm rectangular photocathode is shown connected to the microstrip gate driver.

This design approach has resulted in a mechanically robust state-of-the-art camera mainframe with high performance analog and digital busses and provision for modular PCB-based analog and digital circuitry for easy up grading of current circuitry as improved components and circuits evolve.

The two key camera components are shown in figure 4. These are (1) the stripline MCPII designed by Los Alamos National Laboratory and manufactured by Philips Components, and (2) the HS0512J multiport CCD manufactured by EG&G Reticon. Characteristics of the MCPII and CCD are summarized in table 1.

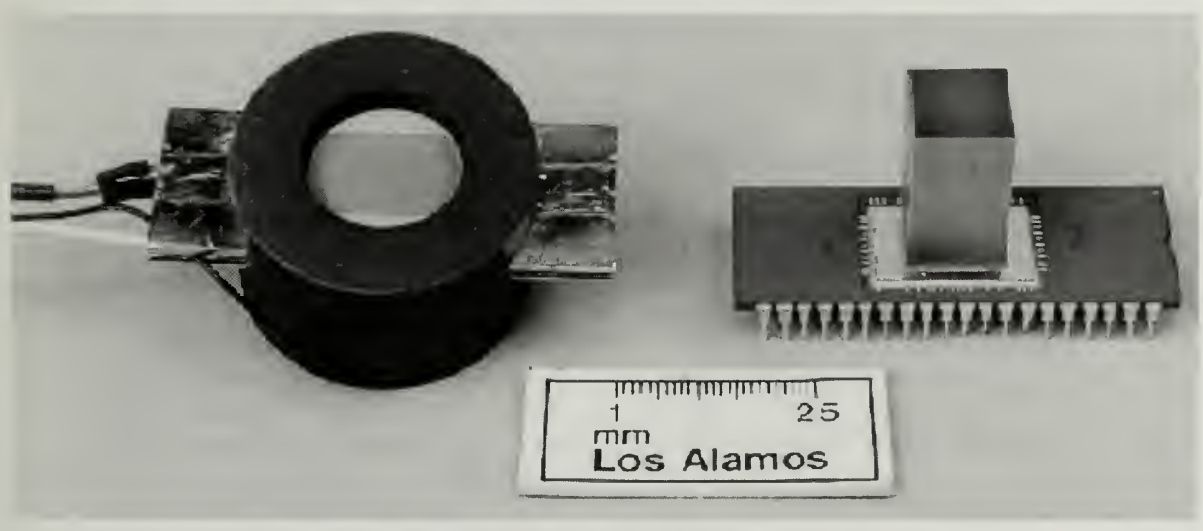


Figure 4. Photo of stripline MCPII (left) and multiport CCD (right) used in GY-11 camera.

Table 1. Reticon HS0512J CCD and Philips XX1412MH/E04 MCPII data

| | CCD | MCPII |
|---|---|---|
| Image Area | 8.2 x 8.2 mm | 12 x 18 mm |
| Pixel/MCP | 16-micron sqd. | 10-micron diam. |
| Sensor | Si | S-20/P-48 |
| Readout/Gate | 250 microsec | 200 picosec |

## CAMERA TEST DATA

The measured parameters required for use of the cameras in radiometric imaging applications include gating/shuttering characteristics, responsivity, dynamic range, resolution, ADC accuracy, gain and bias variances among the individual output video ports, and electrical and optical crosstalk among the individual segments. Preliminary resolution data are shown in figure 5, and other test results are found in Table 2.

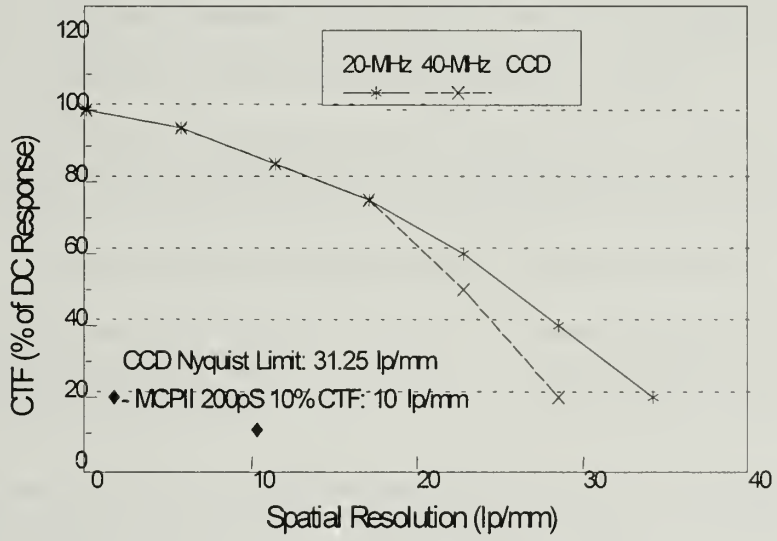


Figure 5. Measured resolutions for individual CCD and MCPII components of GY-11 .

Table 2. GY-11 measured test data

| | |
|---|---|
| Sensitivity: 1-2 picojoules/cm sqd | Sensor Dynamic Range: > 500/1 |
| Amplifier Dynamic Range: > 2x1 E3 | ADC Resolution: 10-bits @50MHz |
| Gated Resolution: > 10 lp/mm | Optical Crosstalk: < .01% |
| Shutter Speed: < 100pS | Shutter Ratio: > 1x10 E6 |
| Gate Control: 10-bits, 1-1024nS | Gain Control: 10-bits, 1-1024V |

## CAMERA RECORDERS

Three independent designs are under development. These are (1) high speed VME-based digital memory capable of storing 1-1000 frames, described earlier (reference 11) and summarized in this paper, high speed data transmission link and CAMAC-based digital memory capable of 1-10 frames storage (reference 12) and (3) high frequency multichannel digital sampling oscilloscope (DSO) digitizer and digital memory system (reference 13).

The VME-based system frame grabber and data memory modules is being developed uniquely for the GY-11 camera because commercially available frame grabbers and data acquisition cards will not meet the high data rates of the camera. The basic function of the frame grabber is to receive the 16 channels of digital data from the GY-11 camera and record the data in resident high-speed storage, then, upon demand,

transfer the data into an archival storage medium such as a removable computer hard-disk drive. The frame grabber software will have the capability of assembling the 64x256 sub-arrays from the 16 CCD segments into one full 512x512 video frame. The frame grabber will have the capability of displaying selected frames of data either in a single frame static mode or a multi-frame dynamic mode, similar to a motion picture. Conceptual design of the frame grabber, referred to as the frame grabber memory module (FGMM), has been completed and detail design is now underway. The FGMM consists of a stand alone memory module that is interfaced to an IBM compatible computer through a SCSI link and the necessary software to control the memory module, transfer video data from the memory module to computer storage, reconstruct full frames from the sub-arrays, and display frames upon request. The FGMM includes a setup mode where frames are recorded from the camera and displayed on the monitor as quickly as possible, which is expected to be approximately 5 frames per second. Each sub-array from the camera will have a unique header that identifies the sub-array with the frame being recorded and indicates location in the frame. In addition, a date-time indicator in included in the header. Unless specified by the user, data recording will be circular, that is, when the end of the FGMM memory is reached, recording automatically starts again at the beginning of the memory and the previous data is overwritten.

The memory module clock is to be synchronized with the GY-11 pixel clock, which is accomplished by a pixel clock signal line for each of the 16 data channels. Circuit designs in the FGMM will allow up to 100 MHz pixel clock frequency. A summary of the storage characteristics of the FGMM is given in Table 3.

Table 3. Data Rate and Storage capabilities of FGMM. (8-bit bytes)

| | |
|---|---|
| Pixel Clock Frequency Range:1-100 M Hz | Frame Rate Range: 4-3500 frames/sec |
| Initial Total Memory Size: 2,048 Mbytes | Initial Frame Storage : 3900 frames |
| Expanded Memory Size: 6,144 Mbytes | Expanded Frame Storage: 11,700 frames |

The FGMM is primarily controlled through the computer. A graphical user interface (GUI) operating under Windows 95 or NT provides a user-friendly operating environment. The following functions are controlled from the computer using the GUI (Table 4) and manually (Table 5).

Table 4. Computer controlled functions for FGMM.

(1) Record M Frames after Every Nth Frame, Stop after Tth Frame: M, N, and T are parameters entered by the user through the control computer. The FGMM will record and store the first M frames after start and skip the next N frames at which time M more frame are stored, and so on, until recording is stopped.
(2) Record M frames: Start collecting frames on trigger and collect M frames.
(3) Display Frames Real-time: This function records frames from the camera and displays them on the monitor as quickly as possible. This function will operate whether or not the FGMM is storing frames.
(4) Display Frame (number): This function displays a single user specified frame and allows the user to step through frames stored in the FGMM or on computer disk from the keyboard.
(5) Display Sequence of Specified Frames: This function allows the user to enter a specified list of frames and to display the frames by stepping through the list in sequence.
(6) Display Movie of Sequence of Frames: This function displays the Sequence of Specified Frames (above) to be viewed as a movie (or motion picture).
(7) Transfer Specified Frames: This function transfers a user specified list of frames from the FGMM and stores them on computer storage disk.
(8) Transfer All Files: This function transfers all stored frames from the FGMM into computer disk .

Table 5. Manual controls for FGGM.

(1) Reset, which causes the FGMM to initialize.
(2) Start, which causes the FGMM to begin recording frames of data.
(3) Stop, which causes the FGMM to stop recording frames .
(4) Single Frame, which causes the FGMM to read and display one frame.

## ACKNOWLEDGMENTS

The authors acknowledge technical support from Claudine Pena of Los Alamos National Laboratory, mechanical design and packaging layout and PCB fabrication support from Rick Diaz of Special Technologies Laboratory (STL) of Bechtel Neveda, and electronics design support for MCPII circuits from Eric Larson, also of STL. The authors also acknowledge PCB layout and fabrication support for CCD circuits from George Ziska of Lawrence Berkeley National Laboratory.

## REFERENCES

(1) G.J. Yates, "FPS Camera Sync and Reset Chassis," Los Alamos National Laborotory Report LA-8255, June 1980

(2) G.J. Yates, S.A. Jaramillo, "Characterization of New Focus Projection and Scan (FPS) Vidicons for Scientific Imaging Applications," SPIE, Vol. 832, High-Speed Photography, Videography, Photonics V, pp. 297-306, San Diego, CA, August 1987.

(3) G.J. Yates, N.S.P. King, "High-frame-rate intensified fast optically shuttered TV cameras with selected imaging applications", (invited paper) SPIE Vol. 2273, pp. 126-148, San Diego, CA.,July 24-29,1994.

(4) Thomas, M.C., G.J. Yates, and P.A. Zagarino, "Fast Optical Gating Using Planar-lead MCPIIs and Linear Microstrip Impedance Transformers," SPIE, Vol. 2273-26, Ultrahigh- and High-Speed Photography, Videography, and Photonics Conference, San Diego, CA, July 24-29, 1994.

(5) G.J. Yates et al, "An Intensified/Shuttered Cooled CCD Camera for Dynamic Proton Radiography", Proceedings of Electronic Imaging '98 Conference, SPIE Vol. 3302, pp.140-151, January 28-29 1998, San Jose, CA.

(6) N.S.P. King et al, "Underwater Mine Detection Utilizing Gated Intensifier Shutters Sychronized with Laser Reflectance Images From Submersed Targets," ISIA Conference on Detection and Analysis of Subsurface Objects and Phenomena, High-Speed Imaging Techniques and Applications Session, Naval Postgraduate School, Monterey, CA., October 19-23, 1998.

(7) J. Payton et al, "Range Gating Experiments Through a Scattering Media," ISIA Conference on Detection and Analysis of Subsurface Objects and Phenomena, High-Speed Imaging Techniques and Applications Session, Naval Postgraduate School, Monterey, CA., October 19-23, 1998.

(8) G.J. Yates, "Real Time Pulse Width Monitor for ICCD Electro-optic Shutters," High-Speed Photography and Photonics Conference, SPIE Vol.2869, pp360-373, Santa Fe, NM, October 27- November 1, 1996.

(9) G. J. Yates , T . E. McDonald, and N. S. P. King, "High-Speed Intensified, Shuttered, Multiport CCD Camera," in ISA proceedings of the 43rd International Instrumentation Symposium, pp. 775-784, Orlando, Florida, May 4-8, 1997.

(10) G.J. Yates, T.E. McDonald, B.T. Turko, "High Frame Rate CCD Camera With Fast Optical Shutter," in ISA proceedings of the 44th International Instrumentation Symposium, . Reno, Nevada, May 3-6, 1998.

(11) T.E. McDonald Jr. and G.J. Yates, "Continuous Recording Camera System for High-Frame Rate High-Resolution Applications," International congress on High-Speed Photography and Photonics (ICHSPP '98), Moscow, Russia, September 20-25,1998.

(12) B.T. Turko et al, "Digital Memory for a 16-port CCD Camera Readout at 40 MHz Pixel Rates," ISIA Conference on Detection and Analysis of Subsurface Objects and Phenomena, High-Speed Imaging Techniques and Applications Session, Naval Postgraduate School, Monterey, CA., October 19-23, 1998.

(13) E.L. Brunholzl and V. Hungerbueller, "A Method for Transmitting High Frame Rate Video Data to Remote Locations," ISIA Conference on Detection and Analysis of Subsurface Objects and Phenomena, High-Speed Imaging Techniques and Applications Session, Naval Postgraduate School, Monterey, CA., October 19-23, 1998.

# Digital Memory for a 16-port CCD Camera Readout at 40 MHz Pixel Rates

B.T. Turko,** N.S.P. King,* T. McDonald,* J. Millaud** and G.J. Yates*
(*Los Alamos National Laboratory; **Lawrence Berkeley National Laboratory)

## Summary

A 16-port very high frame rate CCD camera, developed at the Los Alamos National Laboratory, requires a custom designed digital memory. We describe a modular memory capable of supporting a variety of multi-port CCD sensors. The LANL camera, using EG&G/Reticon, Inc. HS0512J sensor, makes 512x512 pixel video frames split into 16 segments. Each image segment is served by an individual video channel. The segment format is 256 video lines of 64 pixels each, digitized in 10-bit words. Combined, the data make 160-bit wide words, sent to the memory for storage at the rates of up to 40 MSPS. The distance between the camera and the memory should exceed 50 feet.

## Video signal processing at very high pixel rates

I order to read out images in shortest possible time, very high horizontal clock frequencies must be used, far above the nominal rate of the CCD sensor. Consequently, the video line resembles a train of narrow voltage pulses. The peak of each pulse is proportional to the intensity of pixel illumination. Video signal processing at such rates requires somewhat unusual electronic circuitry. One of the sixteen parallel video channels is illustrated in Fig.1. Close to the sensor video port is a buffer amplifier providing the level shifting and voltage gain, and driving the transmission line linking the camera head with the video processing circuits.

The level of video signal is further increased by a wide-band amplifier. An appropriate D.C. offset is also adjusted at this point. The fast voltage comparator is used next as a precision peak detector. The comparator output coincides with the peak of a slightly integrated video waveform (by a R-C network) at the comparator's inverting input. This is illustrated in Fig.1, waveforms A, B and D. A very fast track-and-hold amplifier follows the contour of the video signal. At each peak point the comparator switches the amplifier to hold mode (waveform E). The T/H amplifier output remains flat until the beginning of the next pixel.

A 40 MSPS A/D converter digitizes the stretched video in a 10-bit range. The system clock (coinciding with the pixel readout clock) drives the ADC. A conversion is started on the positive edge of the clock, timed to fall in the flat portion of the input signal (waveforms E, F and G). The ADC data is buffered and transmitted to the remote memory by twisted pair ribbon cables.

## Data transmission

The camera is frequently remote from the data storage and/or processing area. Since the required distance between the camera and memory is over 50', data transmission by twisted pair cables at rates of over 40 MHz, is not an easy task. In order to reduce power dissipation inside the camera, single-ended data buffers/line drivers were used to feed the transmission lines. Since all 16 image sections are running in parallel, the data is sent to the memory in 160-bit words. Using a high-speed differential line driver for each bit was unacceptable due to an excessive use of power and space. The drawback of the acceptable solution, however, was a smaller signal and higher noise at the receiving end.

Two links, one for the data and the other for shaping the camera clock, frame and line timing, are illustrated in Fig.2. Data signal is reduced due to the transmission losses and a lot noisier because of crosstalk (waveforms A and B). The data is sensed by a fast TTL comparator. Resistors R01 and R1 – R2 provide the transmission line termination and threshold bias, respectively. The clock and the sync. pulses, on the other hand, are received by a fast ECL comparator, in order to shape them before the data appear at the output of the slower TTL device. The ECL comparator output is followed by two stages of an ECL line receiver. The negative-going signal edge is delayed by the Rl-Cl network, and then, after an inverting stage, by Rt-Ct. The clock output is both shaped and delayed in order to appear properly timed with respect to the data (waveforms C, D, E and F).

In the laboratory testing of the above circuits data was transmitted successfully over a distance of 70' and rates of up to 50 MHz.

## Data storage

In order to achieve a flexible, expandable system, the memory is split into two modules serving eight video ports each. Each module has four slots for RAM boards. A single RAM board capacity is eight frames. With all slots occupied, the memory can store up to 32 frames. A single frame has 512x512 pixels with a resolution of 10 bits. A programming logic controls the memory modules. They can be used either individually or the two of them working in parallel, depending on how many video ports are configured. The memory operates either in a write mode or in a read mode. The block diagram of a two-module system is shown in Fig.3.

Data write mode.

The camera normally operates continually, sending data, the vertical and horizontal synchronization pulses and the pixel clock signal to the memory. An ARM signal from the computer is sent before commencing the recording in order to enable the write mode. Upon the FIDU command from the camera operation logic, the memory will start storing video frames until full.

Data readout mode.

Prior to data readout the computer has to download the address of the frame and/or the frame segment to be read out. The data is read out serially in 10-bit words, each word representing the signal magnitude of an individual pixel. The rate is dependent on the rate of read clock generated by the computer. Each clock pulse stores the addressed pixel's data into the P.C. memory. The trailing edge of the pulse advances the pixel address. The number of clock pulses defines how many consecutive video frames and/or sections are read out.

Before using the memory in either mode, parameters pertinent to the video format of the CCD camera must be entered. These include the number of lines per frame, number of pixels per line and the number of frames to be recorded. During the period between the lines the recording stops in order to save memory space. However, due to the data latency in A/D converters of the CCD camera, the write cycle must be extended beyond the video line by several pixel clock pulses. The ADC latency is thus also one of parameters to be entered.

Relatively low cost and flexibility in adapting this memory to a number of different high-speed digital CCD cameras makes it a useful tool in many applications.

FIG. 1. VIDEO PROCESSING CHANNEL

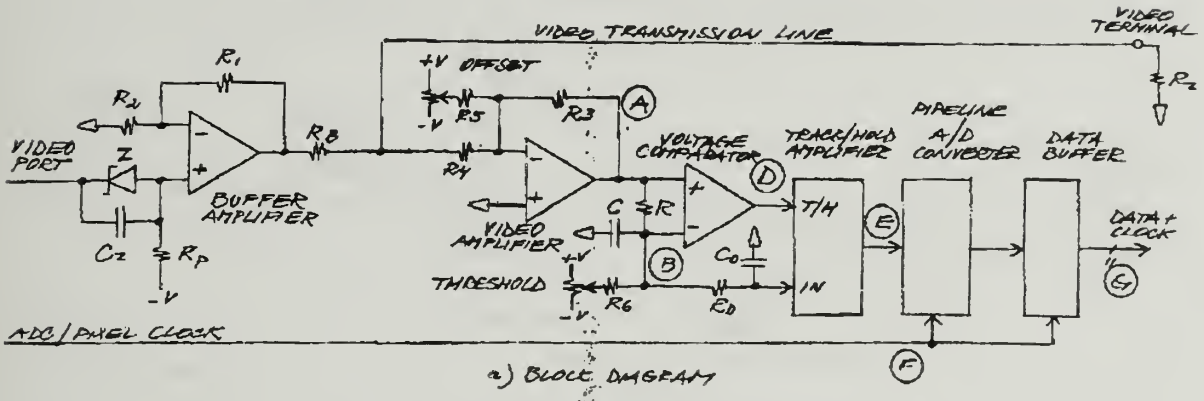


a) BLOCK DIAGRAM

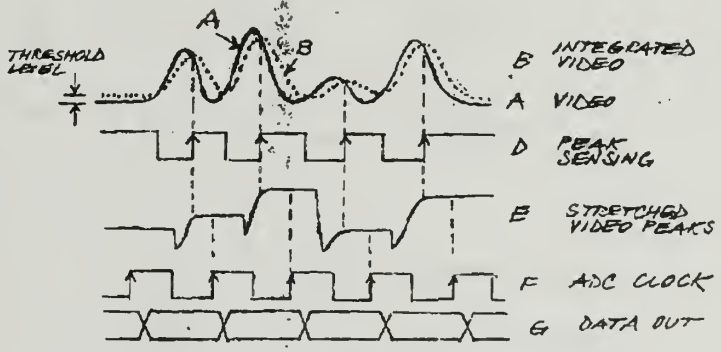


b) TIMING DIAGRAM

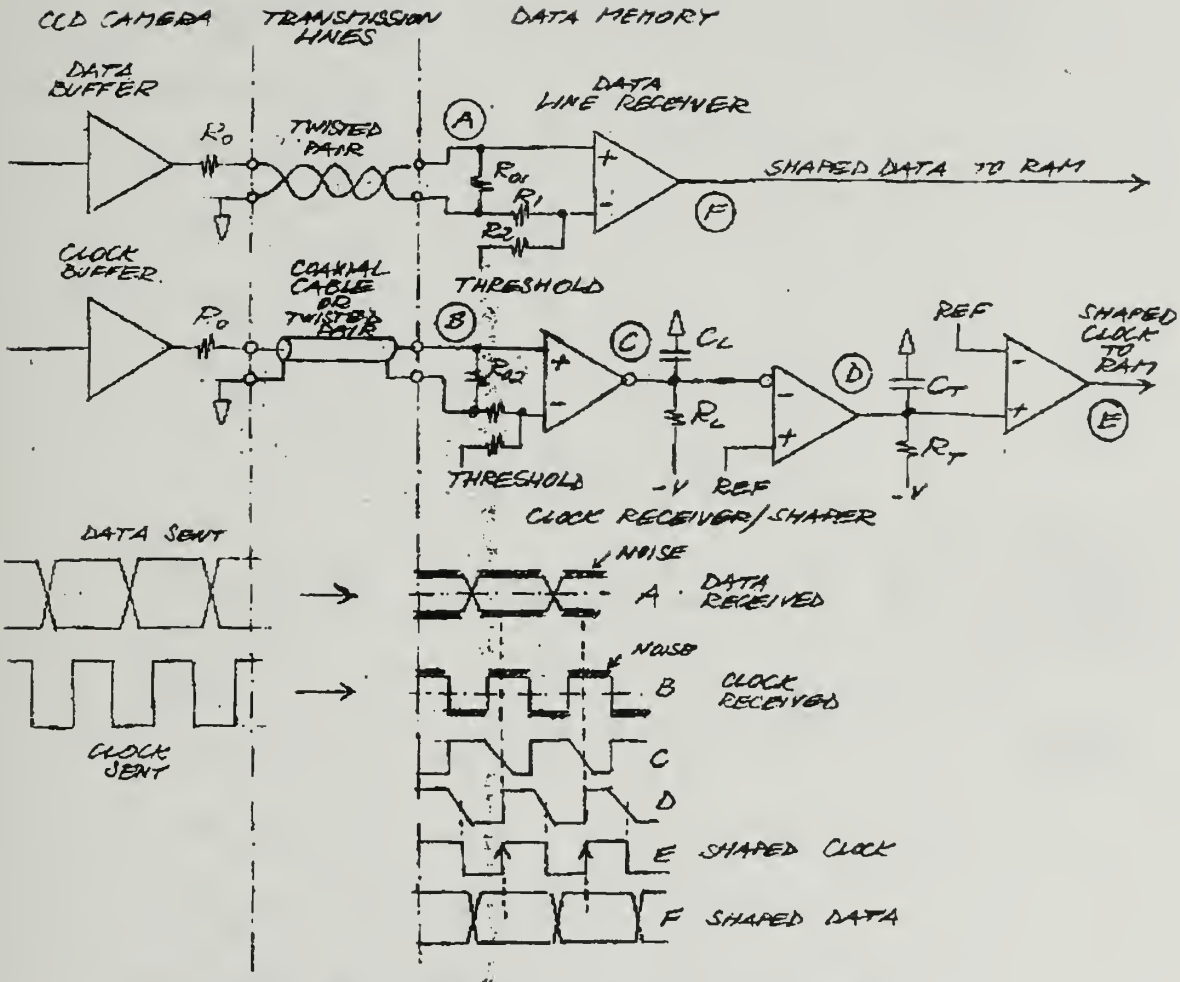


FIG 2. DATA AND CLOCK TRANSMISSION BLOCK DIAGRAM

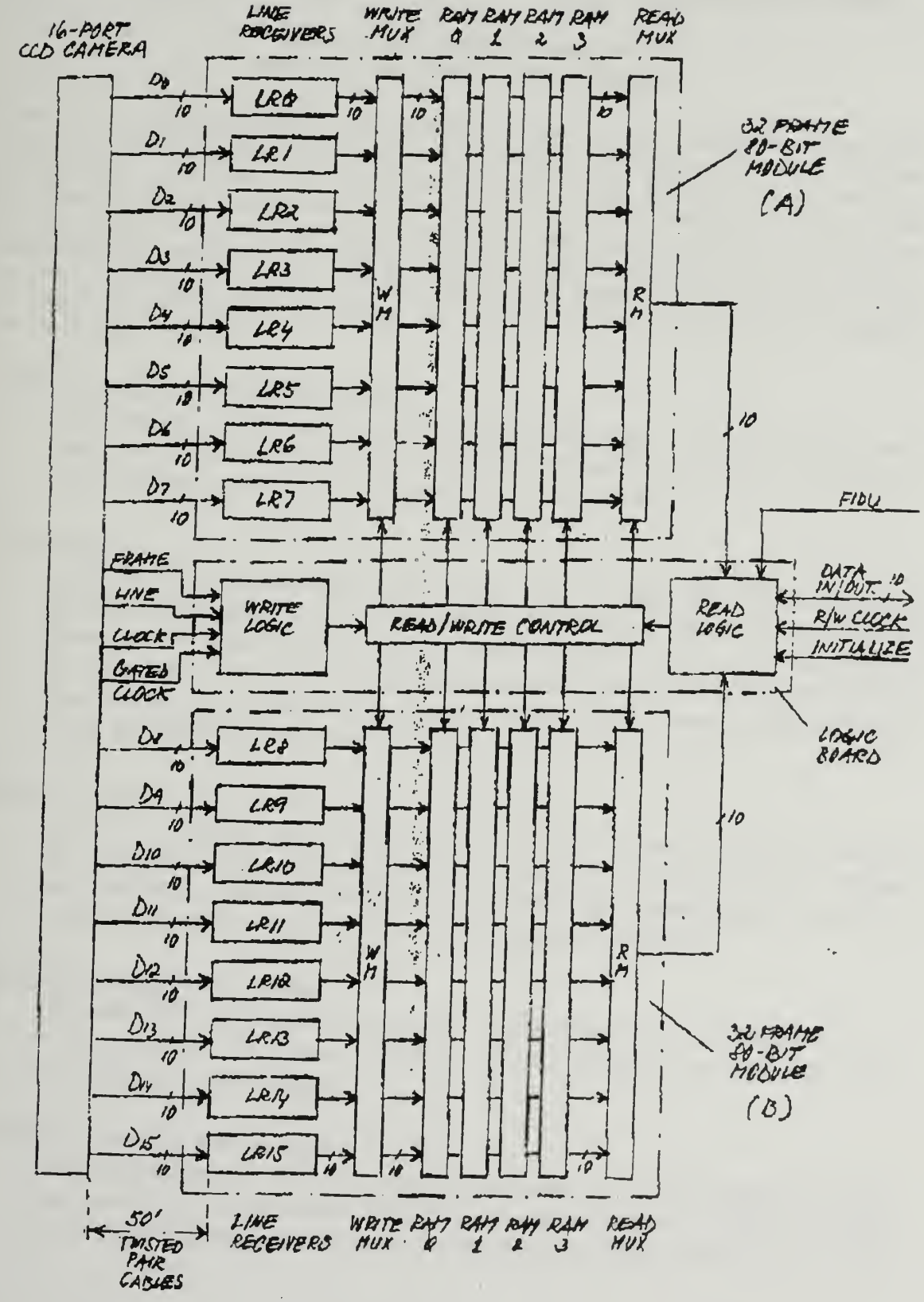


Fig.3. 16-port, 160-bit digital storage of CCD images at rates of 40 Mwords/s

# A Method for Transmitting High Frame Rate Video Data to Remote Locations

**Ernie Brunholzl Acqiris Albuquerque NM**
**Didier LeVanchy Acqiris Geneva Switzerland**

Overview: There are many systems being designed and used today from high speed video as in this example, to real time radar systems which can benefit from integrated digitizing and processing. This approach can make a large difference in the amount of data that the system bus and processor has to handle. The inclusion of a large Field Programmable Gate Array immediately following the digitizer not only can reduce the amount of data passed on, but actually improve the quality of the data that is passed on. The fast clock frequency, in this case 2 GHz is much faster than most other processors, and much of the required processing can occur in real time, therefore not impacting system acquisition speeds.

1.Modern imaging system requirements:

An example is the Los Alamos National Laboratory GY-11 Camera system being developed for DOE and DOD to meet several programmatic requirements. The imaging system salient characteristics are as follows:

The Camera:

The GY-11 is an intensified, CCD camera with the capability of subnanosecond gating and a continuos frame rate of 4000 frames per second. To achieve this frame rate the camera has 16 parallel output ports and a pixel clock frequency of up to 75 MHz. The pixel clock frequency can be varied from 10 kHz and 75 MHz, thus allowing for a variable frame rate. In addition the camera outputs the pixel clock and frame synchronization signals.

High Accuracy:

The GY-11 contains internal 10 bit converters, (one for each output port) and also provides the analog CCD signals for external conversion where even higher accuracy may be required. The CCD data has a high dynamic range and certain requirements require utilizing the maximum accuracy possible.

Large Data Storage Requirements:

Consider 4000 frames/second at 262 ksamples/frame = >1 Gsamples/sec x 2 bytes/sample = 2 Gbytes/sec. Additionally frame identifier and date time data is also included with each frame.

Real Time Processing Requirements:

File management includes adding header information to the incoming data stream and storing the frames either in a dedicated memory system or hard disk array. Some programs desire the data to be transmitted to a remote location in real time.

2. Reducing the amount of data and increasing the accuracy at the input of the acquisition system is the key to faster, more flexible systems in the future.

Signal processing algorithms such as signal averaging, and curve fitting can improve the accuracy of the data.

By sampling the data at much higher rates, with an external A/D converter, many samples per pixel can be obtained. These samples can then be averaged and fitted to achieve higher accuracy than when a single sample is used.

The on board converters of the GY-11 are timed to sample at an optimum point on the readout of the CCD. The optimum point however changes as a function of clock frequency and signal level. The signal processing algorithms in the external converter can compensate for these changes. The accuracy of the pixel value is increased over a wide range of timing and amplitude.

Compression of similar pixel values can result in significant reduction in the amount of the data that the system must store. Temporary storage of a dynamic array of pixel values and executing a suitable compression algorithm can result in significant improvement in reducing the amount of data to be stored.

3. This describes a new digitizer with onboard real time processing that is now available, which can be used to increase the quality of the data and at the same time reduce the amount of data that is passed on to the processing system.

The Acqiris DC210 a 2 GS/s 8 bit digitizer in PXI standard contains a Field Programmable Gate Array clocking at the same frequency as the A/D converter. In this case the FPGA is clocked at up to 2 Ghz. The DC210 also contains an external clock input for variable frame rates.

With the DC210 operating at 2 GS/s, 32 samples per pixel are digitized.

The samples are curve fitted and the resulting value of the maximum or any other definable parameter is read.

In applications where the sampling window is triggered, the Acqiris DC210 almost eliminates trigger jitter allowing signal averaging to reach near theoretical limits.

The Acqiris modules operate with a synchronizing bus built in which means all modules in a system are operated simultaneously without extensive cabling or timing considerations.

The FPGA reads data from acquisition memory and processes it and places the results in post processing memory for storage.

Previous pixel values can be stored as a dynamic array in the FPGA and compressed with the result placed in the post processing memory. The post processing memory is subsequently read by the system bus. A suitable compression algorithm can reduce the amount of subsequent system bus traffic and storage requirements by one half to one third versus conventional system configurations.

# Nuclear Radiation Detection Technology at Los Alamos National Laboratory

W. Robert Scarlett, M. W. Johnson, and Avigdor Gavron
Los Alamos National Laboratory

Abstract: We will discuss recent and ongoing Los Alamos nuclear radiation detection projects related to nonproliferation, treaty monitoring, safeguards, and waste disposal. The presentation will include active and passive methods for detecting and identifying smuggled nuclear material; monitoring technology for arms and fissile material reduction treaties; recent developments in safeguards measurements of hard-to-measure items, and advances in neutron differential die away approaches for waste characterization.

# ENRICHED URANYL FLUORIDE DEPOSIT CHARACTERIZATIONS USING ACTIVE NEUTRON AND GAMMA INTERROGATION TECHNIQUES WITH $^{252}Cf$

T. Uckan, M. S. Wyatt, J. T. Mihalczo, and T. E. Valentine
Oak Ridge National Laboratory
P.O. Box 2008
Oak Ridge, Tennessee 37831 U.S.A.

T. F. Hannon
Bechtel Jacobs Company LLC
P.O. Box 4699
Oak Ridge, Tennessee 37831

## ABSTRACT

A method was developed and successfully applied to characterize large uranyl fluoride ($UO_2F_2$) deposits at the former Oak Ridge Gaseous Diffusion Plant. These deposits were formed by a wet air in-leakage into the $UF_6$ process gas lines over a period of years. The resulting $UO_2F_2$ is hygroscopic, readily absorbing moisture from the air to form hydrates as $UO_2F_2 \cdot nH_2O$. The ratio of hydrogen to uranium, denoted H/U, can vary from 0-16, and has significant nuclear criticality safety impacts for large deposits. In order to properly formulate the required course of action, a non-intrusive characterization of the distribution of the fissile material within the pipe, its total mass, and amount of hydration was needed. The Nuclear Weapons Identification System (NWIS) previously developed at the Oak Ridge Y-12 Plant for identification of uranium weapons components in storage containers was used to successfully characterize the distribution, hydration, and total mass of these deposits. Previous estimates of the mass of the largest deposit from passive gamma and neutron measurements was $1190 \pm 595$ kg of $UO_2F_2$ with an enrichment of $3.30 \pm 0.66$ wt % $^{235}U$ whereas the estimates from interpolation of NWIS measurements at six positions along the pipe were $552 \pm 93$ kg which compared favorably with the measured mass of the deposit when cleaned up of 478.6 kg. In addition the H/U, a parameter interest for nuclear criticality safety, obtained from the measurements agreed with the actual values. The asymmetric distribution obtained from the measurements was also confirmed when the pipes were cut open.

# $^{252}$CF OR INHERENT SOURCE DRIVEN CORRELATIONS FOR NON INTRUSIVE VERIFICATION OF WEAPONS COMPONENTS IN CONTAINERS

J. K. Mattingly, M. S. Wyatt, T. E. Valentine, J. T. Mihalczo, and J. A. Mullens
Oak Ridge National Laboratory
P.O. Box 2008
Oak Ridge, Tennessee, 37831 U.S.A.

S. S. Hughes
Oak Ridge Y-12 Plant
P.O. Box 2009
Oak Ridge, Tennessee 37831 U.S.A.

## ABSTRACT

The $^{252}$Cf source driven time and frequency analyses method has some unique advantages for use in confirming that nuclear weapons components are stored as required. This method of confirmation is in use at the Oak Ridge Y-12 Plant for verification of the contents of containers in storage. The data presented in this paper shows how NWIS signatures can be used to confirm the presence of nuclear weapons components in containers in storage configurations in a nonintrusive way so as not to reveal design information and track them for nuclear material control and accountability. This active neutron interrogation method is particularly useful for components of shielded highly enriched uranium (HEU) where induced fission from $^{252}$Cf neutrons produce a signature that can be used to identify the presence of HEU and the configurations of material. Nonintrusive displays of ratios of signatures can be used for making comparisons. Recent measurements with pits in containers at Los Alamos Scientific Laboratory and PANTEX have shown that passive correlation methods can be used to identify pits in containers.

# Tactical Unattended Ground Sensors

**Dr. Steven G. Peglow**
**Lawrence Livermore National Laboratory**

The Tactical Unattended Ground Sensors (TUGS) Program is a joint (LLNL/Sandia/ENSCO) program, sponsored by the Department of Defense, whose purpose is to provide a capability to monitor underground facilities and communicate real time information to aid in threat assessment. TUGS consists of three major system elements: the sensor field units, the communication infrastructure and the operator work station or Correlator.

The TUGS field unit is the element of the TUGS system that is hand emplaced near a target site or facility and collects, processes and stores data for transmission to the Correlator. The sensor is battery powered, with an expected lifetime of 30 to 90 days.

The sensor is designed to use a downloadable set of on-board algorithms to detect events and sources and produce feature vectors. These feature vectors are formed using the inputs from the on-board transducers and information stored in the program memory. Each sensor has an independent capability to identify and provide location information on transient and continuous sources at demonstrated ranges greater than 400 meters. The baseline field unit architecture includes 12 channels for transducers, 9 of which are used in the current configuration. These channels are dedicated to the seismic transducers (3 axis, dual gain) and the magnetic orientation sensor, with three spare channels for an additional sensor, e.g., acoustic microphone.

12 units built at LLNL were successfully deployed and tested at a series of tests against a facility earlier this year . The current system uses an RF/LOS commercial modem that talks to a local (within 5 miles) INMARSAT terminal. From the relay platform, the data can be sent anywhere in the world that is serviced by an INMARSAT satellite. Once at the ground station, the data is displayed and analyzed on a workstation by a miltary operator/controller who can communicate with the field units to change modes or download additional algorithms. A follow-on program is underway to provide an air delivery capability and direct-to-satellite communications.

# Identification of Motion Events from Fusion of Micropower Impulse Radar and other Sensor Data

James K. Wolford, Jr.[1], Donald J. Mullenhoff, and David A. Kasimatis
University of California
Lawrence Livermore National Laboratory
Livermore CA 94551

## Abstract

*Micropower impulse radar (MIR) is a useful tool for detecting motion at small (<10 meter) object distances from behind opaque barriers with very low power consumption. Combining the returns from two or more sensors also gives direction and velocity information. Knowledge of other physical phenomena through passive infrared, seismic, or magnetic signatures gives still more information about the event. These techniques are well suited to classifying motion through defined pathways such as tunnels and culverts. The choice of features and classification methods affects how accurately these determinations are made. This study presents analysis of data collected in field and laboratory tests and compares algorithms used to identify the event. It applies sensor fusion at the decision level and proposes an improved treatment at the feature level. Identification algorithms include both neural net and model based classifiers. Some are robust in extreme environments where only part of the feature ensemble may be available or reliable.*

[1] e-mail: wolford@llnl.gov; telephone: (925) 422-7236